UNIVERSITY OF CALIFORNIA, SAN DIEGO

Selective inhibitory control and the basal ganglia

A dissertation submitted in partial satisfaction of the requirements of the degree
Doctor of Philosophy

in

Neurosciences

by

Dewan-Syed Adnan Majid

Committee in charge:

Professor Adam Aron, Chair
Professor James Brewer
Professor Anders Dale
Professor Christine Fennema-Notestine
Professor Neal Swerdlow

2013

The Dissertation of Dewan-Syed Adnan Majid is approved, and it is acceptable in quality and form for publication on microfilm and electronically:

Chair

University of California, San Diego

2013

DEDICATION

With much joy and happiness, I would like to express my deep gratitude and dedicate this dissertation to those who have made and continue to make a lasting impact in my life. Firstly, I dedicate this work to my mother, in whose prayers and tender affection I grew and became the person I am today. To this day, I remember her tireless dedication raising my brother and me while pursuing a college degree with high honors. She has always hoped for the best in my brother and me, and that faith in us has always given us constant support. I dedicate this work also to my father, a solid role model throughout my life whom I have always looked up to. It is his example of holding to an impeccable moral standing and a tireless work ethic that has driven me forward, and I am honored to follow in his footsteps in completing this degree. And I dedicate this work to my wife, friend, and soul mate, who has brought me endless happiness and laughter since we first met. Her love and companionship has been my greatest source of strength through the hardest of times, and I look forward to many beautiful years ahead. And I dedicate this work to my brother who will join me as we complete our degrees together, and my grandparents who have taught me through their most beautiful example.

TABLE OF CONTENTS

LIST OF FIGURES

LIST OF TABLES

ACKNOWLEDGEMENTS

With great thanks, I would like to acknowledge the mentorship of my graduate advisor, Dr. Adam Aron, for his tireless support.

Chapter 1, in full, is a reprint of material as it appears in Majid, Cai, George, Verbruggen, and Aron, *Cerebral Cortex*, 2011. I also thank Cathy Stinear for helpful comments on the manuscript and the Alfred P Sloan Foundation and the NIH National Institute on Drug Abuse for financial support. The dissertation author was the primary investigator and author of this paper.

Chapter 2, in full, is a reprint of material as it appears in Majid, Stoffers, Sheldon, Hamza, Thompson, Goldstein, Corey-Bloom, and Aron, *Movement Disorders*, 2011. I thank Anders Dale and Matt Erhart for technical assistance with image preprocessing and CHDI for financial support. The dissertation author was the primary investigator and author of this paper.

Chapter 3, in full, is a reprint of material as it appears in Majid, Aron, Thompson, Sheldon, Hamza, Stoffers, Holland, Goldstein, Corey-Bloom, and Dale, *Movement Disorders*, 2011. I thank Matt Erhart for technical assistance for technical assistance with image processing and CHDI for financial support. The dissertation author was the primary investigator and author of this paper.

Chapter 4, in full, was submitted for publication and may appear in Majid, Cai, Corey-Bloom, and Aron, *Journal of Neurosciences*, 2013. We thank Jody Goldstein and Cait Casey for subject recruitment, Rogier Mars for providing fMRI optimization scripts, Yu-Chin

Chiu for comments on the manuscript, and NIH, the Alfred P Sloan Foundation, and CHDI for financial support. The dissertation author was the primary investigator and author of this paper.

I thank Jan Wessel for assistance in methodological development in Chapter 5.

VITA

2007 Bachelor of Science, Symbolic Systems, Stanford University

2013 Doctor of Philosophy, Neurosciences, University of California, San Diego

PUBLICATIONS

Majid DSA, Cai W, George JS, Verbruggen F, & Aron AR (2012). Transcranial magnetic stimulation reveals dissociable mechanisms for global versus selective corticomotor suppression underlying the stopping of action. *Cerebral Cortex*, *22*(2), 363-371.

Majid DSA, Stoffers D, Sheldon S, Hamza S, Thompson WK, Goldstein J, Corey-Bloom J, & Aron AR (2011). Automated structural imaging analysis detects premanifest Huntington's disease neurodegeneration within 1 year. *Movement Disorders*, *26*(8), 1481-1488.

Majid DSA, Aron AR, Thompson W, Sheldon S, Hamza S, Stoffers D, Holland D, Goldstein J, Corey-Bloom J, & Dale AM (2011). Basal ganglia atrophy in prodromal Huntington's disease is detectable over one year using automated segmentation. *Movement Disorders*, *26*(14), 2544-2551.

Majid DSA, Cai W, Corey-Bloom J, & Aron AR (*under review*). Proactive selective response suppression is implemented via the basal ganglia: functional evidence for the Indirect Pathway in humans. *Journal of Neuroscience*.

Seibert TM, Majid DSA, Aron AR, Corey-Bloom J, Brewer JB (2012). Stability of resting fMRI interregional correlations analyzed in subject-native space: a one-year longitudinal study in healthy adults and premanifest Huntington's disease. *Neuroimage*, 59(3):2452-63.

Wu SS, Chang TT, Majid A, Caspers S, Eickhoff SB, Menon V (2009). Functional heterogeneity of inferior parietal cortex during mathematical cognition assessed with cytoarchitectonic probability maps. *Cerebral Cortex,* 19(12):2930-45.

ABSTRACT OF THE DISSERTATION

Selective inhibition control and the basal ganglia

by

Dewan-Syed Adnan Majid

Doctor of Philosophy in Neurosciences

University of California, San Diego, 2013

Professor Adam Aron, Chair

In our everyday lives, inhibitory control, the ability to stop the actions we are engaged in, is crucial. Though much prior research has explored the neural basis of simple forms of inhibitory control (where an individual must simply stop all initiated actions, for instance), more complex forms of inhibitory control are often necessary. For instance, an individual engaged with her environment might need to selectively stop only one particular action while continuing others without interference. Here, inhibitory control is *selective*. Using a number of experimental methods – including single-pulse transcranial magnetic stimulation (TMS), structural and function magnetic resonance imaging (MRI), and the study of individuals with premanifest Huntington's disease (preHD) – I present evidence that the neural pathways that underlie selective inhibitory control require signaling through basal

ganglia nodes such as the striatum and thus are distinct from those that underlie simple inhibitory control, which does not require the striatum. I first show evidence with TMS that selective inhibitory control is not associated with the “global” motor suppressive side effect commonly associated with simple inhibitory control. I further show functional evidence of striatal involvement in both preparation for and execution of selective inhibitory control. After showing that basal ganglia damage in preHD is specific for basal ganglia nodes such as the striatum, I show that both preparation for and execution of selective inhibitory control are impaired in preHD compared to controls. Lastly, I present a novel methodology by which selective inhibitory control might be trained through real-time feedback.

INTRODUCTION

Importance of inhibitory control

Circumstances in our everyday lives continuously force us to use *inhibitory control* – whether we stop ourselves from walking carelessly into a busy street, hold back from devouring a high-calorie cake, or be careful not to make a faux-pas in a social gathering. Simply put, *inhibitory control* is a crucial executive function by which we stop or control our actions in preference for others.

Inhibitory control develops and changes with age, improving over childhood and adolescence (Dowsett and Livesey, 2000, Carver et al., 2001, Durston et al., 2002) and getting worse with advanced age (Williams et al., 1999, Bedard et al., 2002, Coxon et al., 2012). Furthermore, deficits of inhibitory control underlie a number of neurological and psychiatric disorders, underscoring its importance. These deficits have been noted with regards to Attention Deficit Hyperactivity Disorder (ADHD) (Murphy, 2002, Aron et al., 2003a, Lijffijt et al., 2005), Obsessive Compulsive Disorder (OCD) (Chamberlain et al., 2006a, Menzies et al., 2007, Morein-Zamir et al., 2010), schizophrenia (Vink et al., 2006), drug addiction (Monterosso et al., 2005, Li et al., 2008a, Lawrence et al., 2009), Parkinson's disease (Gauggel et al., 2004, Obeso et al., 2011), and Huntington's disease (HD) (Lawrence et al., 1998b).

The Stop-Signal Task

There are a number of methods by which to study inhibitory control by operationalizing the behavior in the task setting. One such task is the standard Stop-Signal Task (SST) (Logan et al., 1984). The basic features of the stop-signal task are as follows: On each trial, subjects see a go-signal that cues them to make a response, often one of two choices (a left vs. right button press, for instance). Subjects aim to complete this action on a majority of trials (67%, for instance), referred to as Go-trials. On the remainder of trials (33%, for instance), known as Stop-trials, a stop-signal follows the go-signal after a short delay (known as the Stop-Signal Delay or SSD), cuing the subject to hold back from making the response. Since subjects are already in the process of making a response, successful inhibition of the response may be difficult.

Whether an individual is able to successfully stop a response on a particular Stop trial is dependent on the relative timing of the go- and stop-signals and the speed by which the subject can stop the initiated response. This can be modeled mathematically as the "stopping horse-race" model, which assumes that the go- and stop-signals set off *independent* neural processes that compete to reach a particular threshold (Band et al., 2003). Based on this, success in stopping assumes that the Stop process reaches the threshold before the Go process (analogous to reaching the "finish line" first). By contrast, failure to stop on a particular trial assumes that the Go process reaches the threshold before the Stop process.

The speed of the Stop process, know as the Stop-Signal Reaction Time (SSRT), is unobservable since no response is recorded on successful stop-trials. Nonetheless, the

horse-race model's assumption of *independent* Go and Stop processes can be used to estimate an average SSRT. On any given stop-trial, the stop-signal is presented at SSD and thus the completion of the Stop process occurs at SSD+SSRT after the start of the Go process. Assuming a fixed SSRT for estimation purposes, variation in the SSD will lead directly to variation in the time at which the Stop process completes relative to the Go process. Due to the assumption of independence, this Stop process will not affect the concomitant Go process on stop-trials, which can thus be modeled by the Go process on go-trials (i.e. the Go RT distribution). Consequently, the probability of stopping will depend on the completion of the Stop process relative to this Go RT distribution. This probability will be high when the SSD is short and the Stop process completes early relative to the Go RT distribution, since much of the distribution follows Stop process completion. Likewise, stopping probability will be low when the SSD is long. Dynamic variation of the SSD using a "staircasing" method (by which the SSD gets longer after successful stop-trials, making stopping harder, and shorter after failed stop-trials, making stopping easier) will lead to a behavioral equilibrium at which stopping and failing to stop is equally probable (both 50%). At this point, the Stop process completes relative to the midpoint of the Go RT distribution, the median Go RT. Thus, subtracting the SSD from the median Go RT when the stopping probability is 50% will provide an estimate of the SSRT (Band et al., 2003, Verbruggen and Logan, 2009). This basic conception can be modified to allow for SSRT calculation even in situations when the probability is not exactly 50%, which will be discussed further in the dissertation chapters.

SSRT is a useful measure of inhibitory control that has been found to be very stable for an individual in the absence of major developmental change (Logan and Cowan, 1984, Williams et al., 1999, Soreni et al., 2009, Congdon et al., 2012). Furthermore, the Stop-Signal task can be applied to a number of different subject populations, and SSRT calculation can allow for a comparison of response inhibition ability between healthy individuals and those with ADHD (Murphy, 2002, Aron et al., 2003a), OCD (Menzies et al., 2007), schizophrenia (Vink et al., 2006), and Parkinson's disease (Gauggel et al., 2004). SSRT can also be reliably determined at various stages of development from childhood (Carver et al., 2001, van den Wildenberg and van der Molen, 2004) and old age (Bedard et al., 2002, Coxon et al., 2012). Additionally, the Stop-Signal task has been readily adapted for use in both primates (Boucher et al., 2007, Scangos and Stuphorn, 2010) and rodents (Eagle and Robbins, 2003, Bryden et al., 2012), allowing for animal models in which to study inhibitory control (for review, see Keeler and Robbins, 2011). Studies on the effect of pharmacological interventions on Stop-Signal behavior suggest a high degree of translatability between humans and animals; for instance, selective noradrenergic reuptake inhibitors improve SSRT in both humans and rodents (Robinson et al., 2008, Bari et al., 2009) whereas selective serotonin reuptake inhibitors have no such effect in either humans or rodents (Chamberlain et al., 2006b, Bari et al., 2009).

Other tasks used to study inhibitory control, such as the Stop-Change task or the Go/NoGo task, can be described as modifications of the standard Stop-Signal task. Briefly, the Stop-Change task is a variant of the Stop-Signal task where the stop-signal cues the subject to make an alternative response (not one of the cued responses). This response

provides an additional behavioral measure that can give an indication of the stopping process (Verbruggen and Logan, 2009). In the Go/NoGo task, subjects are cued to respond on the majority of trials (Go trials), but must withhold a response on a minority of trials (NoGo trials). Thus, such a task is essentially a variant of the Stop-Signal task with the SSD fixed essentially to 0s (Logan et al., 1984). Because of this SSD invariance, SSRT cannot be determined using a Go/NoGo task. Furthermore, an additional concern with regards to the Go/NoGo task is that an increasing percentage of NoGo trials reduces the prepotency to respond and thus consequently also reduces the need to exert response inhibition. A task in which 50% of trials are NoGo trials may thus be more relevant to the study of response *selection* or *restraint* versus response *inhibition* (Rubia et al., 2001, Eagle et al., 2008a).

The *Selective* Stopping Task

Finally, the Selective Stopping task is a modification of the Stop-Signal Task that directly pertains to the work in this dissertation. In this task, the go-signal cues the subject to make two concurrent responses, such as coupled responses of both hands. On the minority of Stop-trials, subjects are cued to stop only one of the two responses (Aron and Verbruggen, 2008).

Note that subjects, even when successfully stopping a particular response, must continue to make a response with the hand that was not cued to stop. It is often the case that the RT of this hand, known as the Continuing RT, is often prolonged with respect to the RT of Go trials where no stopping occurs. The degree of this prolongation, known as the Stopping Interference Effect, serves as an additional behavioral index of the *selectivity* of

stopping. If stopping were to be completely selective, affecting only the hand that must stop, the Stopping Interference Effect would be essentially zero. By contrast, stopping that is not selective would lead to a prolongation in the Stopping Interference Effect (Aron and Verbruggen, 2008).

Various forms of the selective stopping task exist. For instance, a number of studies have employed task paradigms in which subjects do not know until the time of the stop-signal which of the two initiated responses they might have to stop (Coxon et al., 2007, Coxon et al., 2012, Macdonald et al., 2012). By contrast, other studies first warn subjects which response might have to stop with a cue delivered before the trial begins (Aron and Verbruggen, 2008, Claffey et al., 2010). The latter such paradigms allow subjects to begin to prepare to stop a particular response in advance. Other paradigms, like the *Proactive Selective Stopping Task* discussed in this dissertation, go one step further by making the stop-signal completely uninformative as to which hand to stop (Claffey et al., 2010, Cai et al., 2011). Rather than simply *allowing* subjects to plan in advance, such a paradigm forces subjects to do so, requiring the maintenance of stopping goals in memory. Importantly, this maintenance has been shown to lead to a *proactive* top-down influence over motor response channels that might have to stop – leading to corticomotor suppression of the excitability of the particular effector (Claffey et al., 2010, Cai et al., 2011).

Neural mechanisms of basic stopping

Early EEG and functional imaging studies have long suggested the importance of a right prefrontal cortex in response inhibition (Kawashima et al., 1996, Pliszka et al., 2000,

Schmajuk et al., 2006), especially the right *inferior* prefrontal cortex (Konishi et al., 1998, Garavan et al., 1999, de Zubicaray et al., 2000, Menon et al., 2001, Garavan et al., 2002). Activation of this region in response inhibition occurs in a number of different types of response inhibition tasks (Konishi et al., 1999) including the Stop-Signal task (Rubia et al., 2001, Rubia et al., 2003), regardless of response modality (whether the response is made with the hands or the eyes (Chikazoe et al., 2007). Children, poorer than adults in response inhibition, further show less activity in right inferior prefrontal cortex when engaged in stopping tasks (Bunge et al., 2002). Lastly, studies of lesions, whether precipitated by stroke or induced temporary by transcranial magnetic stimulation, lend further converging evidence for the role of the right inferior prefrontal cortex, particularly the right inferior frontal gyrus (rIFG) in response inhibition (Aron et al., 2003b, Chambers et al., 2006). Lesions in the rIFG led to increased stopping time, SSRT, whereas analogous left IFG lesions did not (Aron et al., 2003b).

Other important regions implicated in simple stopping include the pre-supplementary motor area (preSMA) and the subthalamic nucleus (STN) (for review, see Aron et al., 2007b). Converging evidence from primate tract tracing work and human diffusion tensor imaging have shown that these three regions are directly connected to one another as a single network (Nambu et al., 1997, Inase et al., 1999, Aron et al., 2007a, Madsen et al., 2010, Coxon et al., 2012, King et al., 2012).

The STN is of particular interest due to its role as a basal ganglia input nucleus, receiving projections from both the rIFG and preSMA via the “Hyperdirect” signaling pathway (Mink, 1996, Nambu et al., 1997, Inase et al., 1999, Nambu et al., 2002b, Aron et

al., 2007a, King et al., 2012). Signaling through this pathway is in an ideal position to bring about rapid stopping. STN excitation leads to excitation of GABA-ergic neurons in the basal ganglia's output nuclei, the internal globus pallidus (GPi). These GABA-ergic neurons in turn inhibit the thalamus, quickly reducing thalamic excitation on the cortex (Nambu et al., 2002b).

A number of considerations support the STN's role in response inhibition. Functional imaging evidence shows that the STN, like the rIFG, activates on successful stopping, that the two regions are highly correlated with one another, and moreover, that the degree of STN activation correlates to faster SSRT (Aron and Poldrack, 2006). White matter tract strength between the cortex and the STN, determined using diffusion tensor imaging, also correlates with faster stopping (Coxon et al., 2012, King et al., 2012) STN lesions in rats also lead to lower stopping accuracy (Eagle et al., 2008b). In addition, signaling through the STN in known to be aberrant in Parkinson's disease patients, who are also impaired in response inhibition (Gauggel et al., 2004, Obeso et al., 2011). Local field potential recordings in Parkinson's patients undergoing Deep Brain Stimulation (DBS) show that STN oscillatory activity responds to stopping behavior (Ray et al., 2012). Stimulation of the STN using leads to improvements in SSRT (van den Wildenberg et al., 2006, Swann et al., 2011, Mirabella et al., 2012), though only if baseline (off-stimulation) SSRT was elevated compared to controls (Ray et al., 2009).

However, Hyperdirect Pathway signaling when stopping rapidly may lead to side effects of nonspecific involvement of unrelated motor regions. The STN is known to have diffuse excitatory projections over the GPi (Parent and Hazrati, 1995a, b, Mink, 1996, Gillies

and Willshaw, 1998), and these could lead to a suppression of thalamo-cortical drive not only for the motor effector that is stopping, but also unrelated stopping. As a possible consequence of this, stopping the hands in a basic stop-signal paradigm has been shown to lead to a reduction in the cortico-motor excitability of the task irrelevant leg, as assessed through single-pulse transcranial magnetic stimulation as probing tool (Badry et al., 2009). Likewise, the task irrelevant hand is suppressed when either stopping a vocal response (Cai et al., 2012) or an eye saccade (Wessel et al., *under review*).

Alternatives to nonselective Hyperdirect Stopping

Despite the converging evidence implicating Hyperdirect Pathway signaling in basic stopping, the broad motor side effects of this pathway raise major questions as to whether this is the only pathway by which to stop, a notion first raised in observations of EEG data (De Jong et al., 1995). As everyday life often requires stopping in the context of other ongoing actions, an alternative (selective) mechanism for stopping may be likely.

One such alternative may be the basal ganglia's pathways classical Indirect Pathway, which, like the Hyperdirect Pathway, also has an overall inhibitory effect on the thalamus (Mink, 1996, Nambu et al., 2002b). The Indirect Pathway signals through the basal ganglia's main input nucleus, the striatum, which is composed of the caudate, putamen, and nucleus accumbens. Here the striatal medium spiny neurons of the Indirect Pathway receive both primary input from the cortex and modulatory input from dopaminergic projections synapsing onto D2 receptors (Gerfen et al., 1990, DeLong and Wichmann, 2007). These striatal neurons then send inhibitory GABA-ergic projections onto other inhibitory neurons

in the external globus pallidus (GPe), which in turn reduces the inhibition on the GPi. Thus like the Hyperdirect Pathway, the Indirect Pathway's overall effect is to increase GPi inhibition on thalamo-cortical drive (Mink, 1996). In contrast to the Hyperdirect Pathway, however, the striatally-mediated Indirect Pathway is believed to have the anatomical specificity to allow for selective response inhibition (Nambu et al., 2002a).

The differences between the Hyperdirect and Indirect Pathways above raise some predictions that may help in dissociating stopping through these pathways. For instance, whereas stopping using the Hyperdirect Pathway leads to widespread suppression, affecting task irrelevant effectors, this may not occur in stopping using the Indirect Pathway. Furthermore Hyperdirect pathway-mediated stopping would bypass the striatum, whereas the striatum would likely be implicated in Indirect pathway-mediated stopping.

Importance of the striatum in response inhibition

Many studies have implicated a role for the striatum in various forms of stopping, consistent with the hypothesis that the Indirect Pathway may be involved. For instance, a number of human functional imaging studies have shown greater striatal activation with the increasing probability that a stop signal may occur (Vink et al., 2005, Jahfari et al., 2010, Zandbelt and Vink, 2010), suggesting the striatum may play more of a preparatory role. Other studies report that faster stopping is associated with greater striatal activity (Li et al., 2008b) and greater functional connectivity between the cortex and striatum (Jahfari et al., 2011).

Behavioral studies in animal models further support the importance of the striatum in stopping. For instance, lesions of the dorsomedial striatum in rodents lead to deficits in inhibitory control including prolonged SSRT. Although these inhibitory control deficits however were coupled with a greater number of Go errors and longer Go RT (Eagle and Robbins, 2003), this could be due to the nonspecific effects on lesioning on the striatal Direct Pathway and may be clarified by a more specific targeting of these pathways, to be discussed below. Additionally single-cell electrophysiology recordings in rodents performing a stopping task show that the medium spiny neurons in the striatum encode a NoGo signal that peaks when rats successfully stop (and diminishes when rats fail to stop) (Bryden et al., 2012). Likewise, primate electrophysiology also identifies striatal cells that respond selectively to another form of response inhibition in the Anti-saccade task. Here a monkey must immediately look *away* form a cued stimulus – which requires inhibition of the prepotent tendency to look *to* the cued stimulus (Ford and Everling, 2009, Watanabe and Munoz, 2010).

Note that dopaminergic signaling through the D2 pathway has long been associated with Indirect Pathway signaling in the striatum (Gerfen et al., 1990, DeLong and Wichmann, 2007). Accordingly, manipulation of D2 receptor signaling in rodents using receptor-specific drugs play contrasting roles in stop-signal behavior (Pattij et al., 2007, Eagle et al., 2011). In particular, blocking the D1 pathway lead to specific reductions in SSRT, whereas blocking the D2 pathway lead to increases in SSRT (Eagle et al., 2011). More precise methods of D2 manipulation, by use of optogenetics in mice to selectively activate cells in the D2 pathway,

lead to no-go behavior (inhibition), punishment, and aversion (Kravitz et al., 2010, Kravitz et al., 2012).

Huntington's disease as a model for striatal impairments

As the above work in animal models of response control suggests, damage to the striatum in humans may lead to specific effects in Indirect Pathway mediated stopping (whereas Hyperdirect Pathway mediated stopping may remain intact). Such a possibility raises interesting questions about specific behavioral deficits in Huntington's disease (HD), where there is selective neurodegeneration of the striatum, especially in the early stages of the disease (Reiner et al., 1988, Albin et al., 1992, Storey and Beal, 1993).

Huntington's disease is autosomal dominant genetic disorder arising from an expansion of trinucleotide repeat sequence in the fourth chromosome. This leads to a mutant protein with a lengthened polyglutamate tail, greater than 36 repeats (MacDonald et al., 1993). Although it is not fully known how this mutant protein eventually leads to neurological cell death, the length of the polyglutamate expansion does scale with the degree of neurological severity and the earlier onset of the disease (Snell et al., 1993, Aylward et al., 1996, Penney et al., 1997, Langbehn et al., 2004). At its earliest stages, HD predominantly affects the medium spiny neurons of the striatum (Graveland et al., 1985, Halliday et al., 1998). This significant cell loss in the striatum also begins long before the clinical onset of the disease, at which 50% of striatal volume is already lost when compared to non-diseased controls (Aylward et al., 1996, Aylward et al., 2004).

Notably, even the progression of HD damage of striatal medium spiny neurons is believed to be specific. The key motor symptoms of HD, uncontrolled writhing movements known as *chorea,* are believed to be specifically due to a loss of inhibitory signaling in the striatum, namely cells of the abovementioned Indirect Pathway. Thus early HD may serve as a selective *Indirect Pathway* lesion model (Reiner et al., 1988, Albin et al., 1992, Storey and Beal, 1993). This may particularly be the case in the *premanifest* stage of the disease (preHD) when, despite the absence of open symptoms, cross-sectional volumetric reductions compared to controls have been identified (Thieben et al., 2002, Kipps et al., 2005, Rosas et al., 2005, Hobbs et al., 2009, Stoffers et al., 2010).

HD impairments in fronto-striatal signaling, possibly implicating the Indirect Pathway, may directly lead to cognitive deficits (Ho et al., 2003). For example, reductions in D2 binding in PET studies (a possible marker for the Indirect Pathway) correlates with greater impairments in executive function (Lawrence et al., 1998a). Huntington's patients also seem to specific impairments in attentional set shifting, semantic verbal fluency (Lawrence et al., 1998b), task set switching (Aron et al., 2003d), inhibition of subliminally primed responses (Aron et al., 2003c), and saccade control (Leigh et al., 1983, Lasker et al., 1987). Such response control impairments are highly suggestive of roles of the Indirect Pathway in response control.

Overview of the dissertation

In Chapter 1, I will show that while simple stopping has global effects, stopping that requires more behavioral selectivity does not. Based on much work that implicates the

Hyperdirect Pathway in simple stopping, I argue that these findings are highly suggestive of the existence of an alternative pathway involved in behaviorally selective stopping.

In Chapter 2 and 3, I show that individuals with premanifest Huntington's disease have specific longitudinal atrophy in specific basal ganglia nuclei, such as the striatum and globus pallidus. In addition to establishing useful clinical biomarkers by which to treat Huntington's disease, the work further reaffirms premanifest Huntington's disease as a useful striatal lesion model for further behavioral investigation in Huntington's disease.

In Chapter 4, I show that a key characteristic of selective stopping, that of proactive control in preparation for stopping, requires basal ganglia involvement. With single-pulse TMS and functional MRI, I show that healthy individuals who are better able to suppress a particular effector in advance of stopping have greater activation of the basal ganglia. Furthermore, the basal ganglia once again activates when selective stopping must occur outright. Consistent with the findings of Chapter 1, simple stopping shows no striatal involvement, neither in advance or at the time of stopping. Furthermore, premanifest Huntington's disease patients with atrophy in the striatum are unable to employ selective suppression in advance of stopping and are behaviorally impaired in stopping. Taken together, the work in this chapter highly suggests that the striatally-mediated Indirect Pathway is crucially involved in selective stopping and may be the alternative pathway hypothesized in Chapter 2.

Finally, in Chapter 5, I show evidence that suggests that one can *train* selective suppression, possibly the same phenomenon found to be driven by the basal ganglia in Chapter 5. I present a novel procedural method by which training can occur through trial-

by-trial feedback of corticomotor excitability. I discuss the neurological implications of this training and the possibility as to whether such training can lead to an overall behavioral benefit.

References

Albin R, Reiner A, Anderson K, Dure L, Handelin B, Balfour R, Whetsell W, Penney J, Young A (1992) Preferential loss of striato-external pallidal projection neurons in presymptomatic Huntington's disease. Ann Neurol 31:425-430.

Aron AR, Behrens TE, Smith S, Frank MJ, Poldrack RA (2007a) Triangulating a cognitive control network using diffusion-weighted magnetic resonance imaging (MRI) and functional MRI. J Neurosci 27:3743-3752.

Aron AR, Dowson JH, Sahakian BJ, Robbins TW (2003a) Methylphenidate improves response inhibition in adults with attention-deficit/hyperactivity disorder. Biol Psychiatry 54:1465-1468.

Aron AR, Durston S, Eagle DM, Logan GD, Stinear CM, Stuphorn V (2007b) Converging evidence for a fronto-basal-ganglia network for inhibitory control of action and cognition. J Neurosci 27:11860-11864.

Aron AR, Fletcher PC, Bullmore ET, Sahakian BJ, Robbins TW (2003b) Stop-signal inhibition disrupted by damage to right inferior frontal gyrus in humans. Nat Neurosci 6:115-116.

Aron AR, Poldrack RA (2006) Cortical and subcortical contributions to Stop signal response inhibition: role of the subthalamic nucleus. J Neurosci 26:2424-2433.

Aron AR, Schlaghecken F, Fletcher PC, Bullmore ET, Eimer M, Barker R, Sahakian BJ, Robbins TW (2003c) Inhibition of subliminally primed responses is mediated by the caudate and thalamus: evidence from functional MRI and Huntington's disease. Brain 126:713-723.

Aron AR, Verbruggen F (2008) Stop the presses: dissociating a selective from a global mechanism for stopping. Psychol Sci 19:1146-1153.

Aron AR, Watkins L, Sahakian BJ, Monsell S, Barker RA, Robbins TW (2003d) Task-set switching deficits in early-stage Huntington's disease: implications for basal ganglia function. J Cogn Neurosci 15:629-642.

Aylward EH, Codori AM, Barta PE, Pearlson GD, Harris GJ, Brandt J (1996) Basal ganglia volume and proximity to onset in presymptomatic Huntington disease. Arch Neurol 53:1293-1296.

Aylward EH, Sparks BF, Field KM, Yallapragada V, Shpritz BD, Rosenblatt A, Brandt J, Gourley LM, Liang K, Zhou H, Margolis RL, Ross CA (2004) Onset and rate of striatal atrophy in preclinical Huntington disease. Neurology 63:66-72.

Badry R, Mima T, Aso T, Nakatsuka M, Abe M, Fathi D, Foly N, Nagiub H, Nagamine T, Fukuyama H (2009) Suppression of human cortico-motoneuronal excitability during the Stop-signal task. Clin Neurophysiol 120:1717-1723.

Band GPH, van der Molen MW, Logan GD (2003) Horse-race model simulations of the stop-signal procedure. Acta Psychol (Amst) 112:105-142.

Bari A, Eagle DM, Mar AC, Robinson ES, Robbins TW (2009) Dissociable effects of noradrenaline, dopamine, and serotonin uptake blockade on stop task performance in rats. Psychopharmacology (Berl) 205:273-283.

Bedard AC, Nichols S, Barbosa JA, Schachar R, Logan GD, Tannock R (2002) The development of selective inhibitory control across the life span. Developmental neuropsychology 21:93-111.

Boucher L, Palmeri TJ, Logan GD, Schall JD (2007) Inhibitory control in mind and brain: an interactive race model of countermanding saccades. Psychol Rev 114:376-397.

Bryden DW, Burton AC, Kashtelyan V, Barnett BR, Roesch MR (2012) Response inhibition signals and miscoding of direction in dorsomedial striatum. Front Integr Neurosci 6:69.

Bunge SA, Dudukovic NM, Thomason ME, Vaidya CJ, Gabrieli JD (2002) Immature frontal lobe contributions to cognitive control in children: evidence from fMRI. Neuron 33:301-311.

Cai W, Oldenkamp C, Aron AR (2011) A proactive mechanism for selective suppression of response tendencies. J Neurosci 31:5965-5969.

Cai W, Oldenkamp CL, Aron AR (2012) Stopping speech suppresses the task-irrelevant hand. Brain Lang 120:412-415.

Carver AC, Livesey DJ, Charles M (2001) Age related changes in inhibitory control as measured by stop signal task performance. The International journal of neuroscience 107:43-61.

Chamberlain SR, Fineberg NA, Blackwell AD, Robbins TW, Sahakian BJ (2006a) Motor inhibition and cognitive flexibility in obsessive-compulsive disorder and trichotillomania. Am J Psychiatry 163:1282-1284.

Chamberlain SR, Muller U, Blackwell AD, Clark L, Robbins TW, Sahakian BJ (2006b) Neurochemical modulation of response inhibition and probabilistic learning in humans. Science 311:861-863.

Chambers CD, Bellgrove MA, Stokes MG, Henderson TR, Garavan H, Robertson IH, Morris AP, Mattingley JB (2006) Executive "brake failure" following deactivation of human frontal lobe. J Cogn Neurosci 18:444-455.

Chikazoe J, Konishi S, Asari T, Jimura K, Miyashita Y (2007) Activation of right inferior frontal gyrus during response inhibition across response modalities. J Cogn Neurosci 19:69-80.

Claffey MP, Sheldon S, Stinear CM, Verbruggen F, Aron AR (2010) Having a goal to stop action is associated with advance control of specific motor representations. Neuropsychologia 48:541-548.

Congdon E, Mumford JA, Cohen JR, Galvan A, Canli T, Poldrack RA (2012) Measurement and reliability of response inhibition. Front Psychol 3:37.

Coxon JP, Stinear CM, Byblow WD (2007) Selective inhibition of movement. J Neurophysiol 97:2480-2489.

Coxon JP, Van Impe A, Wenderoth N, Swinnen SP (2012) Aging and inhibitory control of action: cortico-subthalamic connection strength predicts stopping performance. J Neurosci 32:8401-8412.

De Jong R, Coles MG, Logan GD (1995) Strategies and mechanisms in nonselective and selective inhibitory motor control. J Exp Psychol Hum Percept Perform 21:498-511.

de Zubicaray GI, Andrew C, Zelaya FO, Williams SC, Dumanoir C (2000) Motor response suppression and the prepotent tendency to respond: a parametric fMRI study. Neuropsychologia 38:1280-1291.

DeLong MR, Wichmann T (2007) Circuits and circuit disorders of the basal ganglia. Arch Neurol 64:20-24.

Dowsett SM, Livesey DJ (2000) The development of inhibitory control in preschool children: effects of "executive skills" training. Developmental psychobiology 36:161-174.

Durston S, Thomas KM, Yang Y, Ulug AM, Zimmerman RD, Casey BJ (2002) A neural basis for the development of inhibitory control. Developmental science 5:F9-F16.

Eagle DM, Bari A, Robbins TW (2008a) The neuropsychopharmacology of action inhibition: cross-species translation of the stop-signal and go/no-go tasks. Psychopharmacology (Berl) 199:439-456.

Eagle DM, Baunez C, Hutcheson DM, Lehmann O, Shah AP, Robbins TW (2008b) Stop-signal reaction-time task performance: role of prefrontal cortex and subthalamic nucleus. Cereb Cortex 18:178-188.

Eagle DM, Robbins TW (2003) Inhibitory control in rats performing a stop-signal reaction-time task: effects of lesions of the medial striatum and d-amphetamine. Behavioral Neuroscience 117:1302-1317.

Eagle DM, Wong JC, Allan ME, Mar AC, Theobald DE, Robbins TW (2011) Contrasting roles for dopamine D1 and D2 receptor subtypes in the dorsomedial striatum but not the nucleus accumbens core during behavioral inhibition in the stop-signal task in rats. J Neurosci 31:7349-7356.

Ford KA, Everling S (2009) Neural activity in primate caudate nucleus associated with pro- and antisaccades. J Neurophysiol 102:2334-2341.

Garavan H, Ross TJ, Murphy K, Roche RA, Stein EA (2002) Dissociable executive functions in the dynamic control of behavior: inhibition, error detection, and correction. Neuroimage 17:1820-1829.

Garavan H, Ross TJ, Stein EA (1999) Right hemispheric dominance of inhibitory control: an event-related functional MRI study. Proc Natl Acad Sci U S A 96:8301-8306.

Gauggel S, Rieger M, Feghoff T-A (2004) Inhibition of ongoing responses in patients with Parkinson's disease. J Neurol Neurosurg Psychiatr 75:539-544.

Gerfen CR, Engber TM, Mahan LC, Susel Z, Chase TN, Monsma FJ, Jr., Sibley DR (1990) D1 and D2 dopamine receptor-regulated gene expression of striatonigral and striatopallidal neurons. Science 250:1429-1432.

Gillies AJ, Willshaw DJ (1998) A massively connected subthalamic nucleus leads to the generation of widespread pulses. Proc Biol Sci 265:2101-2109.

Graveland GA, Williams RS, DiFiglia M (1985) Evidence for degenerative and regenerative changes in neostriatal spiny neurons in Huntington's disease. Science 227:770-773.

Halliday GM, McRitchie DA, Macdonald V, Double KL, Trent RJ, McCusker E (1998) Regional specificity of brain atrophy in Huntington's disease. Exp Neurol 154:663-672.

Ho AK, Sahakian BJ, Brown RG, Barker RA, Hodges JR, Ane MN, Snowden J, Thompson J, Esmonde T, Gentry R, Moore JW, Bodner T, Consortium N-H (2003) Profile of cognitive progression in early Huntington's disease. Neurology 61:1702-1706.

Hobbs NZ, Henley SMD, Ridgway G, Wild EJ, Barker R, Scahill RI, Barnes J, Fox NC, Tabrizi S (2009) The Progression of Regional Atrophy in Premanifest and Early Huntington's Disease: A Longitudinal Voxel-Based Morphometry Study. J Neurol Neurosurg Psychiatr.

Inase M, Tokuno H, Nambu A, Akazawa T, Takada M (1999) Corticostriatal and corticosubthalamic input zones from the presupplementary motor area in the macaque monkey: comparison with the input zones from the supplementary motor area. Brain Res 833:191-201.

Jahfari S, Stinear CM, Claffey M, Verbruggen F, Aron AR (2010) Responding with restraint: what are the neurocognitive mechanisms? J Cogn Neurosci 22:1479-1492.

Jahfari S, Waldorp L, van den Wildenberg WP, Scholte HS, Ridderinkhof KR, Forstmann BU (2011) Effective connectivity reveals important roles for both the hyperdirect (fronto-subthalamic) and the indirect (fronto-striatal-pallidal) fronto-basal ganglia pathways during response inhibition. J Neurosci 31:6891-6899.

Kawashima R, Satoh K, Itoh H, Ono S, Furumoto S, Gotoh R, Koyama M, Yoshioka S, Takahashi T, Takahashi K, Yanagisawa T, Fukuda H (1996) Functional anatomy of GO/NO-GO discrimination and response selection--a PET study in man. Brain Res 728:79-89.

Keeler JF, Robbins TW (2011) Translating cognition from animals to humans. Biochemical pharmacology 81:1356-1366.

King AV, Linke J, Gass A, Hennerici MG, Tost H, Poupon C, Wessa M (2012) Microstructure of a three-way anatomical network predicts individual differences in response inhibition: a tractography study. Neuroimage 59:1949-1959.

Kipps CM, Duggins AJ, Mahant N, Gomes L, Ashburner J, McCusker EA (2005) Progression of structural neuropathology in preclinical Huntington's disease: a tensor based morphometry study. J Neurol Neurosurg Psychiatr 76:650-655.

Konishi S, Nakajima K, Uchida I, Kikyo H, Kameyama M, Miyashita Y (1999) Common inhibitory mechanism in human inferior prefrontal cortex revealed by event-related functional MRI. Brain 122 (Pt 5):981-991.

Konishi S, Nakajima K, Uchida I, Sekihara K, Miyashita Y (1998) No-go dominant brain activity in human inferior prefrontal cortex revealed by functional magnetic resonance imaging. Eur J Neurosci 10:1209-1213.

Kravitz AV, Freeze BS, Parker PR, Kay K, Thwin MT, Deisseroth K, Kreitzer AC (2010) Regulation of parkinsonian motor behaviours by optogenetic control of basal ganglia circuitry. Nature 466:622-626.

Kravitz AV, Tye LD, Kreitzer AC (2012) Distinct roles for direct and indirect pathway striatal neurons in reinforcement. Nat Neurosci 15:816-818.

Langbehn DR, Brinkman RR, Falush D, Paulsen JS, Hayden MR, Group IHsDC (2004) A new model for prediction of the age of onset and penetrance for Huntington's disease based on CAG length. Clin Genet 65:267-277.

Lasker AG, Zee DS, Hain TC, Folstein SE, Singer HS (1987) Saccades in Huntington's disease: initiation defects and distractibility. Neurology 37:364-370.

Lawrence AD, Hodges JR, Rosser AE, Kershaw A, ffrench-Constant C, Rubinsztein DC, Robbins TW, Sahakian BJ (1998a) Evidence for specific cognitive deficits in preclinical Huntington's disease. Brain 121 (Pt 7):1329-1341.

Lawrence AD, Sahakian BJ, Robbins TW (1998b) Cognitive functions and corticostriatal circuits: insights from Huntington's disease. Trends in Cognitive Science 2:379-388.

Lawrence AJ, Luty J, Bogdan NA, Sahakian BJ, Clark L (2009) Impulsivity and response inhibition in alcohol dependence and problem gambling. Psychopharmacology (Berl) 207:163-172.

Leigh RJ, Newman SA, Folstein SE, Lasker AG, Jensen BA (1983) Abnormal ocular motor control in Huntington's disease. Neurology 33:1268-1275.

Li CS, Huang C, Yan P, Bhagwagar Z, Milivojevic V, Sinha R (2008a) Neural correlates of impulse control during stop signal inhibition in cocaine-dependent men. Neuropsychopharmacology 33:1798-1806.

Li CS, Yan P, Sinha R, Lee TW (2008b) Subcortical processes of motor response inhibition during a stop signal task. Neuroimage 41:1352-1363.

Lijffijt M, Kenemans JL, Verbaten MN, van Engeland H (2005) A meta-analytic review of stopping performance in attention-deficit/hyperactivity disorder: deficient inhibitory motor control? Journal of abnormal psychology 114:216-222.

Logan GD, Cowan WB (1984) On the ability to inhibit thought and action: a theory of an act of control. Psychol Rev 91:295-327.

Logan GD, Cowan WB, Davis KA (1984) On the ability to inhibit simple and choice reaction time responses: a model and a method. J Exp Psychol Hum Percept Perform 10:276-291.

Macdonald H, Stinear CM, Byblow WD (2012) Uncoupling Response Inhibition. J Neurophysiol.

MacDonald ME, Ambrose CM, Duyao MP, Myers RH, Lin C, Srinidhi L, Barnes G, al. e (1993) A novel gene containing a trinucleotide repeat that is expanded and unstable on Huntington's disease chromosomes. Cell 72:971-983.

Madsen KS, Baaré WFC, Vestergaard M, Skimminge A, Ejersbo LR, Ramsøy TZ, Gerlach C, Akeson P, Paulson OB, Jernigan TL (2010) Response inhibition is associated with white matter microstructure in children. Neuropsychologia 48:854-862.

Menon V, Adleman NE, White CD, Glover GH, Reiss AL (2001) Error-related brain activation during a Go/NoGo response inhibition task. Hum Brain Mapp 12:131-143.

Menzies L, Achard S, Chamberlain SR, Fineberg N, Chen C-H, del Campo N, Sahakian BJ, Robbins TW, Bullmore E (2007) Neurocognitive endophenotypes of obsessive-compulsive disorder. Brain 130:3223-3236.

Mink JW (1996) The basal ganglia: focused selection and inhibition of competing motor programs. Prog Neurobiol 50:381-425.

Mirabella G, Iaconelli S, Romanelli P, Modugno N, Lena F, Manfredi M, Cantore G (2012) Deep brain stimulation of subthalamic nuclei affects arm response inhibition in Parkinson's patients. Cereb Cortex 22:1124-1132.

Monterosso JR, Aron AR, Cordova X, Xu J, London ED (2005) Deficits in response inhibition associated with chronic methamphetamine abuse. Drug and alcohol dependence 79:273-277.

Morein-Zamir S, Craig KJ, Ersche KD, Abbott S, Muller U, Fineberg NA, Bullmore ET, Sahakian BJ, Robbins TW (2010) Impaired visuospatial associative memory and attention in obsessive compulsive disorder but no evidence for differential dopaminergic modulation. Psychopharmacology 212:357-367.

Murphy P (2002) Inhibitory control in adults with Attention-Deficit/Hyperactivity Disorder. Journal of attention disorders 6:1-4.

Nambu A, Kaneda K, Tokuno H, Takada M (2002a) Organization of corticostriatal motor inputs in monkey putamen. J Neurophysiol 88:1830-1842.

Nambu A, Tokuno H, Inase M, Takada M (1997) Corticosubthalamic input zones from forelimb representations of the dorsal and ventral divisions of the premotor cortex in the macaque monkey: comparison with the input zones from the primary motor cortex and the supplementary motor area. Neurosci Lett 239:13-16.

Nambu A, Tokuno H, Takada M (2002b) Functional significance of the cortico-subthalamo-pallidal 'hyperdirect' pathway. Neurosci Res 43:111-117.

Obeso I, Wilkinson L, Casabona E, Bringas ML, Alvarez M, Alvarez L, Pavon N, Rodriguez-Oroz MC, Macias R, Obeso JA, Jahanshahi M (2011) Deficits in inhibitory control and

conflict resolution on cognitive and motor tasks in Parkinson's disease. Exp Brain Res 212:371-384.

Parent A, Hazrati LN (1995a) Functional anatomy of the basal ganglia. I. The cortico-basal ganglia-thalamo-cortical loop. Brain research Brain research reviews 20:91-127.

Parent A, Hazrati LN (1995b) Functional anatomy of the basal ganglia. II. The place of subthalamic nucleus and external pallidum in basal ganglia circuitry. Brain research Brain research reviews 20:128-154.

Pattij T, Janssen MC, Vanderschuren LJ, Schoffelmeer AN, van Gaalen MM (2007) Involvement of dopamine D1 and D2 receptors in the nucleus accumbens core and shell in inhibitory response control. Psychopharmacology (Berl) 191:587-598.

Penney JB, Jr., Vonsattel JP, MacDonald ME, Gusella JF, Myers RH (1997) CAG repeat number governs the development rate of pathology in Huntington's disease. Ann Neurol 41:689-692.

Pliszka SR, Liotti M, Woldorff MG (2000) Inhibitory control in children with attention-deficit/hyperactivity disorder: event-related potentials identify the processing component and timing of an impaired right-frontal response-inhibition mechanism. Biol Psychiatry 48:238-246.

Ray NJ, Brittain JS, Holland P, Joundi RA, Stein JF, Aziz TZ, Jenkinson N (2012) The role of the subthalamic nucleus in response inhibition: evidence from local field potential recordings in the human subthalamic nucleus. Neuroimage 60:271-278.

Ray NJ, Jenkinson N, Brittain J, Holland P, Joint C, Nandi D, Bain PG, Yousif N, Green A, Stein JS, Aziz TZ (2009) The role of the subthalamic nucleus in response inhibition: evidence from deep brain stimulation for Parkinson's disease. Neuropsychologia 47:2828-2834.

Reiner A, Albin RL, Anderson KD, D'Amato CJ, Penney JB, Young AB (1988) Differential loss of striatal projection neurons in Huntington disease. Proc Natl Acad Sci U S A 85:5733-5737.

Robinson ES, Eagle DM, Mar AC, Bari A, Banerjee G, Jiang X, Dalley JW, Robbins TW (2008) Similar effects of the selective noradrenaline reuptake inhibitor atomoxetine on three distinct forms of impulsivity in the rat. Neuropsychopharmacology 33:1028-1037.

Rosas HD, Hevelone ND, Zaleta AK, Greve DN, Salat DH, Fischl B (2005) Regional cortical thinning in preclinical Huntington disease and its relationship to cognition. Neurology 65:745-747.

Rubia K, Russell T, Overmeyer S, Brammer MJ, Bullmore ET, Sharma T, Simmons A, Williams SC, Giampietro V, Andrew CM, Taylor E (2001) Mapping motor inhibition: conjunctive brain activations across different versions of go/no-go and stop tasks. Neuroimage 13:250-261.

Rubia K, Smith AB, Brammer MJ, Taylor E (2003) Right inferior prefrontal cortex mediates response inhibition while mesial prefrontal cortex is responsible for error detection. Neuroimage 20:351-358.

Scangos KW, Stuphorn V (2010) Medial frontal cortex motivates but does not control movement initiation in the countermanding task. J Neurosci 30:1968-1982.

Schmajuk M, Liotti M, Busse L, Woldorff MG (2006) Electrophysiological activity underlying inhibitory control processes in normal adults. Neuropsychologia 44:384-395.

Snell RG, MacMillan JC, Cheadle JP, Fenton I, Lazarou LP, Davies P, MacDonald ME, Gusella JF, Harper PS, Shaw DJ (1993) Relationship between trinucleotide repeat expansion and phenotypic variation in Huntington's disease. Nat Genet 4:393-397.

Soreni N, Crosbie J, Ickowicz A, Schachar R (2009) Stop signal and Conners' continuous performance tasks: test--retest reliability of two inhibition measures in ADHD children. Journal of attention disorders 13:137-143.

Stoffers D, Sheldon S, Kuperman JM, Goldstein J, Corey-Bloom J, Aron AR (2010) Contrasting gray and white matter changes in preclinical Huntington disease: an MRI study. Neurology 74:1208-1216.

Storey E, Beal MF (1993) Neurochemical substrates of rigidity and chorea in Huntington's disease. Brain 116 (Pt 5):1201-1222.

Swann N, Poizner H, Houser M, Gould S, Greenhouse I, Cai W, Strunk J, George J, Aron AR (2011) Deep brain stimulation of the subthalamic nucleus alters the cortical profile of response inhibition in the beta frequency band: a scalp EEG study in Parkinson's disease. J Neurosci 31:5721-5729.

Thieben MJ, Duggins AJ, Good CD, Gomes L, Mahant N, Richards F, McCusker E, Frackowiak RSJ (2002) The distribution of structural neuropathology in pre-clinical Huntington's disease. Brain 125:1815-1828.

van den Wildenberg WP, van Boxtel GJ, van der Molen MW, Bosch DA, Speelman JD, Brunia CH (2006) Stimulation of the subthalamic region facilitates the selection and inhibition of motor responses in Parkinson's disease. J Cogn Neurosci 18:626-636.

van den Wildenberg WP, van der Molen MW (2004) Developmental trends in simple and selective inhibition of compatible and incompatible responses. Journal of experimental child psychology 87:201-220.

Verbruggen F, Logan GD (2009) Models of response inhibition in the stop-signal and stop-change paradigms. Neurosci Biobehav Rev 33:647-661.

Vink M, Kahn RS, Raemaekers M, van den Heuvel M, Boersma M, Ramsey NF (2005) Function of striatum beyond inhibition and execution of motor responses. Hum Brain Mapp 25:336-344.

Vink M, Ramsey NF, Raemaekers M, Kahn RS (2006) Striatal dysfunction in schizophrenia and unaffected relatives. Biol Psychiatry 60:32-39.

Watanabe M, Munoz DP (2010) Saccade suppression by electrical microstimulation in monkey caudate nucleus. J Neurosci 30:2700-2709.

Wessel J, Reynoso HS, Aron AR (*under review*) Stopping eye movements has global motor effects.

Williams BR, Ponesse JS, Schachar RJ, Logan GD, Tannock R (1999) Development of inhibitory control across the life span. Developmental psychology 35:205-213.

Zandbelt BB, Vink M (2010) On the role of the striatum in response inhibition. PLoS ONE 5:e13848.

CHAPTER 1

Transcranial Magnetic Stimulation reveals dissociable mechanisms for global versus selective corticomotor suppression underlying the stopping of action

ABSTRACT

Stopping an initiated response is an essential function, investigated in many studies with go/no-go and stop-signal paradigms. These standard tests require rapid action cancellation. This appears to be achieved by a suppression mechanism that has 'global' effects on corticomotor excitability (i.e. affecting task-irrelevant muscles). By contrast, stopping action in everyday life may require selectivity (i.e. targeting a specific response tendency without affecting concurrent action). We hypothesized that while standard stopping engages global suppression, behaviorally selective stopping engages a selective suppression mechanism. Accordingly, we measured corticomotor excitability of the task-irrelevant leg using Transcranial Magnetic Stimulation (TMS) while subjects stopped the hand. Experiment 1 showed that for standard (i.e. nonselective) stopping, the task-irrelevant leg was suppressed. Experiment 2 showed that for behaviorally selective stopping, there was no mean leg suppression. Experiment 3 directly compared behaviorally nonselective and selective stopping. Leg suppression occurred only in the behaviorally nonselective condition. These results argue that global and selective suppression mechanisms are dissociable. Participants may use a global suppression mechanism when speed is stressed; however, they may recruit a more selective suppression mechanism when selective stopping is behaviorally necessary and preparatory information is available. We

predict that different fronto-basal-ganglia pathways underpin these different suppression mechanisms.

INTRODUCTION

The ability to stop is essential in every day life. For example, one must immediately stop an impending movement to step into the street when a car suddenly appears. Experimentally, this behavior has been operationalized using stop-signal and go/no-go tasks. These require participants to try to quickly stop a response whenever a signal occurs (reviewed by Verbruggen and Logan, 2009). As these paradigms typically require rapid action control, it is likely that human subjects use the easiest and fastest suppression mechanism available. By contrast, everyday life often requires behavioral stopping that is selective to a particular tendency. This could engage a selective rather than global suppression mechanism. Here we aimed to dissociate these putative stopping mechanisms physiologically using single-pulse Transcranial Magnetic Stimulation (TMS).

Evidence for a fast suppression mechanism that has widespread effects on the motor system comes from both behavioral and TMS studies. In one behavioral study, participants initiated two responses together on each trial and then, whenever an infrequent signal occurred, tried to stop one response while continuing with the other (Coxon et al., 2007). It was found that the movement of the continuing hand was severely delayed, possibly due to a widespread suppression of motor tendencies that also affected the continuing hand. This interpretation is supported by TMS, which can probe the corticomotor excitability of both task-relevant and -irrelevant muscles. Several studies have

shown that stopping a particular manual response suppresses not only the task-relevant muscle but also the task-irrelevant muscles of the same hand (Leocani et al., 2000, Sohn et al., 2002, Coxon et al., 2006, van den Wildenberg et al., 2010a), the homologous muscles of the opposite hand (Coxon et al., 2006, Badry et al., 2009), and, most impressively, the task-irrelevant leg (Badry et al., 2009). Here we refer to this widespread effect over task-irrelevant muscles as 'global' suppression. At the neural systems level, it is possible that this global suppressive effect arises from recruitment of the subthalamic nucleus (STN) of the basal ganglia [via the "hyperdirect signaling pathway" from the cortex]. Imaging, lesion, and neurophysiology implicate the STN in standard forms of stopping (reviewed by Eagle and Baunez, 2010), and the STN sends a broad output to the pallidum that is thought to have widespread effects on the motor system by reducing thalamocortical drive (Mink, 1996, Gillies and Willshaw, 1998, Nambu et al., 2002).

Yet many everyday situations call for the selective stopping of a particular response. It seems unlikely that this is achieved using the abovementioned global suppression mechanism. For example, it is possible to continue speaking even while one stops an initiated manual movement, and it is possible to keep walking even while one cancels the tendency to say something. Moreover, skilled tasks such as playing music or sports often require selective, often independent, control of one's hands and feet. For example, an American football player can continue running even as he cancels a throw of the ball. Thus, the suppression used in all these cases could engage a mechanism that is selectively targeted at a particular response tendency rather than one that is generally targeted at many muscle representations.

Using a novel behavioral paradigm, we attained preliminary evidence that global and selective mechanisms for stopping are dissociable (Aron and Verbruggen, 2008, Claffey et al., 2010). We adapted the method mentioned above, where two responses are initiated on each trial and where one must be stopped whenever a signal occurs while the other is quickly continued. The reaction time delay to continue this other response on stop trials was taken as a measure of the selectivity of stopping. A key innovation in these recent studies was that in one condition, participants were cued in advance about which response to stop (e.g. "Maybe Stop Left"), while, in the other condition, no cue was given. By cuing people in advance, we encouraged them to engage behaviorally selective stopping because they could prepare which response to stop. Consequently, stopping was indeed more selective but also slower relative to the case when advanced information was not given. We interpreted these findings as indicating different neural pathways for stopping – a selective system that is slower (perhaps because it uses more synapses) vs. a global system that is faster (perhaps on account of the hyperdirect signaling pathway). Here we aimed to dissociate these putative stopping mechanisms physiologically using TMS.

Our key assumption was that if a global suppression mechanism is used to stop the hand, there would be observable suppression of the task-irrelevant leg (cf. Badry et al., 2009). By contrast, if a selective suppression mechanism is used to stop the hand, there would be no leg suppression. We tested these predictions in a series of experiments using TMS to probe the cortico-motor excitability of the task-irrelevant leg while subjects stopped the hand in conditions that did or did not emphasize behavioral selectivity. In Experiment 1 (Figure 1.1A), we aimed to replicate the earlier observation (Badry et al., 2009) that

stopping the hand in a standard stop signal task leads to suppression of the leg. In Experiment 2 (Figure 1.1B), we used a task that emphasized behaviorally selective stopping (cf. Aron and Verbruggen, 2008, Claffey et al., 2010, Cai et al., 2011). We predicted less leg suppression than in Experiment 1. In Experiment 3 (Figure 1.1C), we intermixed trials requiring selective behavioral stopping (stopping one hand, continuing with the other) and nonselective stopping (stopping both hands). Again, we predicted less leg suppression for the selective compared to nonselective case.

METHODS

Participants

There were 25 participants in total (Experiment 1: 7 total, 4 females, mean age, 20.6 ± 1.6 years, all right handed; Experiment 2: 7 total, three females, mean age, 20.7 ± 2.7 years, six right handed; Experiment 3: 11 total, six females, mean age, 21.91 ± 1.8 years, all right-handed). All participants provided written consent in accordance with the Institutional Review Board guidelines of the University of California, San Diego. They also completed a TMS safety-screening questionnaire based on recommendations from the International Workshop on the Safety of Repetitive TMS (Wassermann, 1998). This questionnaire excluded any neurological or psychiatric disorder.

EMG recording preparation

Surface electromyography (EMG) recordings were obtained from the Tibialis Anterior (TA) muscle of both legs using pairs of 10mm silver electrodes. This muscle is

responsible for dorsoflexion of the foot and was completely irrelevant for the behavioral task. A ground electrode was placed over the lateral malleoli (outer ankle protuberance) of both legs.

A Grass QP511 Quad AC Amplifier System (Glass Technologies, West Warwick, RI) amplified the EMG signal using a 30Hz to 1kHz band-pass filter and a 60Hz notch filter. A CED Micro 1401 mk II acquisition system sampled the data at a frequency of 2kHz. The data from both legs were displayed in two channels and recorded using CED Signal v4 (Cambridge Electronic Design, Cambridge, UK).

TMS preparation

TMS was delivered with a MagStim 200-2 system (Magstim, Whitland, UK) and a batwing coil; type no. 15411. The study began with a thresholding procedure. Participants were seated comfortably with heels placed on the floor and toes raised 5cm upon a platform. This leg arrangement increased the likelihood of obtaining a motor-evoked potential (MEP) in the TA muscles. The coil was initially placed over the vertex of the head (midline and halfway between the nasion and the inion), approximately close to the midline M1 representations of the TA muscles. With single-pulse stimulation, the TMS coil was incrementally re-positioned to elicit a maximal response in whichever of the two TA muscles that was most easily stimulated. Participants were requested to slightly activate their legs in order to increase the likelihood of finding the TA motor hotspot. This location averaged about 1cm laterally over the right motor cortex in 22 participants (stimulating the left leg) and the left motor cortex in 3 participants (stimulating the right leg – note this was only in

Experiment 1). After this location was identified and marked, the participant was asked to rest. The lowest stimulation intensity required to elicit MEP amplitudes of at least 0.05mV in at least 5 out of 10 trials was determined as the resting motor threshold (RMT). The stimulation intensity for each subject in each experiment was approximately 110% of the RMT (Table 1.1 and 1.2). This level elicited consistent responses between 0.05mV and 0.2mV.

Experiment 1

Behavioral task

The behavioral task (see Figure 1.1A) was a standard, nonselective stopping paradigm based on Badry et al. (2009). Participants placed left and right index fingers on the "Z" and "/" keys of a standard keyboard. Stimuli were presented on an iMac (19 in. monitor). Each trial began with a yellow fixation "+" for 500ms. This then disappeared, leaving a blank (black) screen for 500ms. An imperative Go signal, an arrow, was then presented. This pointed to the left or right with equal frequency ("<" or ">"), cueing the participant to respond with either the left or right index finger. On Go trials (67% of all trials), this arrow cue remained either until the participant made a response or for a maximum of 900ms. On Stop trials (33% of all trials), a red square stop signal appeared over the arrow after a short delay and remained for the duration of the trial. In the inter-trial interval (ITI), a white fixation "+" was presented for 4 to 6 seconds (mean 5.1 seconds). There were 5 blocks of 105 trials each (70 Go trials and 35 Stop trials). The first block was practice without TMS.

The time interval between the Go signal (the arrow) and the Stop signal (the red square) is known as the stop signal delay (SSD). This was varied dynamically throughout the experiment depending on the subject's performance. The SSD increased by 50ms with every successful stop and decreased by 50ms with every failed stop, leading to an overall stopping probability of approximately 50%. This converging 'tracking' method is optimal for calculating the stop signal reaction time (SSRT, see below) (Band et al., 2003). Two separate SSD staircases were used for left and right hand response trials. SSD values began at 150ms for both staircases.

TMS Delivery

TMS was delivered either during the response period (on 90 of the 105 trials, 60 Go trials and 30 Stop trials) or during the inter-trial interval (before 15 of the 105 trials, 10 Go trials and 5 Stop trials). For the response period, stimulation occurred 100 ms before the mean Go reaction time (RT) of the practice session (GoRT–100ms) (based on Badry et al., 2009). For the inter-trial interval, stimulation occurred 300ms before the onset of the next trial (i.e. before the yellow fixation).

Experiment 2

Behavioral Task

The behavioral task (see Figure 1.1B) was a selective stopping paradigm based on Aron and Verbruggen (2008). Participants placed the index and little fingers of each hand on a standard keyboard (left hand: little finger on "Z" and index on "V"; right hand: index on

"M" and little finger on "/"). Each experimental trial began with a cue ("Maybe Stop Right" or "Maybe Stop Left") written in white text on a black background for 1 sec. The cue then disappeared leaving a blank (black) screen for 1 sec.

An imperative Go stimulus, four horizontally arranged circles, was then presented. Two of the circles on each trial, either the two inner circles or the two outer circles, were colored blue whereas the other two were colored gray. The circles were 2.3° visual angles in diameter. The two inner circles were separated from each other by a 4.6° visual angle and from the two outer circles by a 1.2° visual angle. If the two inner circles were blue, participants responded with both index fingers simultaneously, whereas if the outer circles were blue, participants responded with both little fingers. Inner (index) and outer (little) finger responses were equiprobable. Failure to respond with both hands simultaneously (defined as a difference > 70 ms) resulted in a textual "Decoupled" warning presented for 2 secs.

On Go trials (69% of all trials), the circles remained until either the participant made a response or for a maximum of 1 sec. On stop trials (31% of all trials), a red "X" appeared in the center of the screen (between the inner circles) after a short delay (the SSD) and remained until the end of the trial. Participants were required to stop the response of the hand previously cued in the beginning of the trial (e.g. "Maybe Stop Left") while quickly continuing with the other hand.

An ITI blank screen lasted for 2 to 4 secs (mean 2.6 secs). Each block consisted of 78 trials (54 Go trials and 24 Stop trials). Participants took part in either four or five total blocks

of the experiment proper as well as a single practice block without TMS. SSDs varied dynamically as in Experiment 1.

TMS Delivery

TMS was delivered during the response period (on 72 of the 78 trials, 48 Go trials and 24 Stop trials) or during the inter-trial interval (before the 6 remaining Go trials). As in Experiment 1, stimulation onset was set at practice GoRT–100ms. For the inter-trial interval, stimulation was delivered 300ms before the onset of the next trial. Since ITI stimulation was informative as to the subsequent trial type, these trials were excluded from the behavioral analysis.

Experiment 3

Behavioral Task

This was a modification of the task used in Experiment 2 with a key difference (see Figure 1.1C). In order to test the effects of nonselective stopping in the same design as selective stopping, a third stopping cue, “Maybe Stop Both,” was used in addition to the original two (“Maybe Stop Right” and “Maybe Stop Left”). On “Maybe Stop Both” trials, subjects were required to stop both fingers if a stop signal occurred. The Nonselective “Both” cue was presented on 50% of all trials, whereas the Selective “Left” and “Right” cues were presented with equal frequency on the other 50% of trials. The experiment was otherwise similar to Experiment 2 except that the stop signal probability was 33%, the blank

screen after the cue was 500ms long, the ITI blank screen was 1.5 sec long, and there were trials with and without TMS.

The entire experiment was a maximum of 816 trials long (408 Nonselective and 408 Selective trials), with trial types pseudo-randomized throughout. Participants completed from 8 to a maximum of 16 blocks (mean = 13) within the allotted time. Each block had 51 trials.

SSD varied dynamically as before. Trials had independent SSD staircases based on which of the three stopping cues preceded them and whether TMS was delivered during the trial or not (see below for details). This led to a total of 6 independent SSD staircases.

TMS Delivery

Of the 816 total trials possible, TMS was delivered during the response period on 66% of trials (540 total, 270 Nonselective and 270 Selective). Stimulation was also delivered in the inter-trial interval 200ms before the presentation of the cue in 4% of trials (36 total, 18 Nonselective and 18 Selective). No TMS was delivered in the remaining 30% of trials (240 total, 120 Nonselective and 120 Selective). This preserved a subset of trials without TMS delivery that were used to accurately estimate SSRT. As the estimates for SSRT were discovered to be very similar to the TMS trials, these non-TMS trials are not further analyzed or discussed.

On Stop trials, stimulation was delivered at either 200, 220, or 240ms after the stop signal (60 total at each interval, 30 Nonselective and 30 Selective). On Go trials, stimuli were

delivered in a yoked fashion, i.e. relative to the timing on Stop trials in the respective Nonselective or Selective condition (120 at each interval, 60 Nonselective and 60 Selective).

Behavioral Indices

For Experiment 1, the following indices were calculated: Accuracy of Go trials; Probability of stopping; RT on Go trials, i.e. the mean correct Go RT; Mean SSD; and SSRT. For this and the other experiments, SSRT was calculated using the Integration method (see Verbruggen and Logan, 2009). The two SSD values with the greatest number of trials and a stopping probability between 40% and 60% were determined. For each of these, the failed stop rate was calculated and used to determine the corresponding point in the rank-ordered distribution of Go trials. SSRT was then estimated by subtracting SSD from this Go RT value. The two SSRTs were then averaged.

Some additional indices were also calculated for Experiment 2 and 3. These were: the direction error rate, i.e. how often the subject stopped the wrong hand on stop trials; RT of the alternative response, i.e. the mean RT of the continuing hand on correct stop trials; and the Stopping Interference Effect, i.e. the difference between the alternative response RT and the mean correct Go RT (see Aron and Verbruggen, 2008).

MEP analysis

MEP analysis involved amplitude calculation, trial rejection, trimming, and averaging within condition. An auxiliary analysis examined pre-TMS EMG activity.

Peak-to-peak MEP amplitude was determined using custom software developed in Matlab. Trials were rejected if a) there was no stable baseline tracing in the period leading up to TMS delivery or b) the MEP was less than 0.05mV (Average trials removed per subject: Exp. 1 = 7; Exp. 2 = 12; Exp. 3 = 7). MEP amplitudes in Correct Go, Successful Stop, and Failed Stop trials, as well as in the ITI period, were trimmed (by removing upper and lower 10% of values) and then averaged. In order to verify that the muscle of interest was equally at rest before stimulation, the root mean square of the EMG trace from 200ms to 100ms before TMS onset was calculated.

Relative MEP amplitudes were calculated for Correct Go, Successful Stop, and Failed Stop conditions by dividing by the baseline ITI MEP. In addition, a primary measure of importance was the percentage of leg modulation when stopping. This was calculated as (Successful Stop MEP – Correct Go MEP)*100/Correct Go MEP. Negative leg modulation indicates suppression. In Experiment 3, these values were calculated separately for Nonselective and Selective trials.

Stimulation was delivered to one side of the body while participants made bilateral hand responses. Differential hand movement (moving one hand and not the other) occurred on Go trials in Experiment 1 (based on the direction of the Go cue) or on successful Selective stopping trials in Experiment 2 and 3 (where stopping one hand was coupled to a response in the other hand). To explore the laterality of leg modulation during stopping, we separated trials depending on the recording leg's relationship with the hand that stopped (i.e. whether the hand on the same side as the leg stopped or continued). Percent Leg Modulation was calculated separately for each case.

Statistical Analysis

In Experiments 1 and 2, one-sample *t*-tests and nonparametric Wilcoxon tests were performed to assess the change in leg excitability from baseline (test value: 0). To compare leg excitability and behavior between Experiments 1 and 2, independent-samples *t*-tests and nonparametric Mann-Witney tests were performed. In Experiment 3, paired-samples *t*-tests were used to compare between selective and nonselective conditions for leg excitability and behavior. In Experiment 3, an ANOVA was also performed with the factors pulse time (200, 220, 240) and condition (selective, nonselective). Significant results were followed up with paired-samples *t*-tests using Bonferroni correction. All tests had an alpha level of 0.05.

RESULTS

Experiment 1

Participants performed the same standard stop signal task known to engage a global suppressive mechanism (Badry et al., 2009). As predicted, leg excitability was suppressed on successful stops, a significant modulation of –13.6% (one-sample $t[6]=3.539$, $p=.012$) (Figure 1.2A). Strikingly, this suppression was evident in each of the 7 participants (the result was also significant when using a non-parametric Wilcoxon test, $p=0.018$). This finding successfully replicates the Badry et al. (2009) finding that stopping the hand leads to suppression of the task-irrelevant leg. Behavioral performance was typical for a standard stop signal task (Table 1.1). Importantly, the suppression was not due to differences in pre-

TMS leg excitability for Go and Stop trials (Go = 1.2 μV; Stop = 1.1 μV; n.s.). Furthermore, the leg was suppressed regardless of whether the stopped hand was on the same or opposite side of the recorded leg (same side = –15.4%, opposite side = –13.4%, $t[6] < 1$), providing further evidence of global suppression.

Experiment 2

Participants performed a behaviorally selective stopping task that putatively engages a selective suppressive mechanism (Aron and Verbruggen, 2008, Claffey et al., 2010, Cai et al., 2011). Consistent with our prediction, behaviorally selective stopping did not modulate mean leg excitability from baseline (Leg Modulation = –0.3%, one-sample $t[6] < 1$) (Figure 1.2A). Again, pre-TMS leg excitability did not differ for Go and Stop trials (Go = 8.9 μV; Stop = 8.4 μV; n.s.). Behavioral performance on the selective stopping task was similar to our prior reports (Aron and Verbruggen, 2008, Claffey et al., 2010) (Table 1.1). Importantly, participants were highly selective in performing the task, as the delay in continuing the other hand response on Stop trials (the Stopping Interference Effect) was short – only 74 ms on average.

The apparent absence of leg suppression contrasts with Experiment 1 where simple stopping did globally suppress the leg. An independent samples t-test showed significantly greater leg suppression in Experiment 1 than in Experiment 2, as hypothesized (Exp 1: –13.6%; Exp2: –0.3%; $t[12] = 1.97$, p=0.04, one-tailed, Cohen's $d = 1.07$) (Figure 1.2A). This difference was marginally significant when using a nonparametric Mann-Whitney Test, p=0.055. Comparing the two experiments behaviorally, there was no difference in Go

accuracy (t[12] = 1.513, n.s.), Stopping probability (t[12] < 1), Go RT (t[12] < 1), Stop Signal Delay (SSD, t[12] = 1.041, n.s.), or SSRT (t[12] < 1). However, stimulation was delivered earlier in Experiment 1 (t[12] = 3.231, p < .01). Experiment 3 controls for this.

Finally, we note that in Experiment 2, participants were required to stop one response while continuing the other. This raises the possibility of an alternative explanation of our findings. Behaviorally selective stopping may also engage the global suppression mechanism (which affects the leg as in Experiment 1), but this suppression may subsequently be masked by re-initiation of the continuing action (which elevates leg excitability). This global-suppression-plus-reinitiation account predicts that the masking effect is greater when the leg is on the same side as the continuing hand (i.e. if leg excitability is increased when the hand responds, one would expect this to occur more strongly when hand and leg are in the same hemisphere). Our task paradigm allowed us to test this prediction by comparing leg modulation when the recorded leg was on the same side as the continuing hand or the same side as the stopped hand (Figure 1.3). The leg was significantly suppressed when it was on the side of the continuing hand (–11.5%, one-sample t[6] = 2.999, p = .024), whereas there was no reliable leg modulation when the leg was on the side of the stopped hand (6.8%, one-sample t[6] < 1) (Figure 1.3B). This contradicts the global-suppression-plus-reinitiation account and will be further discussed below.

Experiment 3

Experiment 3 compared behaviorally nonselective and selective stopping with a randomized, within-block design. The task-irrelevant leg was significantly suppressed in the Nonselective condition (Leg Modulation = –8.0%, one-sample $t[10] = 2.648$, $p = .024$) but not in the Selective condition (Leg Modulation = 6.8%, one-sample $t[10] = 1.303$, $p = .222$). A paired-sample t-test showed more leg suppression in the Nonselective compared to Selective condition ($t[10] = 4.205$, $p = .002$, Cohen's $d = 1.56$) (Figure 1.2B).

The Nonselective and Selective conditions did not differ behaviorally in Go RT ($p = .35$), SSD ($p = .47$), or SSRT ($p = .27$), although Go accuracy was greater on Nonselective trials (Nonselective = 95.6%, Selective = 89.9%, $t[10] = 4.715$, $p=.001$) (Table 1.2). Additionally, there were no differences in stimulation onset after the Go signal ($p = .19$) or in pre-TMS leg excitability before Go trials (Nonselective = 3.3 μV; Selective = 3.5 μV; $p=.44$) and Stop trials (Nonselective = 3.2 μV; Selective = 3.6 μV; $p=.25$).

We further examined the temporal specificity of the nonselective and selective stopping processes because we had stimulated at three different timepoints after stop signal onset, i.e. after 200, 220, and 240 ms. There was a significant interaction between stimulation time and stopping condition ($F[10,2] = 5.920$, $p = .023$). Subsequent analysis revealed that Nonselective suppression was greater than Selective suppression at 200 and 220 ms ($t[10] = 3.275$, $p = .008$, Cohen's $d = 1.05$ and $t[10] = 3.569$, $p = .005$, Cohen's $d = 1.15$, respectively) but not at 240ms ($t[10] < 1$) (Table 1.2, Figure 1.2C). Moreover, Nonselective stopping led to suppression from baseline at the first two timepoints (200ms: $t[10] = 2.155$, $p = .057$; 220ms: $t[10] = 4.533$, $p = .001$) but not at 240 ms ($t[10] < 1$).

Selective stopping did not effect leg modulation at any timepoint (200ms: $t[10] < 1$, $p = .35$; 220ms: $t[10] = 1.406$, $p = .19$; 240ms: $t[10] < 1$).

As in Experiment 2, we examined leg modulation on Selective Stop trials as a function of whether the recorded leg was on the same side as either the continuing or stopped hand. Again, as in Experiment 2, the leg was slightly suppressed when it was on the side of the continuing hand (although not significantly this time, –1.4%, $t[10] < 1$, n.s.) but not when it was on the side of the stopped hand (8.3%, $t[10] = 1.171$, n.s.) (Figure 1.3C). Again this contradicts the global-suppression-plus-reinitiation account and will be discussed further below.

DISCUSSION

In three experiments we measured the corticomotor excitability of the task-irrelevant leg while participants performed manual stop signal tasks. In Experiment 1 we showed that stopping the hand in the standard stop signal paradigm is accompanied by suppression of the task-irrelevant leg. In Experiment 2 we used a behavioral paradigm that emphasized selective stopping of the hand. In this case there was no mean leg suppression. In Experiment 3 we directly compared trials requiring behaviorally selective and nonselective stopping. In the behaviorally selective condition (stop one hand, continue with the other) there was no leg suppression, while in the behaviorally nonselective condition (stop both hands) there was leg suppression. Moreover, we observed that the leg suppression in the nonselective condition was temporally specific, occurring at 200 and 220 ms after the stop signal, but not at 240 ms.

Experiment 1: Stopping in the standard paradigm is associated with leg suppression

The suppression of the task-irrelevant leg in Experiment 1 replicates Badry et al. (2009). It is also consistent with several earlier studies showing that behaviorally nonselective stopping is associated with widespread corticomotor excitability reductions and increased GABAergic inhibition across M1 (Leocani et al., 2000, Sohn et al., 2002, Coxon et al., 2006). This global effect may involve the STN of the basal ganglia, which has been implicated in stopping during stop-signal and go/no-go studies (Aron and Poldrack, 2006, van den Wildenberg et al., 2006, Isoda and Hikosaka, 2008, Li et al., 2008, Eagle and Baunez, 2010, Hershey et al., 2010). Furthermore, the STN is a node of the hyperdirect pathway with direct connections from prefrontal regions involved in stopping, such as the right inferior frontal gyrus and the presupplementary motor area (Nambu et al., 1997, Aron et al., 2007, Forstmann et al., 2010). Since the STN is known to have a very broad inhibitory effect on basal ganglia output (Mink, 1996, Gillies and Willshaw, 1998, Nambu et al., 2002), the global suppression we observe in the leg could be a "side-effect" of using this fast STN-mediated hyperdirect stopping mechanism.

We speculate that in Experiment 1, and in most stopping studies, subjects resort to using this global stopping mechanism because there is no cost to the global "side-effect" (i.e. this mechanism may be the quickest and easiest to use). However this global mechanism is unlikely to be used in all situations in which stopping is required. In everyday life, selectively stopping one action while continuing others is important, and global suppression of motor excitability in such situations would interfere with these continuing

actions. Thus, we set out to show that an alternative mechanism of selective suppression exists. We provide evidence for this selective suppressive mechanism in Experiment 2.

Experiment 2: Behaviorally selective stopping is not associated with leg suppression.

In this experiment, participants responded with both hands and stopped the response of one hand upon stop signal presentation while continuing with the other hand as quickly as possible. Since the stop signal contained no information about which hand to stop, participants were forced to use the advance information provided by the initial cue. As we have shown before, this advance information is key for behaviorally selective stopping. In one study, we showed that those participants with greater knowledge of the cue (tested after the trial was complete) were those who stopped more selectively (Claffey et al., 2010). In another study we showed that the advance information (e.g. “Maybe Stop Right”) is manifest in reduced motor excitability of the right hand even before the go signal occurs, and moreover the extent of this suppression predicts the subsequent selectivity of stopping (Cai et al., 2011). Yet in the current experiment, in contrast to Experiment 1, there was no mean suppression of the leg when the hand was stopped. This is consistent with our hypothesis that behaviorally selective stopping recruits a more selective suppression mechanism. Experiment 3 provided further support for this.

Experiment 3: Directly contrasting selective and nonselective behavioral stopping

This experiment compared behaviorally selective stopping (stopping one hand, continuing with the other) with nonselective stopping (stopping both hands). There was

significantly greater leg suppression for behaviorally nonselective than selective stopping. This experiment also provided greater information about the timing of the effect relative to the stop signal. Previous TMS studies have shown that motor suppression occurs towards the end of the SSRT (Coxon et al., 2006, van den Wildenberg et al., 2010a). Thus we stimulated at 200, 220, and 240 ms after the stop signal. This proved judicious since SSRT averaged approximately 260 ms (Nonselective SSRT was 246 ms and Selective SSRT was 271 ms, a non-significant difference but one that was in the same direction and magnitude as our earlier report, see Aron and Verbruggen, 2008). In the behaviorally nonselective condition, leg suppression was temporally specific – it was present at both 200 and 220 ms after the stop signal, but it had evidently expired before 240ms just before SSRT ended.

Discounting the global-suppression-plus-reinitiation account

We considered an alternative interpretation of the absent leg suppression in Experiments 2 and 3, i.e. the global-suppression-plus-reinitiation account. This account assumes that stopping, even in the behaviorally selective condition, leads to suppression of task-irrelevant muscles such as those of the leg, but that the requirement to continue with the other response leads to a re-initiation of that response tendency that also elevates the motor excitability of the leg representation. To address this possibility we compared leg excitability in the case where the leg was on the same side as the continuing hand to when the leg was on the same side as the stopped hand (and opposite to the continuing hand). Figures 1.3B and 1.3C show that the leg is suppressed when the hand on the same side continues movement, though this suppression is significant only in Experiment 2. By

contrast, there is no significant leg modulation on the same side as the stopped hand, opposite to the continuing hand.

If stopping one hand did initially cause leg suppression via a global mechanism, it would be unlikely for re-initiation of the continuing hand to abolish leg suppression on the side *opposite* to that continuing hand while sparing the suppression on the *same* side of that hand (see Figure 1.4C). The pattern of data is best explained by selective suppression that targets the hand needing to stop without affecting the leg in the same hemisphere (Figure 1.4B).

In Experiment 2, the suppression on the same side as the continuing hand movement on selective stop trials may be a manifestation of the phenomenon of 'motor surround inhibition' – i.e. activating the representations in M1 for one effector suppresses the representations of other effectors in that same hemisphere (documented by Stinear and Byblow, 2003, Sohn and Hallett, 2004, Coxon et al., 2007, Beck et al., 2009, Shin et al., 2009). Although we do not clearly identify this phenomenon outside of Experiment 2 (it is neither significant in Selective Stop trials in Experiment 3 or unimanual Go trials in Experiment 1), the selective suppression observed in Experiment 3 is at least consistent with that of Experiment 2 to suggest further evidence against the global-suppression-plus-reinitiation account.

Another important consideration against the global-suppression-plus-reinitiation account is that here, as previously (Claffey et al., 2010), there was a very small Stopping Interference Effect in some subjects. In Experiment 2, for example, the mean Stopping Interference Effect was just 74 ms and as low as 9 ms in some participants, indicating

almost perfect selectivity when stopping. Yet the Stopping Interference Effect would likely be larger if stopping employed an initial global suppression followed by a subsequent re-initiation of movement.

Taken together these observations argue for a selective mechanism of inhibitory control that targets the particular hand that needs to stop while sparing irrelevant effectors such as the leg.

What are the neural mechanisms?

Our findings are compatible with different possible accounts of neural stopping mechanisms. On one account there are two different neural mechanisms for stopping that are implemented via different fronto-basal-ganglia circuits; on another account there is a single neural mechanism for stopping that can operate in different modes – for example, broad vs. focused effects on primary motor cortex. When combined with other evidence, we speculate that our findings point more strongly to the former case, that of two different neural mechanisms. Specifically, behaviorally nonselective stopping may be implemented via a hyperdirect fronto-subthalamic pathway (as suggested by prior results, see Aron and Poldrack, 2006), and we speculate that behaviorally selective stopping is implemented via an indirect fronto-striatal-pallidal pathway. While this requires empirical verification, the preliminary evidence is as follows:

First, in two earlier reports we showed that a condition with more selective stopping was associated with slower SSRT than one that was associated with nonselective stopping (Aron and Verbruggen, 2008, Claffey et al., 2010). The difference was around 30 ms [which

is close to the difference in the current Experiment 3 (25 ms)]. Although the indirect pathway only has two or three extra synapses compared with the hyperdirect pathway, an approximately 30 ms delay for the indirect pathway has been observed when stimulating the cortex and recording from the basal ganglia (Magill et al., 2004).

Second, while the hyperdirect pathway via the STN may send a massive pulse to the pallidum and broadly affect basal ganglia output (Gillies and Willshaw, 1998), the indirect pathway has the requisite neural specificity to target a particular response tendency (Mink, 1996). Admittedly the standard model of the indirect pathway does include the STN; however, the STN's role in that pathway may not cause the same broad effects as its involvement in the hyperdirect pathway. Alternatively, the indirect pathway may be implemented via striatal–external pallidal–internal pallidal connections that bypass the STN (Mink, 1996). Notwithstanding, a key feature of the indirect pathway is striatal involvement. Notably, other research has pointed to the importance of the striatum for selective stopping, such as studies of antisaccade performance (Ford and Everling, 2009, Watanabe and Munoz, 2010). We predict that neuroimaging or neurophysiology will be able to dissociate global and selective stopping mechanisms to different fronto-basal ganglia pathways (Aron, 2010).

Summary and implications

Standard stopping, assessed by many stop-signal and go/no-go tasks, may employ an expedient mechanism that leads to a diffuse suppression in both task-relevant and -irrelevant motor representations. The hyperdirect basal ganglia pathway that signals

through the STN may underlie this mechanism due to its speed and diffuse effect in reducing thalamo-cortical drive. However, this form of rapid and global stopping has limitations as a model of human control, which often involves both advance preparation for what to stop, as well as selectivity in stopping (Aron, 2010, van den Wildenberg et al., 2010b). Accordingly we have developed a behavioral paradigm that gives participants advance information of what to stop, and 'forces' behaviorally selective stopping (Aron and Verbruggen, 2008). With this paradigm, and using TMS, we have shown that this advance preparation is associated with below-baseline suppression of the effectors that might need to be stopped in the future. Furthermore, the greater this neural suppression, the more selective the subsequent behavioral stopping (Cai et al., 2011). The current results add important information by showing that neural suppression at the time of stopping is mechanistically selective. We predict that this kind of control will be implemented via fronto-striatal interactions and will target the motor system via the indirect pathway of the basal ganglia.

This behavioral and neural model may be useful for research into impulse control disorders such as Tourette syndrome, Obsessive Compulsive Disorder, and Attention Deficit Hyperactivity Disorder. All of these are disorders characterized by failures to control particular urges, of which motor response tendencies are an important part, and all have been characterized as involving deficiencies in fronto-striatal circuits (Casey et al., 1997, Fineberg et al., 2010, Mazzone et al., 2010). It is likely that the poor control in these disorders relates at least partly to weaknesses in setting up (or maintaining) particular stopping goals, and in implementing these goals to target particular response tendencies.

In the absence of disorder, however, participants can use a stopping goal to setup neural suppression of a particular response tendency. Here we show that this proactive, targeted stopping is not only mechanistically selective but also physiologically dissociable from one that leads to global suppression when participants stop quickly and nonselectively.

ACKNOWLEDGEMENTS

This chapter, in full, is a reprint of material as it appears in Majid, Cai, George, Verbruggen, and Aron, *Cerebral Cortex*, 2011. I also thank Cathy Stinear for helpful comments on the manuscript and the Alfred P Sloan Foundation and the NIH National Institute on Drug Abuse for financial support. The dissertation author was the primary investigator and author of this paper.

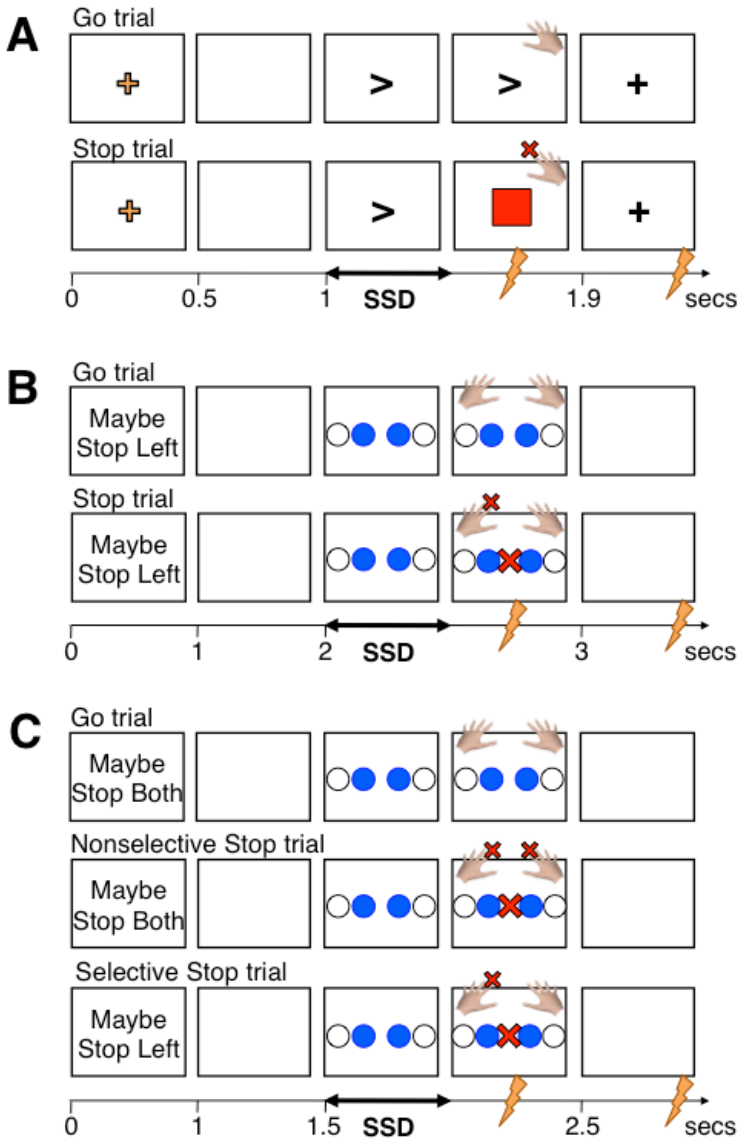

Figure 1.1: *Task designs.* (A) Experiment 1. A left or right arrow indicated the Go response, followed by a red box as a stop signal on 1/3 of trials. TMS was delivered during the Go response time at *Practice* GoRT – 100ms or, on a minority of trials, during the ITI 300ms before the onset of the next trial. (B) Experiment 2. A cue informed the participant which hand may need to stop. Blue circles indicated the Go response (inner = index; outer = little fingers), followed by a central red "X" as a stop signal on 1/3 of trials. On these stop trials, participants continued one response while stopping the other. TMS was delivered as in Experiment 1. (C) Experiment 3. Trials began with a cue indicating possible stopping of both hands (Nonselective: 50% of trials) or either the left or right hand (Selective: each 25%). TMS was delivered either 200, 220, or 240ms after the stop signal on Stop trials or at comparative times on Go trials. On a minority of trials, TMS was delivered 200 ms before the onset of the next trial.

Table 1.1: *Comparison of Experiment 1 (standard stopping) and 2 (selective stopping)*

	Experiment 1 (N=7)	Experiment 2 (N=7)
Resting motor threshold (%)*	62.5 ± 4.1	55.6 ± 6.1
Experimental intensity (%)*	71.8 ± 4.1	61.7 ± 6.6
Mean stimulation time (ms)*	307 ± 61	404 ± 51
Behavior		
Accuracy on Go trials (%)	93.5 ± 8.5	88.4 ± 2.3
Probability of stopping (%)	41.4 ± 11.9	42.6 ± 7.2
Direction error rate (%)	N/A	8.2 ± 4.8
RT on Go trials (ms)	507 ± 131	472 ± 49
Mean SSD (ms)	247 ± 192	168 ± 52
SSRT (ms)	288 ± 127	294 ± 32
RT of continuing response (ms)	N/A	545 ± 70
Stopping Interference Effect (ms)	N/A	74 ± 47
Raw motor evoked potential amplitude		
Correct Go trials (μV)	517 ± 188	459 ± 165
Successful Stop trials (μV)	436 ± 139	447 ± 128
Failed Stop trials (μV)	529 ± 211	458 ± 156
Intertrial interval (μV)	533 ± 239	349 ± 201
Percent Leg Modulation (%)*	–13.6 ± 10.2	–0.3 ± 14.8

All values given as mean ± standard deviation.
RT = reaction time; SSD = stop signal delay; SSRT = stop signal reaction time
* Significantly different between experiments ($p < .05$).

Table 1.2: *Results of Experiment 3 (N=11)*

	Nonselective trials	Selective trials
Resting motor threshold (%)	56.0 ± 4.6	
Experimental intensity (%)	62.7 ± 3.6	
Mean stimulation time (ms)	478 ± 62	451 ± 93
Behavior with TMS		
Accuracy on Go trials (%)*	95.6 ± 3.2	89.9 ± 4.2
Probability of stopping (%)	54.6 ± 6.6	45.2 ± 10.8
Direction error rate (%)	N/A	4.6 ± 2.8
RT on Go trials (ms)	518 ± 47	529 ± 39
Mean SSD (ms)	257 ± 61	239 ± 107
SSRT (ms)	246 ± 38	271 ± 100
RT of continuing response (ms)	N/A	663 ± 57
Stopping Interference Effect (ms)	N/A	134 ± 60
Raw motor evoked potential amplitude		
Correct Go trials (μV)	648 ± 380	660 ± 389
Successful Stop trials (μV)	596 ± 367	694 ± 382
Failed Stop trials (μV)	675 ± 364	700 ± 389
Intertrial interval (μV)	599 ± 397	
Percent Leg Modulation (%)*	–8.0 ± 10.1	6.8 ± 17.3
At 200 ms (%)*	–11.9 ± 18.3	3.6 ± 12.1
At 220 ms (%)*	–16.1 ± 11.8	9.8 ± 23.2
At 240 ms (%)	2.5 ± 21.1	0.9 ± 28.0

All values given as mean ± standard deviation.
RT = reaction time; SSD = stop signal delay; SSRT = stop signal reaction time
* Significantly different between conditions ($p < .05$).

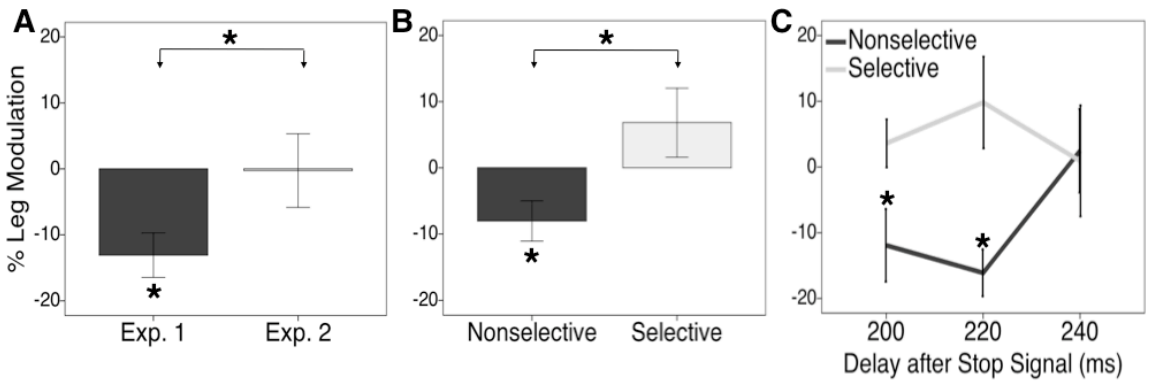

Figure 1.2: *Leg modulation when stopping*. (A) Leg Modulation was negative in Experiments 1 and absent in Experiment 2. (B) Leg Modulation was negative in Nonselective trials and non-significant in Selective trials in Experiment 3. (C) Leg Modulation in Experiment 3 was temporally specific. Nonselective modulation was significantly negative at 200 and 220ms after the stop signal but not at 240ms. Percent Leg Modulation calculated as (Successful Stop MEP – Correct Go MEP)*100/Correct Go MEP. Error bars indicate one standard error from the mean.

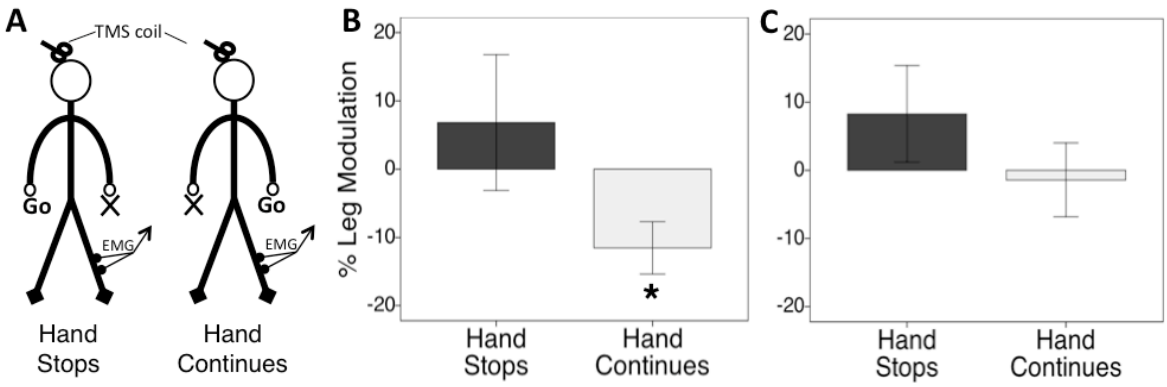

Figure 1.3: *Lateralized leg modulation when stopping and going.* (A) Successful Stop trials in Experiments 2 and 3 were separated as to whether the stimulated leg was on the same side as the hand that *stopped* or the hand that *continued*. (B) The leg is negatively modulated in Experiment 2 when on the same side as the alternative hand movement *(hand continues)*. (C) Leg modulation in Experiment 3 Selective Stop trials was similar in direction to that in Experiment 2. Error bars indicate one standard error from the mean.

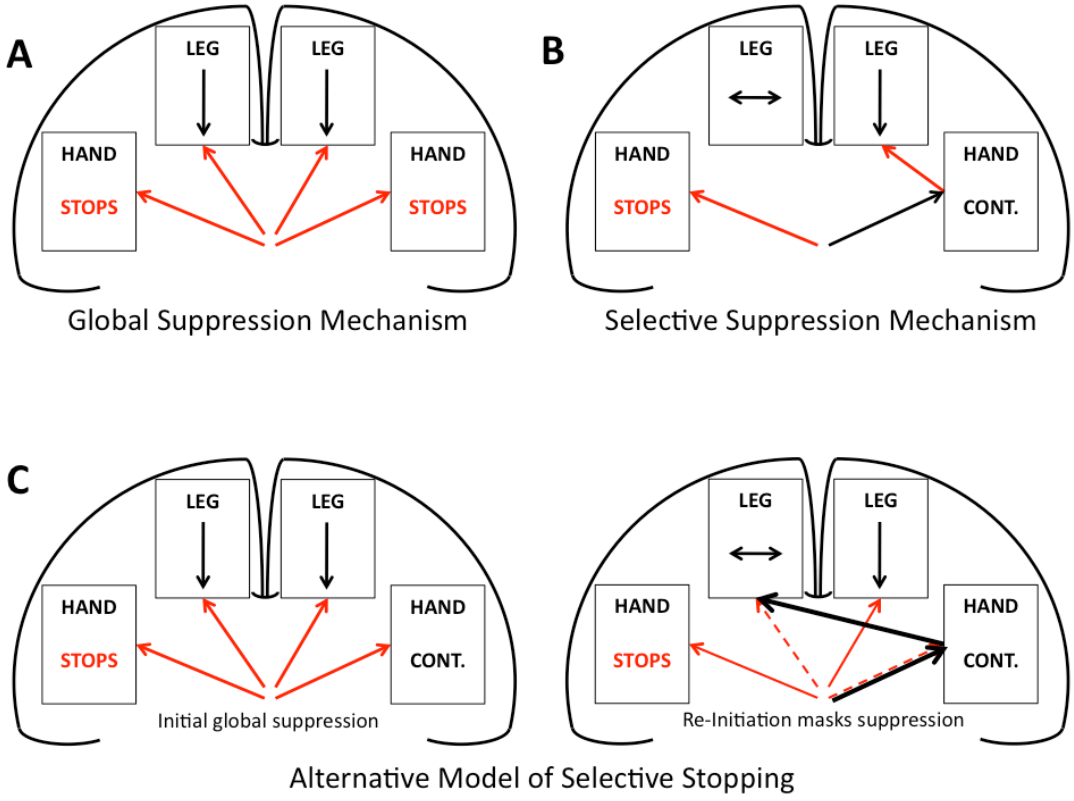

Figure 1.4. *Model of global and selective inhibitory control.* (A) Global suppression. Standard stopping causes suppression (red arrows) across the motor cortex, affecting the task-irrelevant legs in both Experiments 1 and 3 (downward pointing black arrows in boxes indicate reduced excitability). (B) Selective suppression. Stopping selectively while continuing an alternative movement likely involves an alternative mechanism in which suppression is only directed towards the effector in question. However, there is also leg suppression on the same side as the continuing hand, which is significant only in Experiment 2. We suggest that this may be the signature of a different mechanism associated with making the continuing movement (rather than stopping), i.e. intrahemispheric hand-arm surround inhibition. (C) Global-supression-plus-reinitiation alternative model. Global suppression (red arrows in left panel) is subsequently masked by activation from re-initiating the continuing hand (black arrows in right panel), which only affects the leg representation of the opposite hemisphere and spares that of the same hemisphere.

References

Aron AR (2010) From Reactive to Proactive and Selective Control: Developing a Richer Model for Stopping Inappropriate Responses. Biol Psychiatry.

Aron AR, Behrens TE, Smith S, Frank MJ, Poldrack RA (2007) Triangulating a cognitive control network using diffusion-weighted magnetic resonance imaging (MRI) and functional MRI. J Neurosci 27:3743-3752.

Aron AR, Poldrack RA (2006) Cortical and subcortical contributions to Stop signal response inhibition: role of the subthalamic nucleus. J Neurosci 26:2424-2433.

Aron AR, Verbruggen F (2008) Stop the presses: dissociating a selective from a global mechanism for stopping. Psychol Sci 19:1146-1153.

Badry R, Mima T, Aso T, Nakatsuka M, Abe M, Fathi D, Foly N, Nagiub H, Nagamine T, Fukuyama H (2009) Suppression of human cortico-motoneuronal excitability during the Stop-signal task. Clin Neurophysiol 120:1717-1723.

Band GPH, van der Molen MW, Logan GD (2003) Horse-race model simulations of the stop-signal procedure. Acta Psychol (Amst) 112:105-142.

Beck S, Schubert M, Richardson SP, Hallett M (2009) Surround inhibition depends on the force exerted and is abnormal in focal hand dystonia. J Appl Physiol 107:1513-1518.

Cai W, Oldenkamp C, Aron AR (2011) A proactive mechanism for selective suppression of response tendencies. J Neurosci 31:5965-5969.

Casey BJ, Castellanos FX, Giedd JN, Marsh WL, Hamburger SD, Schubert AB, Vauss YC, Vaituzis AC, Dickstein DP, Sarfatti SE, Rapoport JL (1997) Implication of right frontostriatal circuitry in response inhibition and attention-deficit/hyperactivity disorder. J Am Acad Child Adolesc Psychiatry 36:374-383.

Claffey MP, Sheldon S, Stinear CM, Verbruggen F, Aron AR (2010) Having a goal to stop action is associated with advance control of specific motor representations. Neuropsychologia 48:541-548.

Coxon JP, Stinear CM, Byblow WD (2006) Intracortical inhibition during volitional inhibition of prepared action. J Neurophysiol 95:3371-3383.

Coxon JP, Stinear CM, Byblow WD (2007) Selective inhibition of movement. J Neurophysiol 97:2480-2489.

Eagle DM, Baunez C (2010) Is there an inhibitory-response-control system in the rat? Evidence from anatomical and pharmacological studies of behavioral inhibition. Neurosci Biobehav Rev 34:50-72.

Fineberg NA, Potenza MN, Chamberlain SR, Berlin HA, Menzies L, Bechara A, Sahakian BJ, Robbins TW, Bullmore ET, Hollander E (2010) Probing compulsive and impulsive behaviors, from animal models to endophenotypes: a narrative review. Neuropsychopharmacology 35:591-604.

Ford KA, Everling S (2009) Neural activity in primate caudate nucleus associated with pro- and antisaccades. J Neurophysiol 102:2334-2341.

Forstmann BU, Anwander A, Schafer A, Neumann J, Brown S, Wagenmakers EJ, Bogacz R, Turner R (2010) Cortico-striatal connections predict control over speed and accuracy in perceptual decision making. Proc Natl Acad Sci U S A 107:15916-15920.

Gillies AJ, Willshaw DJ (1998) A massively connected subthalamic nucleus leads to the generation of widespread pulses. Proc Biol Sci 265:2101-2109.

Hershey T, Campbell MC, Videen TO, Lugar HM, Weaver PM, Hartlein J, Karimi M, Tabbal SD, Perlmutter JS (2010) Mapping Go-No-Go performance within the subthalamic nucleus region. Brain 133:3625-3634.

Isoda M, Hikosaka O (2008) Role for subthalamic nucleus neurons in switching from automatic to controlled eye movement. J Neurosci 28:7209-7218.

Leocani L, Cohen LG, Wassermann EM, Ikoma K, Hallett M (2000) Human corticospinal excitability evaluated with transcranial magnetic stimulation during different reaction time paradigms. Brain 123 (Pt 6):1161-1173.

Li CS, Yan P, Sinha R, Lee TW (2008) Subcortical processes of motor response inhibition during a stop signal task. Neuroimage 41:1352-1363.

Magill PJ, Sharott A, Bevan MD, Brown P, Bolam JP (2004) Synchronous unit activity and local field potentials evoked in the subthalamic nucleus by cortical stimulation. J Neurophysiol 92:700-714.

Mazzone L, Yu S, Blair C, Gunter BC, Wang Z, Marsh R, Peterson BS (2010) An FMRI study of frontostriatal circuits during the inhibition of eye blinking in persons with Tourette syndrome. The American journal of psychiatry 167:341-349.

Mink JW (1996) The basal ganglia: focused selection and inhibition of competing motor programs. Prog Neurobiol 50:381-425.

Nambu A, Kaneda K, Tokuno H, Takada M (2002) Organization of corticostriatal motor inputs in monkey putamen. J Neurophysiol 88:1830-1842.

Nambu A, Tokuno H, Inase M, Takada M (1997) Corticosubthalamic input zones from forelimb representations of the dorsal and ventral divisions of the premotor cortex in the macaque monkey: comparison with the input zones from the primary motor cortex and the supplementary motor area. Neurosci Lett 239:13-16.

Shin H-W, Sohn YH, Hallett M (2009) Hemispheric asymmetry of surround inhibition in the human motor system. Clin Neurophysiol 120:816-819.

Sohn YH, Hallett M (2004) Surround inhibition in human motor system. Exp Brain Res 158:397-404.

Sohn YH, Wiltz K, Hallett M (2002) Effect of volitional inhibition on cortical inhibitory mechanisms. J Neurophysiol 88:333-338.

Stinear CM, Byblow WD (2003) Role of intracortical inhibition in selective hand muscle activation. J Neurophysiol 89:2014-2020.

van den Wildenberg WP, van Boxtel GJ, van der Molen MW, Bosch DA, Speelman JD, Brunia CH (2006) Stimulation of the subthalamic region facilitates the selection and inhibition of motor responses in Parkinson's disease. J Cogn Neurosci 18:626-636.

van den Wildenberg WPM, Burle B, Vidal F, van der Molen MW, Ridderinkhof KR, Hasbroucq T (2010a) Mechanisms and dynamics of cortical motor inhibition in the stop-signal paradigm: a TMS study. J Cogn Neurosci 22:225-239.

van den Wildenberg WPM, Wylie SA, Forstmann BU, Burle B, Hasbroucq T, Ridderinkhof KR (2010b) To head or to heed? Beyond the surface of selective action inhibition: a review. Front Hum Neurosci 4:222.

Verbruggen F, Logan GD (2009) Models of response inhibition in the stop-signal and stop-change paradigms. Neurosci Biobehav Rev 33:647-661.

Wassermann EM (1998) Risk and safety of repetitive transcranial magnetic stimulation: report and suggested guidelines from the International Workshop on the Safety of Repetitive Transcranial Magnetic Stimulation, June 5-7, 1996. Electroencephalogr Clin Neurophysiol 108:1-16.

Watanabe M, Munoz DP (2010) Saccade suppression by electrical microstimulation in monkey caudate nucleus. J Neurosci 30:2700-2709.

CHAPTER 2

Automated structural imaging analysis detects premanifest Huntington's disease neurodegeneration within one year

ABSTRACT

Background: Intense efforts are underway to evaluate neuroimaging measures as biomarkers for neurodegeneration in premanifest Huntington's disease (preHD). We used a completely automated longitudinal analysis method to compare structural scans in preHD and controls.

Methods: Using a one-year longitudinal design, we analyzed T_1-weighted structural scans in 35 preHD individuals and 22 age-matched controls. We used the SIENA software tool (Structural Image Evaluation, using Normalization, of Atrophy) to yield overall Percentage Brain Volume Change (PBVC) and voxel-level changes in atrophy. We calculated sample sizes for a hypothetical disease modifying (neuroprotection) study.

Results: We found significantly greater yearly atrophy in preHD vs. controls (Mean PBVC controls = –0.149%; preHD = –0.388%; p=.031, Cohen's d=.617). For a preHD subgroup closest to disease onset, yearly atrophy was over three times that of controls (Mean PBVC close-to-onset preHD = –0.510%; p=.019, Cohen's d=.920). This atrophy was evident at the voxel level in periventricular regions – consistent with well-established preHD basal ganglia atrophy. We estimated that a neuroprotection study using SIENA would only need 74 close-to-onset individuals in each arm (treatment vs. placebo) to detect a 50% slowing in yearly atrophy with 80% power.

Conclusions: Automated whole-brain analysis of structural MRI can reliably detect preHD disease progression over one year. These results were attained with a readily available imaging analysis tool – SIENA – which is observer-independent, automated, and robust with respect to image quality, slice thickness, and different pulse sequences. This MRI biomarker approach could be used to evaluate neuroprotection in preHD.

INTRODUCTION

The discovery of the Huntington's disease (HD) triplet repeat gene expansion (The Huntington's Disease Collaborative Research Group, 1993) makes possible the early identification of individuals who will eventually develop manifest HD. Intense efforts are underway to develop disease modifying therapies to slow down or prevent neurodegeneration in Huntington's disease (Beal and Ferrante, 2004, Bonelli et al., 2004, Handley et al., 2006, Fecke et al., 2009, Gil and Rego, 2009, Mestre et al., 2009). Such efforts aim to halt disease progression long before any motor, cognitive, or affective symptoms emerge in gene-positive HD individuals. Consequently, there is an urgent need for biomarkers such as MRI that may be able to detect the degree of neurodegeneration during the premanifest stage of the disease (preHD) (Aylward, 2007, Bohanna et al., 2008, Hersch and Rosas, 2008, Paulsen, 2009). There are several desiderata for MRI biomarkers if they are to be useful for multi-center trials. MRI acquisition should be standard (e.g. a typical high resolution T1 scan), and image analysis should be fully automated with readily available tools that are robust to differences in pulse sequences and image quality.

Moreover, an MRI biomarker that meets these criteria must also be shown capable of detecting longitudinal change over the shortest possible period.

There are few longitudinal MRI results in preHD, and even fewer use observer-independent, automated analysis methods. An early longitudinal study in preHD demonstrated significant decreases in striatal volumes at intervals shorter than two years (Aylward et al., 1997). Subsequent results suggested that striatal degeneration occurs non-linearly, with a precipitous increase in atrophy occurring a decade before estimated diagnosis (Aylward et al., 2004). These longitudinal studies, which used manually drawn regions-of-interest, have been complemented by more recent studies using automated segmentation of the striatum (Kipps et al., 2005, Hobbs et al., 2009b). However, the striatum is not the only structure altered in preHD. Cross-sectional studies comparing preHD and controls have shown cortical thinning (Rosas et al., 2005), cortical gray matter intensity changes (Thieben et al., 2002, Stoffers et al., 2010), white-matter volume and integrity reductions (Ciarmiello et al., 2006, Squitieri et al., 2009, Stoffers et al., 2010), and decreases in cortical glucose metabolism (Ciarmiello et al., 2006). Thus, a longitudinal MRI biomarker is needed with wider sensitivity to these changes, and a whole-brain measure may serve this role. A few whole-brain, automated, longitudinal studies in preHD have been performed, demonstrating changes in white matter (fractional volume and anisotropy) (Ciarmiello et al., 2006, Squitieri et al., 2009, Weaver et al., 2009) and glucose metabolism (Ciarmiello et al., 2006). However, these findings were observed in relatively small samples, and were not always compared to controls. A promising approach is automated, unbiased whole-brain analysis of atrophy.

We evaluated the utility of the software tool SIENA (Structural Image Evaluation, using Normalization, of Atrophy) (Smith et al., 2001, Smith et al., 2002) for characterizing longitudinal changes in brain volume in preHD over the course of one year. SIENA is capable of detecting genuine change across time that is not confounded by registration, smoothing, and other processing steps. Briefly, SIENA performs subject-specific registration whereby the scans from the two timepoints are aligned. Brain edges in each image are then identified using segmentation, and the displacement between edge images is used to estimate atrophy. SIENA has several important strengths: it is completely automated (reducing labor intensiveness and obviating inter-rater reliability concerns), whole-brain based (obviating regions-of-interest), and robust to image quality, slice thickness, and different pulse sequences (Smith et al., 2001). Thus SIENA meets the criteria for biomarker use in multi-center longitudinal studies. First, however, it is important to establish whether this approach can in fact detect neurodegeneration in preHD over a period as short as one year.

METHODS

Participants

All participants were recruited from the Huntington's Disease Center of Excellence at the University of California, San Diego. At the start of the study (July 2008) we recruited 37 participants who tested positive for the HD gene expansion yet did not fulfill diagnostic criteria for clinical HD (preHD) and 22 healthy age- and sex-matched control participants. The control group, which was recruited from the friends and spouses of participants with

preHD, reported no psychiatric or neurological history and no use of psychoactive substances. Participants provided written consent in accordance with an Institutional Review Board protocol of the University of California, San Diego. Participants were studied longitudinally, on two visits, with an average interval between visits of approximately one year (Table 2.1).

Global cognitive ability was measured using the Mini-Mental State Exam (MMSE) (Folstein et al., 1975) at both timepoints. A movement disorder specialist (JCB) evaluated the preHD participants with the Unified Huntington's Disease Rating Scale (Folstein et al., 1975, Huntington Study Group, 1996). Using this scale, the neurologist assessed each participant for motor abnormalities to determine a 'motor score' (range: 0 to 124) and then assigned a rating from 0 to 4 indicating the level of confidence that the presenting motor abnormalities represent symptoms of HD. A confidence rating of 0 represents a normal evaluation and no motor abnormalities, a rating of 1 represents < 50% confidence of an HD diagnosis, and a rating of 4 represents a definitive diagnosis of HD. UHDRS scores were obtained from all participants at timepoint one and only from preHD participants at timepoint two. All participants at timepoint one were rated below 2, confirming their preHD status (Table 2.1). At the second timepoint, two participants from the preHD group were rated 4, indicating conversion to manifest Huntington's disease. These two participants were removed from the primary statistical analyses, leaving a preHD group of 35 participants.

Participants were defined as gene-expansion positive if they had one allele with 38 or more cytosine-adenine-guanine (CAG) repeats. Repeat size was determined by the UCSD

Medical Genetics laboratory using a polymerase chain reaction assay (accuracy of analysis to determine repeat size: 99%). The length of the CAG repeat expansion was used to calculate estimated years-to-onset (YTO) using two different methods. The Aylward method uses all of CAG repeat length, current age, and parental age of onset in a simple regression equation (Aylward et al., 1996), whereas the method of Langbehn and colleagues uses only CAG repeat length and current age in a parametric survival model (Langbehn et al., 2004).

MR Image acquisition and pre-processing

Data were acquired with a General Electric (Milwaukee, WI, USA) 1.5 T EXCITE HD scanner with an 8-channel phased-array head coil. Image acquisition included a General Electric "PURE" calibration sequence and a high-resolution three-dimensional T_1-weighted sequence (echo time = 2.798 msec, repetition time = 6.496 msec, inversion time = 600 msec, flip angle = 12˚, bandwidth = 244.141 Hz/pixel, field of view = 24 cm, matrix = 256 x 192, slice thickness = 1.2 mm). T_1-images were corrected for non-linear warping using tools developed by the Morphometry Biomedical Informatics Research Network.

Quantifying volumetric change using SIENA

We computed Percentage Brain Volume Change (PBVC) for each participant using SIENA (Smith et al., 2001, Smith et al., 2002) – part of the FSL suite of tools (Smith et al., 2004, Woolrich et al., 2009). First, brain and skull images are extracted from the whole-head input data for the two timepoints separately (Smith, 2002). Next, the two brain images are aligned using the skull to constrain the registration scaling (this corrects for distortions in

imaging geometry related to scans on different occasions) (Jenkinson and Smith, 2001, Jenkinson et al., 2002). The registration transform between the two timepoints is deconstructed into two intermediary transforms that put each brain image into a space halfway between the two. This is done so each brain image undergoes the same amount of interpolation-related blurring (Jenkinson et al., 2002). Next, tissue-type segmentation is carried out in order to find the brain/non-brain edge boundary (Zhang et al., 2001). Then edge detection is performed on both the registered brain images (Smith et al., 2001). For every edge point in image 1, voxels along a line perpendicular to the edge at that point are searched in image 2 using intensity gradients in the same direction in order to find the closest matching edge point. Once the edge is found in image 2, the subvoxel position is taken into account in order to quantify the movement (change). This is repeated for many edge points. The total Brain Volume Change is the sum of all edge point motions. This number is divided by the number of edge points and the voxel 'area' and is subsequently converted into Percentage Brain Volume Change (PBVC) (Smith et al., 2002).

Voxel-wise analysis of volumetric change

Following SIENA, an edge displacement image was obtained for each participant. This encodes the outward and inward perpendicular displacement between the two timepoints for every point along the participant's brain/non-brain boundary, including the internal ventricular boundary. This was dilated, transformed into MNI152 standard space, and masked by a standard 2mm brain edge image (Bartsch et al., 2004). The resulting

standardized edge images from all participants were fed into voxel-wise statistical analysis to test for differences between groups.

Sample size calculations and power analysis

We computed estimates of sample sizes needed to achieve 80% power using a two-sided significance test with level α = 5% in a hypothetical two-arm study that would use SIENA to compare a neuroprotective HD treatment with a placebo over a one-year period. For each arm of the study, the minimum sample size required to detect slowing in the yearly atrophy rate can be computed using the following formula:

$$n = 2\sigma^2(z_{(1-\alpha/2)} + z_{power})^2/(\Delta\beta)^2$$

$$= 2\sigma^2(z_{(1-.05/2)} + z_{.80})^2/(\Delta\beta)^2 \qquad (1)$$

Here, σ^2 is the variance of the PBVC values in the preHD group in question, and z_p is the *p*th quantile of the standard normal distribution. The variable β denotes the magnitude of the yearly atrophy relative to a baseline condition, as assessed through SIENA (Hua et al., 2010), and Δ denotes the desired detectible slowing in atrophy. In a model in which the study drug is expected to modify both the disease- and normal aging-related rates of atrophy, the baseline condition is "no atrophy," and β is simply the mean PBVC of the preHD group. Possibly more informative, however, is a model that assumes the study drug's effect is on the disease-related process alone. In this case, the baseline condition is "normal rate of atrophy," and β is equivalent to the difference between mean PBVC of the preHD group and mean PBVC of normal controls.

Sample sizes were calculated for both a 50% and 20% desired slowing in atrophy [Δ in Equation (1)]. Sample size point estimates relative to the "no atrophy" baseline condition were obtained by computing the mean rate of atrophy and variance of the PBVC within the preHD group and substituting these values for β and σ^2 in Equation (1). Sample size point estimates relative to the "normal rate of atrophy" baseline condition were obtained by computing the difference in mean rates of atrophy between the preHD group and an age- and sex-based pair-matched subset of control subjects. This value and the variance of the preHD group were then substituted for β and σ^2 in Equation (1). Sample size 95% confidence intervals (CIs) were computed using the Matlab bootstrapping function *bootci* with 100,000 sample size estimates.

Statistical analysis

Statistical analyses were carried out at a significance level of 5% (two-tailed) using either PASW Statistics 18 (SPSS Inc., Chicago, IL, USA) for participant characteristics and PBVC values or with FSL's randomize tool, version 4.1.2, for voxel-wise statistics of the brain edge image. The randomize tool uses non-parametric inference and corrects for multiple comparisons (Nichols and Holmes, 2002). The number of permutations was 5,000.

RESULTS

Participant characteristics

At study entry, control and preHD groups had similar age and MMSE score (p=.833 and .495, respectively). For MMSE, ANOVA revealed a main effect of time, with scores decreasing, (F(1,55)=7.126, p=.010), but no between-group difference (F<1). Therefore, the groups were well-matched for longitudinal analysis. Regarding UHDRS motor scores, these were significantly elevated in preHD compared to controls at baseline (t[55]=3.912, p<.001), consistent with subtle motor signs, albeit insufficient to meet the criteria for manifest HD. Second timepoint UHDRS motor scores were significantly elevated in the preHD group after the one-year duration, indicating a slightly worsening condition (t[34]=3.254, p=.003).

Analysis of SIENA Percentage Brain Volume Change

The preHD group showed significantly greater PBVC (increased atrophy) over the year compared to controls (Mean PBVC controls = –0.149%; preHD = –0.388%, t[55]=2.217, p=.031, Cohen's d = .617) (Table 2.3, Figure 2.1A). In controls, there was slight atrophy, consistent with aging; however, this was not a significant effect (t[21]=2.006, p=.058). As group gender ratios differed slightly, auxiliary analyses were performed. Atrophy did not differ between males and females within either group (both p>0.05). A bootstrapping analysis procedure additionally sampled 10,000 pairs of equally sized, gender-balanced groups from among controls and preHD. This showed that there was a significant difference (p<0.001) even when matching for gender distribution and group size. This confirms that

uneven sex distributions and group sizes do not explain the observed difference in PBVC between controls and preHD.

To examine whether the brain volume loss in preHD was greater in those individuals with greater disease burden, we correlated PBVC with the UHDRS motor score and the two measures of YTO separately (i.e. YTO calculated by Aylward and Langbehn methods). PBVC did not correlate with the UHDRS motor score at either timepoint nor with the change in motor score between timepoints (all $t < 1$). This is consistent with prior findings that the UHDRS motor score is insensitive to atrophy in premanifest individuals (de Boo et al., 1998). PBVC was correlated with the Aylward estimate of YTO – such that those preHD individuals with greater brain atrophy were the closest to onset (Spearman's rho = .296, p=.042, one-tailed). However, PBVC did not correlate significantly with the Langbehn YTO estimate (Spearman's rho = .261, p=.065, one-tailed).

This correlation between the Aylward YTO estimate and PBVC is consistent with a previously reported finding of accelerating atrophy as onset approaches (Aylward et al., 2004). Together, these findings motivate a comparison of preHD subgroups defined by proximity to onset. To do this, we performed a median split using Aylward YTO (6 years-to-onset) (Table 2.2). The subgroups (close-to-onset and far-from-onset) did not differ in CAG repeat length (t[33]=.788, p=.436). At timepoint 1, the subgroups were also well-matched on MMSE and UHDRS motor score (p=.169 and .380, respectively). For MMSE and UHDRS motor scores, ANOVA revealed a main effect of time (F[1,33]=7.951, p=.008 and F[1,33]=10.263, p=.003, respectively), but no effect of group (F[1,33]=3.254, p=.080 and

F[1,33]=.989, p=.327, respectively). However, the close-to-onset group was significantly older than the far-from-onset group (*t*[33]=2.051, p=.048).

Consistent with worsening atrophy with approaching disease onset, close-to-onset preHD had larger PBVC than far-from-onset preHD (Mean PBVC close-to-onset preHD = –0.510%; far-from-onset preHD = –0.259%; *t*[33]=1.801, p=.041, one-tailed) (Table 2.3). However, the difference between preHD subgroups did not remain significant after covarying for age (*F*[1,33]=1.584, p=.221).

To compare preHD subgroups with controls, ANOVA was performed with PBVC and all three groups. There was a main effect of group (*F*[2,54]=4.401, p=.017) (Figure 2.1B). Scheffé post-hoc tests showed that while there was no significant difference between the far-from-onset group and controls (p=.781), the close-to-onset group had significantly larger PBVC than controls (p=.019, Cohen's d = .92). This was an over three-fold difference in yearly atrophy. Notably, controls did not differ in age with either the close-to-onset group (*t*[38]=1.127, p=.267) or the far-from-onset group (*t*[37]=.935, p=.356), and the ANOVA's main effect of group remained even after covarying for age (*F*[2,54]= 2.898, p=.043).

The two participants who were excluded from the main analyses above because of conversion to manifest HD had year-end PBVC values greater than any of the other participants in either the preHD or control groups (PBVC = –1.49% and –1.69% in manifest HD individuals vs. maximum values of –1.40% in preHD or –0.70% in controls).

Voxel-wise analysis of volumetric change

The larger PBVC for close-to-onset individuals vs. controls was also evident in voxel-wise analysis of individual edge-displacement images ($p<.05$, corrected over the 2mm MNI152 edge image). Figure 2.2 shows the changes around the lateral ventricles, consistent with the well-established basal ganglia degeneration in HD. There were no significant differences for the voxel-wise analysis when comparing the overall preHD group with controls.

Sample size calculations and power analysis

We used Equation 1 to compute the sample sizes needed to power a two-arm neuroprotective treatment study designed to detect both a 50% and 20% slowing in yearly SIENA-derived PBVC. We specified that such a study have a power of 80% and a 5% two-tailed significance level. Sample size estimates (Table 2.4) were calculated for a hypothetical study that would recruit only those estimated to be six or less years from estimated disease onset (where we found the largest effect size – Cohen's d = .92). Relative to the "no atrophy" baseline condition, detecting a 50% slowing in atrophy requires a sample size of 45 individuals in each study arm (95% CI: 17 to 188) and a 20% slowing requires 281 individuals (95% CI: 106 to 1225). Relative to the "normal rate of atrophy" baseline condition, detecting a 50% slowing requires 74 individuals (95% CI: 35 to 433) and a 20% slowing requires 460 individuals (95% CI: 218 to 2713). Sample sizes are about twice as large if such a study includes preHD individuals without regard for disease onset proximity (Table 2.4).

DISCUSSION

In this longitudinal study of preHD, we used the completely automated SIENA tool to evaluate whole-brain change. We found significantly larger PBVC (more severe atrophy) in preHD individuals compared to controls over the course of one year. The increased PBVC was particularly striking in a close-to-onset preHD subgroup, supporting a previous finding of accelerating preHD atrophy in the striatum using manual segmentation (Aylward et al., 2004). The longitudinal decrease in brain volume was also evident at the voxel-level in periventricular regions – consistent with the well-established basal ganglia atrophy in preHD.

The ideal MRI biomarker for assessing neurodegeneration in preHD would be objectively measured, consistent with known disease pathology, and serve as a predictor for clinical outcomes (such as conversion to manifest HD) (Aylward, 2007, Bohanna et al., 2008, Hersch and Rosas, 2008, Paulsen, 2009). Our results were achieved with a fully-automated analysis. We used the SIENA software tool, which has been shown to be very reliable with an estimated error in brain volume change as low as 0.15% and to be robust to varying image quality, slice thickness, and different pulse sequences (Smith et al., 2001, Smith et al., 2002). This error rate is smaller than the group differences we identify in our study. In comparison with other semi-automated techniques to assess longitudinal change, SIENA has demonstrated lower error rates and higher sensitivity in the detection of subtle differences in atrophy (Sormani et al., 2004). Moreover, SIENA is freely available and quick to run. Clearly, this fully-automated analysis method meets the objectivity criterion of a preHD biomarker.

A useful longitudinal MRI biomarker should also reveal atrophy that is consistent with known preHD pathology. Here, voxel-wise analysis of longitudinal brain edge displacement revealed changes to periventricular regions, consistent with the well-established profile of basal ganglia atrophy in preHD (Thieben et al., 2002, Aylward et al., 2004, Kipps et al., 2005, Hobbs et al., 2009a, Paulsen et al., 2010, Stoffers et al., 2010). However, preHD pathology also includes non-striatal changes such as decreases in white matter volume (Ciarmiello et al., 2006, Squitieri et al., 2009) and cortical changes (Rosas et al., 2005, Paulsen et al., 2006, Nopoulos et al., 2007, Stoffers et al., 2010). Although our voxel-wise analysis points to basal ganglia atrophy, a striking (and probably the most useful) finding here is the overall brain atrophy measure (i.e. PBVC). This measure reflects the total amount of brain edge displacement across time. Thus it is likely sensitive to pathology at multiple levels, including basal ganglia, cortical gray, and white matter, even if not all these changes are reflected in voxel-level differences.

Biomarkers in preHD should also serve as predictors for known future clinical outcomes (Aylward, 2007, Bohanna et al., 2008, Hersch and Rosas, 2008, Paulsen, 2009). We have shown that individuals closest to estimated disease onset drove group differences in atrophy, suggesting that SIENA-derived PBVC may be a good predictor of manifest HD conversion. Furthermore, of the 37 preHD participants who entered our study at the beginning of the year, the two who later converted to manifest HD also had the largest PBVC, consistent with the possibility that PBVC predicts imminent clinical onset. A survival analysis after future follow-up of our remaining 35 preHD participants will further clarify the utility of PBVC as a predictor of clinical onset.

PBVC correlated with the Aylward YTO estimate but not the Langbehn YTO estimate. Differences in methodology may account for this discrepancy. The Langbehn YTO estimate is constrained to always be positive (Langbehn et al., 2004, Langbehn et al., 2010), whereas the Aylward YTO estimate may be negative when the current age exceeds the estimated age-of-onset (Aylward et al., 1996). Thus the Aylward method may allow for greater variability among those closest to onset that is lost when using the Langbehn method.

A limitations of SIENA is the inability to provide full regional specificity as to the locus of atrophy. Our findings of periventricular change, though suggestive regional atrophy, remain unspecific as to the actual locus of change. Indeed, future regionally specific automated analysis tools hold great promise as preHD biomarkers. To date, the sole automated study of caudate atrophy found a high effect size of 0.9 when comparing preHD and controls over a two year period (Hobbs et al., 2009b). Though we show a medium effect size when comparing preHD and control groups, we note that the SIENA whole-brain methodology detected group differences in a shorter time period, i.e. one year. A longer study period would likely accentuate group differences. Moreover, SIENA has the advantage of being freely available, quick, and easy to run.

Furthermore, we observed a high effect size (0.92), as large as that for the abovementioned caudate specific measure(Hobbs et al., 2009b), when comparing PBVC in controls with close-to-onset preHD participants (Aylward YTO ≤ 6 years). This provides useful information about statistical power needed to plan neuroprotective treatment studies in preHD individuals over a one-year period. For instance, a study designed using SIENA to test a treatment that can slow the yearly rate of atrophy by 50% may only require

about 74 close-to-onset preHD individuals in each experimental arm (treatment vs. placebo). Although the assumption of a 50% benefit may be overly optimistic, the feasibility of such a study strongly argues for the utility of SIENA as a preHD biomarker.

In summary, we have demonstrated the potential of SIENA, a fully-automated and robust method, to detect atrophy in preHD over a mere one year period. We have also shown that year-end PBVC values may predict known disease outcomes such as conversion to manifest disease. These findings provide proof-of-concept regarding biomarker development for disease detection in preHD, as well as quantitative insights into how to power upcoming trials of neuroprotection.

ACKNOWLEDGEMENTS

This chapter, in full, is a reprint of material as it appears in Majid, Stoffers, Sheldon, Hamza, Thompson, Goldstein, Corey-Bloom, and Aron, *Movement Disorders*, 2011. I thank Anders Dale and Matt Erhart for technical assistance with image preprocessing and CHDI for financial support. The dissertation author was the primary investigator and author of this paper.

Table 2.1: *Participant characterization by group*

	Controls (N=22)		PreHD (N=35)	
	Visit 1	Visit 2	Visit 1	Visit 2
Age at start (yrs, mean± SD)	40.1±12.2		40.8±10.2	
Sex (F/M)	15/7		20/15	
Between-scan interval (yrs, mean ± SD)	1.0±.1		1.0±.1	
MMSE (mean ± SD) *	28.8±1.4	28.4±1.7	29.2±1.0	28.4±1.5
Number of CAG repeats (mean ± SD) [range]	N/A		42.4±2.4 [38–48]	
Estimated years-to-onset, Aylward method (yrs, mean ± SD)	N/A		5.8±6.9	
Estimated years-to-onset, Langbehn method (yrs, mean ± SD)	N/A		14.0±7.0	
UHDRS motor score (mean ± SD) **	0.1±0.3	N/A	1.6±1.8	3.9±4.6
UHDRS confidence score (*score*: # of participants)	*0*: 22	N/A	*0*: 23 *1*: 12	*0*: 15 *1*: 10 *2*: 9 *3*: 1

SD = standard deviation, MMSE = Mini-mental state exam, CAG = cytosine-adenine-guanine, UHDRS = Unified Huntington's Disease Rating Scale, PreHD = preclinical Huntington's disease, N/A = not applicable

* = ANOVA revealed main effect of time (p=.010) but no effect of group.

** = significantly different between groups at timepoint 1 (p<.001) and between timepoints in preHD group (p=.003). UHDRS was not obtained for controls at timepoint 2.

Table 2.2: *PreHD subgroups by median Aylward years-to-onset (6 years)*

	Far from Onset (N=17)		Close to Onset (N=18)	
	Visit 1	Visit 2	Visit 1	Visit 2
Age at start (yrs, mean ± SD) *	37.3±10.4		44.1±9.1	
Sex (F/M)	8/9		12/6	
Between-scan interval (yrs, mean ± SD)	1.0±.1		1.0±.2	
MMSE (mean ± SD) **	29.5±0.5	28.7±1.4	29.0±1.3	28.1±1.6
Number of CAG repeats (mean ± SD)	42.7±2.8		42.1±2.0	
Estimated years-to-onset, Aylward method (years, mean± SD)	11.8±3.8		0.2±3.6	
UHDRS motor score (mean ± SD) **	1.3±1.5	3.2±4.9	1.8±1.9	4.5±4.3
UHDRS confidence score (*score*: # of participants)	*0*: 12 *1*: 5	*0*: 10 *1*: 4 *2*: 3	*0*: 11 *1*: 7	*0*: 5 *1*: 6 *2*: 6 *3*: 1

Subgroups determined by median split using Aylward YTO of 6 years-to-onset.
SD = standard deviation, MMSE = Mini-mental state exam, CAG = cytosine-adenine-guanine, UHDRS = Unified Huntington's Disease Rating Scale, N/A = not applicable
* = significantly different between groups (p=.048)
** = ANOVA reveals main effect of time (p<.01) but no effect of group.

Table 2.3: *SIENA derived Percentage Brain Volume Change (PBVC) by group*

	PBVC (%, Mean ± SD)
Controls (N=22)	–0.149 ± .348
PreHD (N=35)	–0.388 ± .425
Far-from-onset (N=17)	–0.259 ± .390
Close-to-onset (N=18)	–0.510 ± .431

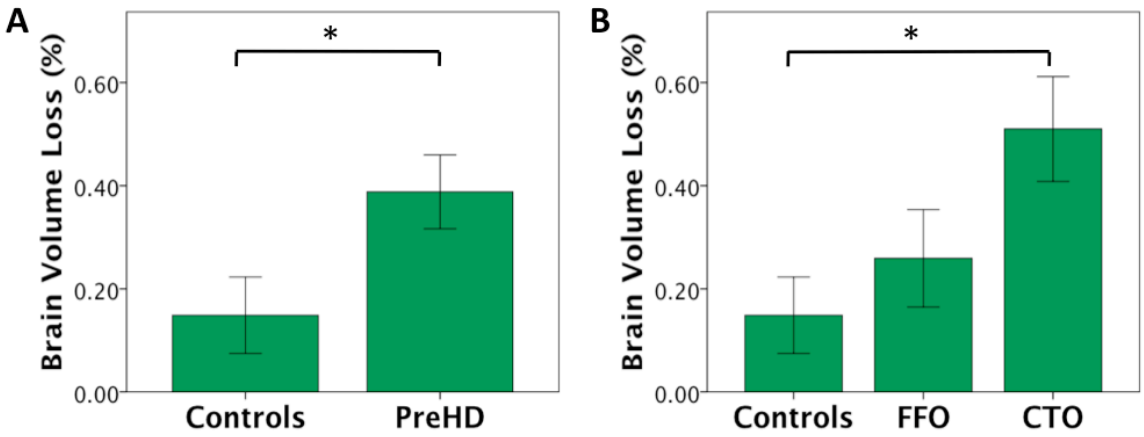

Figure 2.1: *Longitudinal results derived from SIENA.* A. Brain Volume Loss (%) is significantly greater in the premanifest Huntington's disease group when compared to controls. B. Changes in the close-to-onset group drive group differences in Percentage Brain Volume Change. Close-to-onset preHD (Aylward YTO ≤ 6) had greater atrophy than far-from-onset preHD, but this was not significant after covarying for age. Far-from-onset preHD were not significantly different from controls. Error bars represent ± 1 standard error of the mean. Brain Volume Loss (%) equals negative PBVC. PreHD = premanifest Huntington's disease, FFO = far-from-onset preHD, CTO= close-to-onset preHD.

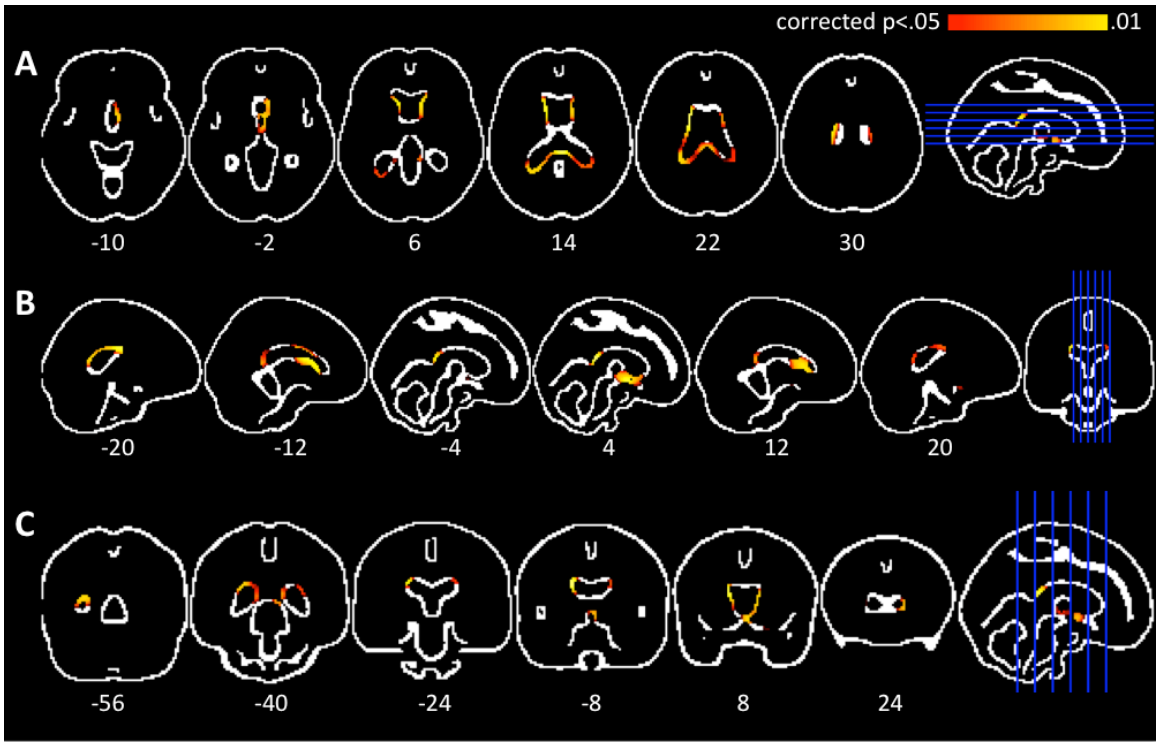

Figure 2.2. *Voxel-wise edge displacement results.* Axial (A), saggital (B), and coronal (C) images of the MNI152 edge image overlaid with areas of significant differences between close-to-onset individuals and controls (p<.05, corrected over the edge image). There is significant periventricular edge displacement, consistent with progressive basal ganglia atrophy in premanifest Huntington's disease.

Table 2.4: *Power analysis*

	Study of close-to-onset preHD alone		Study of all preHD individuals	
Desired atrophy reduction	50%	20%	50%	20%
"No atrophy" baseline	45 (17–188)	281 (106–1225)	76 (36–210)	470 (222–1293)
"Normal atrophy rate" baseline	74 (35–433)	460 (218–2713)	149 (89–12,302)	926 (556–78,284)

Sample sizes needed to detect a given slowing in yearly atrophy in a two-arm neuroprotection study powered at 80% using a 5% two-sided significance level. Parentheses indicated 95% confidence interval. Treatment effect is relative to an either a baseline of "no atrophy" or one of the "normal atrophy rate."

References

Aylward E, Li Q, Stine O, Ranen N, Sherr M, Barta P, Bylsma F, Pearlson G, Ross C (1997) Longitudinal change in basal ganglia volume in patients with Huntington's disease. Neurology 48:394-399.

Aylward EH (2007) Change in MRI striatal volumes as a biomarker in preclinical Huntington's disease. Brain research bulletin 72:152-158.

Aylward EH, Codori AM, Barta PE, Pearlson GD, Harris GJ, Brandt J (1996) Basal ganglia volume and proximity to onset in presymptomatic Huntington disease. Arch Neurol 53:1293-1296.

Aylward EH, Sparks BF, Field KM, Yallapragada V, Shpritz BD, Rosenblatt A, Brandt J, Gourley LM, Liang K, Zhou H, Margolis RL, Ross CA (2004) Onset and rate of striatal atrophy in preclinical Huntington disease. Neurology 63:66-72.

Bartsch A, Bendszus N, De Stefano N, Homola G, Smith S (2004) Extending SIENA for a multi-subject statistical analysis of sample-specific cerebral edge shifts: substantiation of early brain regeneration through abstinence from alcoholism. In: Tenth International Conference on Functional Mapping of the Human Brain.

Beal MF, Ferrante RJ (2004) Experimental therapeutics in transgenic mouse models of Huntington's disease. Nat Rev Neurosci 5:373-384.

Bohanna I, Georgiou-Karistianis N, Hannan AJ, Egan GF (2008) Magnetic resonance imaging as an approach towards identifying neuropathological biomarkers for Huntington's disease. Brain research reviews 58:209-225.

Bonelli RM, Wenning GK, Kapfhammer HP (2004) Huntington's disease: present treatments and future therapeutic modalities. Int Clin Psychopharmacol 19:51-62.

Ciarmiello A, Cannella M, Lastoria S, Simonelli M, Frati L, Rubinsztein DC, Squitieri F (2006) Brain white-matter volume loss and glucose hypometabolism precede the clinical symptoms of Huntington's disease. J Nucl Med 47:215-222.

de Boo G, Tibben A, Hermans J, Maat A, Roos RA (1998) Subtle involuntary movements are not reliable indicators of incipient Huntington's disease. Mov Disord 13:96-99.

Fecke W, Gianfriddo M, Gaviraghi G, Terstappen GC, Heitz F (2009) Small molecule drug discovery for Huntington's Disease. Drug Discov Today 14:453-464.

Folstein M, Folstein S, McHugh P (1975) "Mini-mental state". A practical method for grading the cognitive state of patients for the clinician. J Psychiatr Res 12:189-198.

Gil JM, Rego AC (2009) The R6 lines of transgenic mice: a model for screening new therapies for Huntington's disease. Brain research reviews 59:410-431.

Handley OJ, Naji JJ, Dunnett SB, Rosser AE (2006) Pharmaceutical, cellular and genetic therapies for Huntington's disease. Clin Sci 110:73-88.

Hersch SM, Rosas HD (2008) Neuroprotection for Huntington's disease: ready, set, slow. Neurotherapeutics : the journal of the American Society for Experimental NeuroTherapeutics 5:226-236.

Hobbs NZ, Henley SMD, Ridgway G, Wild EJ, Barker R, Scahill RI, Barnes J, Fox NC, Tabrizi S (2009a) The Progression of Regional Atrophy in Premanifest and Early Huntington's Disease: A Longitudinal Voxel-Based Morphometry Study. J Neurol Neurosurg Psychiatr.

Hobbs NZ, Henley SMD, Wild EJ, Leung KK, Frost C, Barker RA, Scahill RI, Barnes J, Tabrizi SJ, Fox NC (2009b) Automated quantification of caudate atrophy by local registration of serial MRI: evaluation and application in Huntington's disease. Neuroimage 47:1659-1665.

Hua X, Lee S, Hibar DP, Yanovsky I, Leow AD, Toga AW, Jack CR, Bernstein MA, Reiman EM, Harvey DJ, Kornak J, Schuff N, Alexander GE, Weiner MW, Thompson PM, Initiative AsDN (2010) Mapping Alzheimer's disease progression in 1309 MRI scans: power estimates for different inter-scan intervals. Neuroimage 51:63-75.

Huntington Study Group (1996) Unified Huntington's Disease Rating Scale: reliability and consistency. Mov Disord 11:136-142.

Huntington's Disease Collaborative Research Group (1993) A novel gene containing a trinucleotide repeat that is expanded and unstable on Huntington's disease chromosomes. Cell 72:971-983.

Jenkinson M, Bannister P, Brady M, Smith S (2002) Improved optimization for the robust and accurate linear registration and motion correction of brain images. Neuroimage 17:825-841.

Jenkinson M, Smith S (2001) A global optimisation method for robust affine registration of brain images. Med Image Anal 5:143-156.

Kipps CM, Duggins AJ, Mahant N, Gomes L, Ashburner J, McCusker EA (2005) Progression of structural neuropathology in preclinical Huntington's disease: a tensor based morphometry study. J Neurol Neurosurg Psychiatr 76:650-655.

Langbehn DR, Brinkman RR, Falush D, Paulsen JS, Hayden MR, International Huntington's Disease Collaborative Group (2004) A new model for prediction of the age of onset and penetrance for Huntington's disease based on CAG length. Clin Genet 65:267-277.

Langbehn DR, Hayden MR, Paulsen JS, PREDICT-HD Investigators of the Huntington Study Group (2010) CAG-repeat length and the age of onset in Huntington disease (HD): a review and validation study of statistical approaches. Am J Med Genet B Neuropsychiatr Genet 153B:397-408.

Mestre T, Ferreira J, Coelho MM, Rosa M, Sampaio C (2009) Therapeutic interventions for disease progression in Huntington's disease. Cochrane Database Syst Rev CD006455.

Nichols TE, Holmes AP (2002) Nonparametric permutation tests for functional neuroimaging: a primer with examples. Hum Brain Mapp 15:1-25.

Nopoulos P, Magnotta V, Mikos A, Paulson H, Andreasen N, Paulsen J (2007) Morphology of the cerebral cortex in preclinical Huntington's disease. The American journal of psychiatry 164:1428-1434.

Paulsen JS (2009) Biomarkers to predict and track diseases. Lancet Neurol 8:776-777.

Paulsen JS, Magnotta VA, Mikos AE, Paulson HL, Penziner E, Andreasen NC, Nopoulos PC (2006) Brain structure in preclinical Huntington's disease. Biol Psychiatry 59:57-63.

Paulsen JS, Nopoulos PC, Aylward E, Ross CA, Johnson H, Magnotta VA, Juhl A, Pierson RK, Mills J, Langbehn D, Nance M, PREDICT-HD Investigators and Coordinators of the Huntington's Study Group (HSG) (2010) Striatal and white matter predictors of estimated diagnosis for Huntington disease. Brain research bulletin.

Rosas HD, Hevelone ND, Zaleta AK, Greve DN, Salat DH, Fischl B (2005) Regional cortical thinning in preclinical Huntington disease and its relationship to cognition. Neurology 65:745-747.

Smith S (2002) Fast robust automated brain extraction. Hum Brain Mapp 17:143-155.

Smith S, De Stefano N, Jenkinson M, Matthews P (2001) Normalized accurate measurement of longitudinal brain change. J Comput Assist Tomogr 25:466-475.

Smith S, Jenkinson M, Woolrich M, Beckmann C, Behrens T, Johansen-Berg H, Bannister P, De Luca M, Drobnjak I, Flitney D, Niazy R, Saunders J, Vickers J, Zhang Y, De Stefano N, Brady J, Matthews P (2004) Advances in functional and structural MR image analysis and implementation as FSL. Neuroimage 23 Suppl 1:S208-219.

Smith SM, Zhang Y, Jenkinson M, Chen J, Matthews PM, Federico A, De Stefano N (2002) Accurate, robust, and automated longitudinal and cross-sectional brain change analysis. Neuroimage 17:479-489.

Sormani M, Rovaris M, Valsasina P, Wolinsky J, Comi G, Filippi M (2004) Measurement error of two different techniques for brain atrophy assessment in multiple sclerosis. Neurology 62:1432-1434.

Squitieri F, Cannella M, Simonelli M, Sassone J, Martino T, Venditti E, Ciammola A, Colonnese C, Frati L, Ciarmiello A (2009) Distinct brain volume changes correlating with clinical stage, disease progression rate, mutation size, and age at onset prediction as early biomarkers of brain atrophy in Huntington's disease. CNS neuroscience & therapeutics 15:1-11.

Stoffers D, Sheldon S, Kuperman JM, Goldstein J, Corey-Bloom J, Aron AR (2010) Contrasting gray and white matter changes in preclinical Huntington disease: an MRI study. Neurology 74:1208-1216.

Thieben MJ, Duggins AJ, Good CD, Gomes L, Mahant N, Richards F, McCusker E, Frackowiak RSJ (2002) The distribution of structural neuropathology in pre-clinical Huntington's disease. Brain 125:1815-1828.

Weaver KE, Richards TL, Liang O, Laurino MY, Sami A, Aylward EH (2009) Longitudinal diffusion tensor imaging in Huntington's Disease. Exp Neurol.

Woolrich MW, Jbabdi S, Patenaude B, Chappell M, Makni S, Behrens T, Beckmann C, Jenkinson M, Smith SM (2009) Bayesian analysis of neuroimaging data in FSL. Neuroimage 45:S173-186.

Zhang Y, Brady M, Smith S (2001) Segmentation of brain MR images through a hidden Markov random field model and the expectation-maximization algorithm. IEEE Trans Med Imaging 20:45-57.

CHAPTER 3

Basal ganglia atrophy in prodromal Huntington's disease is detectable over one year using automated segmentation

ABSTRACT

Background: Future clinical trials of neuroprotection in prodromal Huntington's (known as *preHD*) require sensitive *in vivo* imaging biomarkers to track disease progression over the shortest period. Since basal ganglia atrophy is the most prominent structural characteristic of Huntington's pathology, systematic assessment of longitudinal subcortical atrophy holds great potential for future biomarker development.

Methods: We studied 36 preHD and 22 age-matched controls using a novel method to quantify regional change from T_1-weighted structural images acquired one year apart. We assessed cross-sectional volume differences and longitudinal volumetric change in seven subcortical structures – the accumbens, amygdala, caudate, hippocampus, pallidum, putamen, and thalamus.

***Results*:** At baseline, accumbens, caudate, pallidum, and putamen volumes were reduced in preHD vs. controls (all $p<.01$). Longitudinally, atrophy was greater in preHD than controls in the caudate, pallidum, and putamen (all $p<.01$). Each structure showed a large between-group effect size, especially the pallidum where Cohen's *d* was 1.21. Using pallidal atrophy as a biomarker, we estimate that a hypothetical one-year neuroprotection study would require only 35 preHD per arm to detect a 50% slowing in atrophy and only 138 preHD per arm to detect a 25% slowing in atrophy.

Conclusions: The effect sizes calculated for preHD basal ganglia atrophy over one year are some of the largest reported to date. Consequently, this translates to strikingly small sample size estimates that will greatly facilitate any future neuroprotection study. This underscores the utility of this automatic image segmentation and longitudinal nonlinear registration method for upcoming studies of preHD and other neurodegenerative disorders.

INTRODUCTION

Intense efforts are underway to develop therapeutic agents that modify the course of Huntington's disease (HD) (Fecke et al., 2009). For example, methods such as RNA interference have shown potential in mouse models of HD by reducing the expression of the mutant gene (Boudreau et al., 2009). However, before such strategies can be translated towards human benefit, the validation of disease-sensitive biomarkers is crucial. This is especially important for the prodromal stage of HD (also known as premanifest HD (Tabrizi et al., 2011), preclinical HD (Aylward, 2007, Bohanna et al., 2008), or abbreviated preHD (Aylward, 2007, Bohanna et al., 2008, Tabrizi et al., 2011)), i.e. before the onset of major neuronal cell death (Aylward, 2007, Bohanna et al., 2008). Additionally, the most useful biomarkers are those that are automated (which will facilitate multi-center deployment) and that can identify longitudinal change over a short period of time (e.g. one year).

Structural magnetic resonance imaging (MRI) has emerged as a strong potential source of preHD biomarkers. When comparing preHD with controls, cross-sectional structural differences are evident in cortical gray matter (Rosas et al., 2005, Nopoulos et al., 2007, Tabrizi et al., 2009, Paulsen et al., 2010, Stoffers et al., 2010), white matter (Squitieri

et al., 2009, Tabrizi et al., 2009, Paulsen et al., 2010, Stoffers et al., 2010), and subcortical structures, especially the striatum (Aylward et al., 1994, Aylward et al., 1996, Paulsen et al., 2006, Tabrizi et al., 2009, van den Bogaard et al., 2010). However, longitudinal studies that assess the magnitude of neurodegeneration across time can provide better insights for preHD biomarker development. While early longitudinal studies of volumetric change used manual tracing to delineate structures such as the caudate (Aylward et al., 1997, Aylward et al., 2004) – something both time consuming and prone to error due to inter-rater variability – recent studies have employed automated analysis methods (Kipps et al., 2005, Henley et al., 2009, Hobbs et al., 2009a, Hobbs et al., 2009b, Aylward et al., 2010, Wild et al., 2010, Tabrizi et al., 2011, Majid et al., 2011a). However, the available automated methods differ in sensitivity (to change across time) and specificity (in terms of the precision of affected structures). Several methods focus on whole-brain volumetric change, which can be detected in a period as short as one year with moderate between-group effect sizes (Tabrizi et al., 2011, Majid et al., 2011a). One of these analyses, by Majid and colleagues (2011a), also estimated the number of individuals needed to detect a 50% slowing of atrophy in a hypothetical neuroprotection study, with the result that both treatment and placebo arms would require 74 preHD individuals, assuming they are within 6 years of clinical onset (i.e. near-onset).

An alternative to the whole-brain approach is to use regional volumetric measures, e.g. biomarkers focused on individual basal ganglia structures. These may be more sensitive to preHD change and thus require smaller sample sizes for future studies. In a two-year follow-up of the PREDICT-HD study, Aylward and colleagues (2010) showed greater preHD

longitudinal change compared to controls in the caudate, putamen, pallidum, and thalamus. The effect sizes of these changes were moderate, ranging between 0.50 and 0.75, and the authors calculated that approximately 150 to 400 near-onset preHD individuals would be needed to detect a 50% slowing in atrophy.

In the above study, Aylward and colleagues (2010) determined longitudinal change by taking the difference of volumetric measures obtained separately from the T_1 image at each timepoint. However, an alternative method of longitudinal analysis is to determine change by registering the two T_1 images together. This reduces variability and leads to larger between-group effect sizes. One such tool is the Caudate-specific Boundary Shift Integral (C-BSI) (Hobbs et al., 2009b, Tabrizi et al., 2011). Whereas Aylward and colleagues (2010) report a moderate two-year caudate atrophy effect size of 0.6, this effect size increased to 0.9 when using C-BSI for the same two-year period (Hobbs et al., 2009b). Furthermore, C-BSI is also sensitive enough to detect preHD caudate atrophy in a shorter one-year period, increasing the feasibility of any future study (Tabrizi et al., 2011).

A limitation of the C-BSI method is that it is constrained to the caudate, yet change in other subcortical structures could be even greater. Indeed, cross-sectional volume differences between preHD and controls suggest that atrophy in the accumbens, pallidum, and putamen is more predictive of HD motor disturbances than atrophy in the caudate (van den Bogaard et al., 2010). In addition, Aylward and colleagues (2010) report that two-year putamen and pallidum longitudinal atrophy exceeds that of the caudate.

Here, we acquired T_1-weighted images at two timepoints one year apart. We used the Quarc (Quantitative anatomical regional change) analysis method, recently developed

and validated in the Alzheimer's Disease Neuroimaging Initiative (ADNI) (Holland et al., 2009, Holland and Dale, 2011). This measured longitudinal change in seven subcortical structures (accumbens, amygdala, caudate, hippocampus, pallidum, putamen, and thalamus). Here we show that this produces a very precise assessment of longitudinal change capable of detecting preHD atrophy with large effect sizes within just one year.

METHODS

Participants

There were 38 preHD (≥ 38 CAG repeats) and 22 healthy age- and sex-matched control participants. Consent was provided in accordance with an Institutional Review Board at the University of California, San Diego. Participants were studied longitudinally, on two visits, with a one-year interval between visits (Table 3.1).

Global cognitive ability was measured using the Mini-Mental State Exam (MMSE) (Folstein et al., 1975) at both timepoints. A movement disorder specialist (JCB) evaluated the preHD participants with the Unified Huntington's Disease Rating Scale (UHDRS) (Huntington's Study Group, 1996). Based on this scale, participants were assigned a 'motor score' (range: 0 to 124) and were rated as to the level of confidence that the presenting motor abnormalities represent symptoms of HD (range: 0 to 4). A confidence rating of 0 represents a normal evaluation and no motor abnormalities, a rating of 1 represents < 50% confidence of an HD diagnosis, and a rating of 4 represents a definitive HD diagnosis. UHDRS scores were obtained from all participants at baseline and only from preHD participants at follow-up. All participants were rated below 2 at baseline, confirming preHD

status. At follow-up, two initially preHD participants were rated 4, indicating conversion to manifest HD. These were removed from the analysis, leaving a preHD group of 36. The length of the CAG repeat expansion was used to calculate estimated years-to-onset (YTO) using both the Aylward and Langbehn methods (Aylward et al., 1996, Langbehn et al., 2004).

MR Image acquisition

Data were acquired with a General Electric (Milwaukee, WI, USA) 1.5 T EXCITE HDx scanner (Software Version 14x) with an 8-channel phased-array head coil. Image acquisition included a General Electric "PURE" calibration sequence and a high-resolution three-dimensional T_1-weighted IRSPGR sequence (echo time = 2.798 msec, repetition time = 6.496 msec, inversion time = 600 msec, flip angle = 12˚, bandwidth = 244.141 Hz/pixel, field of view = 24 cm, matrix = 256x192, slice thickness = 1.2 mm).

Baseline cross-sectional analysis of regional volume

Baseline images were corrected for spatial distortion due to gradient non-linearity (Jovicich et al., 2006) and B_1 field inhomogeneity (Sled et al., 1998). Volumetric segmentation (Fischl et al., 2002, Fischl et al., 2004) – using a probabilistic atlas and applying a Bayesian classification to assign a neuroanatomic label to each voxel – was performed using a data analysis pipeline based on the FreeSurfer software package (http://surfer.nmr.mgh.harvard.edu/) and customized Matlab code. The method is fully

automated except for qualitative review by a trained operator in the case of occasional technical failures in segmentation.

The left and right volumes for each structure were summed and normalized based on a participant's total intracranial volume, e.g. (left caudate volume + right caudate volume)/intracranial volume.

Longitudinal analysis of regional volume change

The longitudinal analysis was performed on a subject-specific basis, using a recently developed method, Quarc (Quantitative anatomical regional change) (Holland et al., 2009, Holland and Dale, 2011). Follow-up MRIs for each subject were fully affine-registered to the baseline image, and intensities were brought to local agreement (i.e. corrected for relative B_1-induced intensity distortion) using an iterative procedure. A deformation field was then calculated from the nonlinear registration and used to align scans at the sub-voxel level. From the deformation field a volume-change field is calculated, which, when integrated over the baseline segmentation for each subcortical structure, gives that structure's percentage volume change from baseline. The percentage change of the left and right hemisphere structures was then averaged and compared between groups.

Sample size calculations and power analysis

Based on our longitudinal results we estimated the sample sizes needed for a hypothetical two-arm study of neuroprotection in preHD. For each arm of the study

(treatment vs. placebo), the minimum sample size required to detect slowing in the yearly atrophy rate can be computed using the following formula (Fitzmaurice et al., 2004):

$$n = 2\sigma^2(z_{(1-\alpha/2)} + z_{power})^2/(\Delta\beta)^2$$

Here, σ^2 is the variance of the longitudinal change for a particular structure in the preHD group, and z_x is the *x*th quantile of the standard normal distribution. Sample sizes were calculated for a study powered at either 90% or 80% and with a 5% two-sided significance level (α). Δ denotes the desired detectible slowing in atrophy, calculated for both a 50% and 25% estimate. β denotes the magnitude of the yearly atrophy relative to controls (Fox et al., 2000), calculated by taking the difference between the mean change of the preHD group versus an age- and sex-based pair-matched subset of control subjects. Sample size 95% confidence intervals (CIs) were computed using the Matlab bootstrapping function *bootci* with 100,000 iterations.

RESULTS

Participant characteristics

At study entry, control and preHD groups had similar age and MMSE scores (p=.941 and .132, respectively) (Table 3.1). For MMSE, ANOVA [group x timepoint] revealed no between-group difference ($F(1,56)=1.347$, p=.25), but did show a main effect of time ($F(1,56)=7.658$, p=.008), with scores decreasing in both groups as time progressed. There was no interaction (F<1). Therefore, the groups were well-matched longitudinally. UHDRS motor scores were significantly elevated in preHD compared to controls at baseline

(t[56]=3.809, p<.001), consistent with subtle motor signs, albeit insufficient to meet diagnostic criteria for manifest HD. Follow-up UHDRS motor scores were significantly elevated in the preHD group after the one-year duration, indicating a slightly worsening condition (t[35]=3.292, p=.002).

Baseline cross-sectional analysis

At baseline, volume was reduced in the accumbens, amygdala, caudate, pallidum, and putamen in preHD compared to controls (Table 3.2, Figure 3.1A). After Bonferroni correction, group differences were significant only for the accumbens, caudate, pallidum, and putamen. Within the preHD group, those patients with greater atrophy of the amygdala and pallidum had greater subclinical motor signs on the UHDRS (both p<.05) (Table 3.3). Furthermore, atrophy correlated with greater proximity to disease onset – caudate, pallidum, and putamen atrophy correlated with both the Langbehn and Aylward years-to-onset estimates, while accumbens atrophy correlated with the Langbehn estimate alone (all p<.05) (Table 3.3).

Longitudinal analysis using Quarc

Using the Quarc algorithm to assess longitudinal change, preHD showed greater change in the amygdala, caudate, pallidum, and putamen (Table 3.4, Figure 3.1B). After Bonferroni correction for multiple comparisons, the atrophy was significant only in the caudate, pallidum, and putamen. One-year preHD atrophy in each of these three structures correlated weakly with one or both years-to-onset estimates. Caudate change correlated

with the Aylward estimate (r[36]=.379, p=.022) but not with the Langbehn estimate (r[36]=.313, p=.063). Putamen change correlated with the Langbehn estimate (r[36]=.334, p=.046) but not with the Aylward estimate (p=.34). Pallidal change correlated with both the Aylward estimate (r[36]=.371, p=.026) and the Langbehn estimate (r[36]=.341, p=.042). Longitudinal change did not correlate with change in UHDRS motor score in any brain structure (all p>.1).

Sample size estimates

We estimated the sample sizes needed to power a two-arm neuroprotective treatment study (treatment vs. placebo) designed to detect either a 50% or 25% slowing of atrophy in each of the subcortical structures for which group differences were identified (Table 3.5).

Relative to controls, detecting a 50% slowing in atrophy with 90% power requires sample sizes of 103 for the caudate (95% CI: 91–2038), 58 for the putamen (95% CI: 53–829), and 35 for the pallidum (95% CI: 26–213) (Figure 3.1D). Detecting a more moderate 25% slowing with the same power requires sample sizes of 412 for the caudate (95% CI: 360–8038), 230 for the putamen (95% CI: 213–3221), and 138 for the pallidum (95% CI: 104–822).

Stratifying based on proximity to disease onset has been shown to further reduce the sample sizes needed (Aylward et al., 2010, Tabrizi et al., 2011, Majid et al., 2011a). Using a subset of individuals in our preHD sample closest to disease onset (18 preHD out of total 36; ≤11.7 years to onset, Langbehn method), we find that sample sizes reduce only

modestly. For instance, to detect a 25% slowing in pallidal atrophy, 115 individuals (95% CI: 57-597) would be required in each study arm with such stratification vs. 138 without (see above).

DISCUSSION

We used Freesurfer-based automatic segmentation to examine cross-sectional volume differences and Quarc to examine longitudinal volume change in preHD vs. controls. Seven subcortical structures were investigated at baseline and over a one-year period. At baseline, the accumbens, caudate, pallidum, and putamen were significantly smaller in preHD vs. controls. Moreover, the longitudinal analysis after follow-up showed that neurodegeneration in preHD can be identified within merely one year with large effect sizes for caudate, putamen and pallidum. For the pallidum, which showed the largest effect size, we estimate that only 35 preHD individuals would be required in both the treatment and placebo arms of a hypothetical study to detect a 50% slowing in atrophy with 90% power.

One-year subcortical atrophy did not correlate with change in UHDRS motor score. This, however, is expected in this preHD population, in whom, by definition, overt motor symptoms are too low to warrant diagnosis of manifest HD. Indeed, one of the strongest motivations for developing MRI biomarkers is to detect brain changes *before* symptoms emerge.

Striatal medium spiny neurons are disproportionally affected in HD (Graveland et al., 1985). Consistent with this, cross-sectional preHD volume reductions were found in those structures populated by medium spiny cell bodies (i.e. the accumbens, caudate, and

putamen, which collectively make up the striatum). Changes were also found in the pallidum, which receives axonal input from the striatum. Many cross-sectional studies have corroborated this pallidal involvement (Aylward et al., 1994, Aylward et al., 1996, Campodonico et al., 1998, Jurgens et al., 2008, Paulsen et al., 2010, van den Bogaard et al., 2010). It should be noted that the pallidal changes we see are unlikely due to the death of cells whose bodies are within the pallidum. In histopathological studies of late stage HD, for instance, volume loss in the pallidum is accompanied by a relative sparing of neuronal cell count and an increase in cell density (Wakai et al., 1993). This suggests that pallidal volume loss may be due to the loss of striatopallidal fibers projecting from striatal medium spiny neurons (see Douaud et al. (2009) for in vivo imaging evidence). Both striatal and pallidal atrophy in preHD thus may result from the same pathological process of striatal medium spiny neuron loss.

Effect sizes for cross-sectional comparisons were large for each of these structures, ranging from 0.81 for the caudate to 1.50 for the putamen. Furthermore, volumes in all these structures correlated with years-to-onset estimates, suggesting a progressive course of the disease that our subsequent longitudinal findings confirm.

Within the one-year period, Quarc successfully detected volumetric change in the caudate, pallidum, and putamen with large effect sizes for all three structures (0.88, 1.21, and 1.12, respectively, Figure 3.1C). By contrast, the corresponding effect sizes reported in the two-year follow-up of the PREDICT-HD study were moderate (0.60, 0.67, and 0.63, respectively) (Aylward et al., 2010). This suggests that Quarc may provide a definitive improvement in identifying change in shorter amounts of time. Furthermore, Quarc extends

the benefit of tools that have been specialized for longitudinal analysis, such as the Caudate Boundary Shift Integral (C-BSI) method (Hobbs et al., 2009b, Tabrizi et al., 2011), to a greater number of subcortical structures. Indeed, as we have shown, yearly preHD atrophy in both the pallidum and putamen shows considerably larger effect sizes compared to caudate atrophy in this and other studies (Aylward et al., 2010, van den Bogaard et al., 2010) and may thus serve as a stronger biomarker.

Confirming the benefits of Quarc over other analysis tools will require a comparison of each method applied to the same subject data, which we have not done here. We cannot therefore conclude that Quarc is superior to all other methods previously used to assess longitudinal change in preHD. However, head-to-head comparison of similar methods in the ADNI dataset has revealed benefits of Quarc (in terms of larger identifiable effect sizes in detecting Alzheimer's disease-related changes) when compared to the standard FreeSurfer-cross-sectional and FreeSurfer-longitudinal methods (Holland and Dale, 2011). These are related to the method previously used by Aylward and colleagues (2010). Additionally, Quarc also showed some slight benefit in whole-brain quantification of change compared to the standard BSI method (KN-BSI), though this was not found to be significant (Holland and Dale, 2011). Thus, while the other longitudinal analysis methods applied to preHD may also yield results as strong as what we have shown here, our findings do flag the use of Quarc as having great potential in future studies of preHD neuroprotection.

These findings – effect sizes larger than any previously reported in preHD research to date – have clinical relevance in translating into smaller sample sizes required for such future therapeutic trials. Here, we calculated that approximately 103 preHD individuals

would be required in each therapeutic study arm (treatment vs. placebo) to detect a 50% slowing in caudate atrophy with 90% power. This dropped to 58 preHD individuals in each study arm for the putamen and to only 35 for the pallidum (Figure 3.1D).

Focusing on a subgroup of preHD participants who are closer to disease onset has been shown to reduce sample sizes (Aylward et al., 2010, Tabrizi et al., 2011, Majid et al., 2011a). Here we find only moderate sample size reductions with this approach. Although subject stratification does provide some benefit, Quarc's ability to yield small, feasible sample sizes in a non-stratified preHD population further argues for the strength of the Quarc longitudinal methodology.

By contrast, the two-year follow-up of the PREDICT-HD study estimated sample sizes of 235 near-onset preHD individuals (≤10 years to onset, Langbehn method) to detect a 50% slowing of caudate atrophy and 188 for pallidal atrophy (Aylward et al., 2010). The most useful biomarker reported by the PREDICT-HD study, however, was change in cerebral white matter volume, which we did not study. Even with this measure, an estimated 61 near-onset preHD individuals are needed to detect a 50% slowing in atrophy over two years (Aylward et al., 2010). Thus, Quarc may offer the ability to detect a similar therapeutic improvement with fewer preHD individuals, within a time period that is half the length, and without constraints on participant inclusion based on proximity to estimated disease onset.

Future HD therapies are likely to have a moderate protective effect, and the expectation of a 50% slowing in atrophy may be difficult to achieve. A moderate expectation of a 25% slowing is more likely but will also require larger sample sizes (see

Table 3.5). Nonetheless, the Quarc-based estimates still remain well within feasibility, requiring only 138 individuals in each study arm when using pallidal atrophy as a biomarker.

In summary, our results complement and extend recent results, showing that automated subcortical segmentation combined with longitudinal nonlinear registration can detect disease-related volumetric change within a short one-year time period. We used Quarc, which evidently shows improvements over available methods, be they whole brain (Tabrizi et al., 2011, Majid et al., 2011a) or regionally specific (Hobbs et al., 2009b, Aylward et al., 2010, Tabrizi et al., 2011). Quarc can simultaneously evaluate longitudinal change in several subcortical structures, yielding large effect sizes for the caudate, pallidum, and putamen between preHD and controls. In the case of the pallidum, effect sizes were larger than any yet reported. This sets the stage for large-scale clinical trials of neuroprotective agents, which will be highly feasible given the relatively small sample size and study length requirements demonstrated here.

ACKNOWLEDGEMENTS

This chapter, in full, is a reprint of material as it appears in Majid, Aron, Thompson, Sheldon, Hamza, Stoffers, Holland, Goldstein, Corey-Bloom, and Dale, *Movement Disorders*, 2011. I thank Matt Erhart for technical assistance for technical assistance with image processing and CHDI for financial support. The dissertation author was the primary investigator and author of this paper.

Table 3.1: *Participant characterization by group*

	Controls (N=22)		PreHD (N=36)	
	Baseline	Follow-up	Baseline	Follow-up
Age at start (yrs, mean± SD)	40.1±12.2		40.4±10.3	
Sex (F/M)	15/7		20/16	
Between-scan interval (yrs, mean ± SD)	1.0±.1		1.0±.1	
MMSE (mean ± SD) *	28.8±1.4	28.4±1.7	29.2±1.0	28.4±1.5
Number of CAG repeats (mean ± SD) [range]	N/A		42.4±2.4 [38–48]	
Estimated years-to-onset, Aylward method (yrs, mean ± SD)	N/A		6.3±7.3	
Estimated years-to-onset, Langbehn method (yrs, mean ± SD)	N/A		14.4±7.2	
UHDRS motor score (mean ± SD) **	0.1±0.3	N/A	1.5±1.7	3.8±4.5
UHDRS confidence score (*score*: # of participants)	*0*: 22	N/A	*0*: 24 *1*: 12	*0*: 16 *1*: 10 *2*: 9 *3*: 1

SD = standard deviation, MMSE = Mini-mental state exam, CAG = cytosine-adenine-guanine, UHDRS = Unified Huntington's Disease Rating Scale, PreHD = prodromal/premanifest Huntington's disease, N/A = not applicable

* ANOVA revealed main effect of time (p=.008) but no effect of group.

** Significantly different between groups at baseline (p<.001) and between timepoints in preHD group (p=.002). UHDRS was not obtained for controls at follow-up.

Table 3.2: *Baseline volume differences*

	Control (N=22)	PreHD (N=36)	*t*-statistic (56 d.f.)	*p*-value	Effect size (Cohen's *d*)
Accumbens*	0.08 ± 0.01	0.07 ± 0.01	3.100	.003	0.84
Amygdala	0.21 ± 0.02	0.20 ± 0.02	2.107	.040	0.58
Caudate*	0.46 ± 0.05	0.42 ± 0.06	2.949	.005	0.81
Hippocampus	0.54 ± 0.04	0.51 ± 0.05	1.809	.076	0.49
Pallidum*	0.23 ± 0.02	0.21 ± 0.03	3.166	.002	0.88
Putamen*	0.67 ± 0.06	0.57 ± 0.08	5.379	<.001	1.50
Thalamus	0.89 ± 0.07	0.88 ± 0.08	0.609	.545	0.17

Values indicate percent total intracranial volume summed bilaterally ± standard deviation
* Significantly different after Bonferroni correction ($p < .05/7 = .007$)

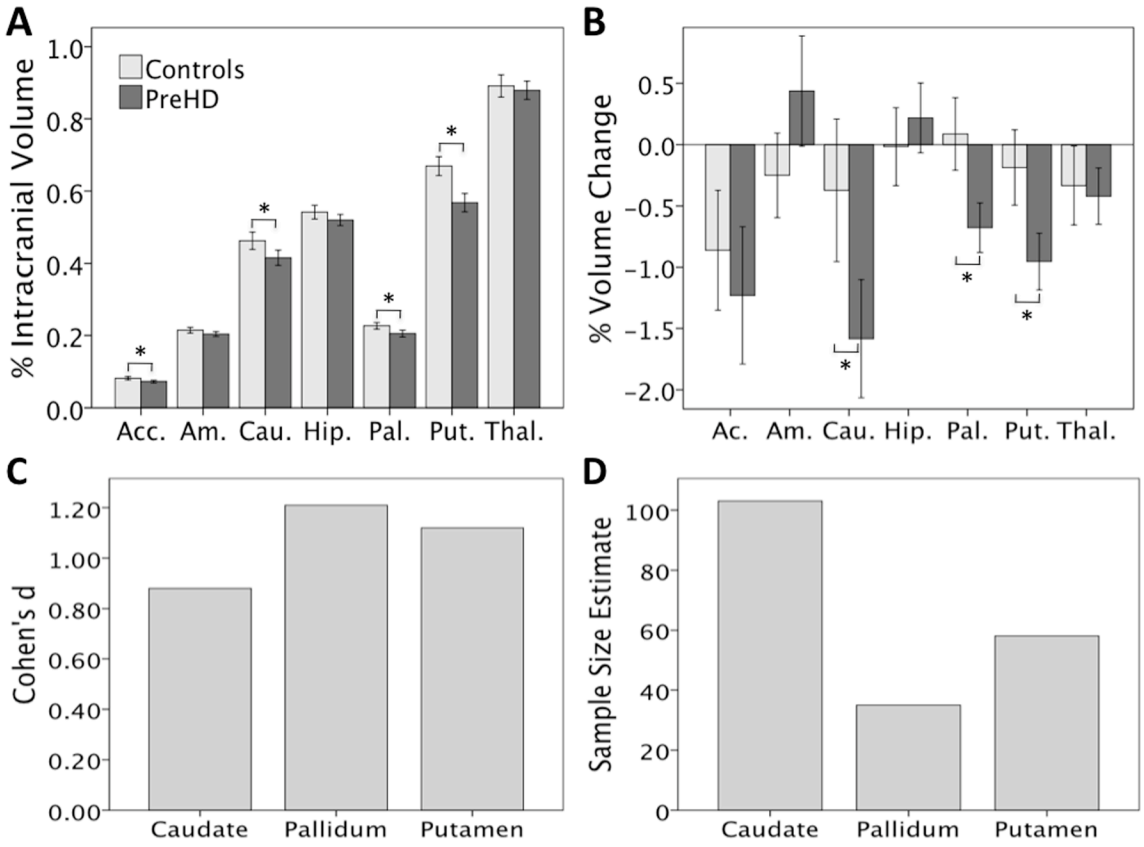

Figure 3.1: *Subcortical atrophy over one year can provide powerful preHD biomarkers.* A) Cross-sectional differences at baseline. PreHD volume reductions in the accumbens, caudate, pallidum, and putamen were significant after Bonferroni correction. B) Longitudinal volume change. One-year percent volume change in the caudate, pallidum, and putamen was significantly greater in preHD after Bonferroni correction. C) Longitudinal between-group effect sizes for structures with significant preHD change. D) Estimated sample sizes needed for both arms (treatment vs. placebo) of a hypothetical neuroprotection study to detect a 50% slowing in atrophy of a particular structure. The study is powered at 90% with a 5% two-sided significance level.
Abbreviations: Ac. – Accumbens; Am. – Amygdala; Cau. – Caudate; Hip. – Hippocampus; Pal. – Pallidum; Put. – Putamen; Thal. – Thalamus.

Table 3.3: *Baseline volume correlations to preHD disease burden (N=36)*

	Langbehn YTO	Aylward YTO	UHDRS Motor
Accumbens	.403*	.205	.149
Amygdala	.322	.321	.434*
Caudate	.379*	.453**	.269
Hippocampus	.248	.297	.239
Pallidum	.358*	.357*	.338*
Putamen	.467**	.439**	.269
Thalamus	.269	.187	.129

Values indicate Pearson Correlation Coefficients. For YTO (years-to-onset) estimates, smaller volumes correlated with greater proximity to estimated disease onset. For UHDRS Total motor score, smaller volumes correlated with greater motor symptoms.
* Significantly different at $p < .05$
** Significantly different after Bonferroni correction

Table 3.4: *Percent volume change from baseline over one year*

	Control (N=22)	PreHD (N=36)	*t*-statistic (56 d.f.)	*p*-value	Effect size (Cohen's *d*)
Accumbens	-0.86 ± 1.10	-1.23 ± 1.66	0.924	.36	0.26
Amygdala	-0.25 ± 0.78	0.44 ± 1.33	-2.200	.032	0.63
Caudate*	-0.37 ± 1.31	-1.58 ± 1.42	3.234	.002	0.88
Hippocampus	-0.02 ± 0.72	0.22 ± 0.84	-1.087	.282	0.30
Pallidum*	0.09 ± 0.67	-0.68 ± 0.59	4.541	<.001	1.21
Putamen*	-0.19 ± 0.69	-0.95 ± 0.68	4.132	<.001	1.12
Thalamus	-0.33 ± 0.73	-0.42 ± 0.68	0.461	.646	0.12

Values indicate percent volume change averaged bilaterally ± standard deviation
* Significantly different after Bonferroni correction ($p < .05/7 = .007$)

Table 3.5: *Power analysis*

Study Power	90%		80%	
Atrophy Slowing	50%	25%	50%	25%
Caudate	103 (91–2038)	412 (360–8038)	77 (68–1521)	308 (269–5999)
Pallidum	35 (26–213)	138 (104–822)	26 (20–159)	103 (78–614)
Putamen	58 (53–829)	230 (213–3221)	43 (40–619)	172 (159–2404)

Sample sizes needed to detect a given slowing in yearly atrophy in a two-arm neuroprotection study using a 5% two-sided significance level compared to controls. Parentheses indicated 95% confidence interval.

References

Aylward E, Brandt J, Codori A, Mangus R, Barta P, Harris G (1994) Reduced basal ganglia volume associated with the gene for Huntington's disease in asymptomatic at-risk persons. Neurology 44:823-828.

Aylward E, Li Q, Stine O, Ranen N, Sherr M, Barta P, Bylsma F, Pearlson G, Ross C (1997) Longitudinal change in basal ganglia volume in patients with Huntington's disease. Neurology 48:394-399.

Aylward EH (2007) Change in MRI striatal volumes as a biomarker in preclinical Huntington's disease. Brain research bulletin 72:152-158.

Aylward EH, Codori AM, Barta PE, Pearlson GD, Harris GJ, Brandt J (1996) Basal ganglia volume and proximity to onset in presymptomatic Huntington disease. Arch Neurol 53:1293-1296.

Aylward EH, Nopoulos PC, Ross CA, Langbehn DR, Pierson RK, Mills JA, Johnson HJ, Magnotta VA, Juhl AR, Paulsen JS, Group tP-HIaCotHS (2010) Longitudinal change in regional brain volumes in prodromal Huntington disease. J Neurol Neurosurg Psychiatr.

Aylward EH, Sparks BF, Field KM, Yallapragada V, Shpritz BD, Rosenblatt A, Brandt J, Gourley LM, Liang K, Zhou H, Margolis RL, Ross CA (2004) Onset and rate of striatal atrophy in preclinical Huntington disease. Neurology 63:66-72.

Bohanna I, Georgiou-Karistianis N, Hannan AJ, Egan GF (2008) Magnetic resonance imaging as an approach towards identifying neuropathological biomarkers for Huntington's disease. Brain research reviews 58:209-225.

Boudreau RL, Mcbride JL, Martins I, Shen S, Xing Y, Carter BJ, Davidson BL (2009) Nonallele-specific silencing of mutant and wild-type huntingtin demonstrates therapeutic efficacy in Huntington's disease mice. Mol Ther 17:1053-1063.

Campodonico J, Aylward E, Codori A, Young C, Krafft L, Magdalinski M, Ranen N, Slavney P, Brandt J (1998) When does Huntington's disease begin? J Int Neuropsychol Soc 4:467-473.

Douaud G, Behrens TE, Poupon C, Cointepas Y, Jbabdi S, Gaura V, Golestani N, Krystkowiak P, Verny C, Damier P, Bachoud-Lévi A-C, Hantraye P, Remy P (2009) In vivo evidence for the selective subcortical degeneration in Huntington's disease. Neuroimage 46:958-966.

Fecke W, Gianfriddo M, Gaviraghi G, Terstappen GC, Heitz F (2009) Small molecule drug discovery for Huntington's Disease. Drug Discov Today 14:453-464.

Fischl B, Salat D, Busa E, Albert M, Dieterich M, Haselgrove C, van der Kouwe A, Killiany R, Kennedy D, Klaveness S, Montillo A, Makris N, Rosen B, Dale A (2002) Whole brain segmentation: automated labeling of neuroanatomical structures in the human brain. Neuron 33:341-355.

Fischl B, Salat DH, van der Kouwe AJW, Makris N, Ségonne F, Quinn BT, Dale AM (2004) Sequence-independent segmentation of magnetic resonance images. Neuroimage 23 Suppl 1:S69-84.

Fitzmaurice G, Laird N, Ware J (2004) Applied Longitudinal Analysis. New York: John Wiley and Sons.

Folstein M, Folstein S, McHugh P (1975) "Mini-mental state". A practical method for grading the cognitive state of patients for the clinician. J Psychiatr Res 12:189-198.

Fox NC, Cousens S, Scahill R, Harvey RJ, Rossor MN (2000) Using serial registered brain magnetic resonance imaging to measure disease progression in Alzheimer disease: power calculations and estimates of sample size to detect treatment effects. Arch Neurol 57:339-344.

Graveland GA, Williams RS, DiFiglia M (1985) Evidence for degenerative and regenerative changes in neostriatal spiny neurons in Huntington's disease. Science 227:770-773.

Huntington Study Group (1996) Unified Huntington's Disease Rating Scale: reliability and consistency. Mov Disord 11:136-142.

Henley SMD, Wild EJ, Hobbs NZ, Frost C, Macmanus DG, Barker RA, Fox NC, Tabrizi SJ (2009) Whole-brain atrophy as a measure of progression in premanifest and early Huntington's disease. Mov Disord 24:932-936.

Hobbs NZ, Henley SMD, Ridgway G, Wild EJ, Barker R, Scahill RI, Barnes J, Fox NC, Tabrizi S (2009a) The Progression of Regional Atrophy in Premanifest and Early Huntington's Disease: A Longitudinal Voxel-Based Morphometry Study. J Neurol Neurosurg Psychiatr.

Hobbs NZ, Henley SMD, Wild EJ, Leung KK, Frost C, Barker RA, Scahill RI, Barnes J, Tabrizi SJ, Fox NC (2009b) Automated quantification of caudate atrophy by local registration of serial MRI: evaluation and application in Huntington's disease. Neuroimage 47:1659-1665.

Holland D, Brewer JB, Hagler DJ, Fenema-Notestine C, Dale AM, the Alzheimer's Disease Neuroimaging Initiative (2009) Subregional neuroanatomical change as a biomarker for Alzheimer's disease. Proc Natl Acad Sci USA 106:20954-20959.

Holland D, Dale AM (2011) Nonlinear registration of longitudinal images and measurement of change in regions of interest. Med Image Anal.

Jovicich J, Czanner S, Greve D, Haley E, van der Kouwe A, Gollub R, Kennedy D, Schmitt F, Brown G, Macfall J, Fischl B, Dale A (2006) Reliability in multi-site structural MRI studies: effects of gradient non-linearity correction on phantom and human data. Neuroimage 30:436-443.

Jurgens CK, van de Wiel L, van Es ACGM, Grimbergen YM, Witjes-Ané M-NW, van der Grond J, Middelkoop HAM, Roos RAC (2008) Basal ganglia volume and clinical correlates in 'preclinical' Huntington's disease. J Neurol 255:1785-1791.

Kipps CM, Duggins AJ, Mahant N, Gomes L, Ashburner J, McCusker EA (2005) Progression of structural neuropathology in preclinical Huntington's disease: a tensor based morphometry study. J Neurol Neurosurg Psychiatr 76:650-655.

Langbehn DR, Brinkman RR, Falush D, Paulsen JS, Hayden MR, International Huntington's Disease Collaborative Group (2004) A new model for prediction of the age of onset and penetrance for Huntington's disease based on CAG length. Clin Genet 65:267-277.

Majid DS, Stoffers D, Sheldon S, Hamza S, Thompson WK, Goldstein J, Corey-Bloom J, Aron AR (2011a) Automated structural imaging analysis detects premanifest Huntington's disease neurodegeneration within 1 year. Mov Disord.

Nopoulos P, Magnotta V, Mikos A, Paulson H, Andreasen N, Paulsen J (2007) Morphology of the cerebral cortex in preclinical Huntington's disease. The American journal of psychiatry 164:1428-1434.

Paulsen JS, Magnotta VA, Mikos AE, Paulson HL, Penziner E, Andreasen NC, Nopoulos PC (2006) Brain structure in preclinical Huntington's disease. Biol Psychiatry 59:57-63.

Paulsen JS, Nopoulos PC, Aylward E, Ross CA, Johnson H, Magnotta VA, Juhl A, Pierson RK, Mills J, Langbehn D, Nance M, PREDICT-HD Investigators and Coordinators of the Huntington's Study Group (HSG) (2010) Striatal and white matter predictors of estimated diagnosis for Huntington disease. Brain research bulletin.

Rosas HD, Hevelone ND, Zaleta AK, Greve DN, Salat DH, Fischl B (2005) Regional cortical thinning in preclinical Huntington disease and its relationship to cognition. Neurology 65:745-747.

Sled JG, Zijdenbos AP, Evans AC (1998) A nonparametric method for automatic correction of intensity nonuniformity in MRI data. IEEE Trans Med Imaging 17:87-97.

Squitieri F, Cannella M, Simonelli M, Sassone J, Martino T, Venditti E, Ciammola A, Colonnese C, Frati L, Ciarmiello A (2009) Distinct brain volume changes correlating with clinical stage, disease progression rate, mutation size, and age at onset prediction as early biomarkers of brain atrophy in Huntington's disease. CNS neuroscience & therapeutics 15:1-11.

Stoffers D, Sheldon S, Kuperman JM, Goldstein J, Corey-Bloom J, Aron AR (2010) Contrasting gray and white matter changes in preclinical Huntington disease: an MRI study. Neurology 74:1208-1216.

Tabrizi SJ, Langbehn DR, Leavitt BR, Roos RA, Durr A, Craufurd D, Kennard C, Hicks SL, Fox NC, Scahill RI, Borowsky B, Tobin AJ, Rosas HD, Johnson H, Reilmann R, Landwehrmeyer B, Stout JC, TRACK-HD Investigators (2009) Biological and clinical manifestations of Huntington's disease in the longitudinal TRACK-HD study: cross-sectional analysis of baseline data. Lancet Neurol 8:791-801.

Tabrizi SJ, Scahill RI, Durr A, Roos RA, Leavitt BR, Jones R, Landwehrmeyer GB, Fox NC, Johnson H, Hicks SL, Kennard C, Craufurd D, Frost C, Langbehn DR, Reilmann R, Stout JC, TRACK-HD Investigators (2011) Biological and clinical changes in premanifest and early stage Huntington's disease in the TRACK-HD study: the 12-month longitudinal analysis. Lancet Neurol 10:31-42.

van den Bogaard SJA, Dumas EM, Acharya TP, Johnson H, Langbehn DR, Scahill RI, Tabrizi SJ, van Buchem MA, van der Grond J, Roos RAC, TRACK-HD Investigator Group (2010) Early atrophy of pallidum and accumbens nucleus in Huntington's disease. J Neurol.

Wakai M, Takahashi A, Hashizume Y (1993) A histometrical study on the globus pallidus in Huntington's disease. J Neurol Sci 119:18-27.

Wild EJ, Henley SMD, Hobbs NZ, Frost C, Macmanus DG, Barker RA, Fox NC, Tabrizi SJ (2010) Rate and acceleration of whole-brain atrophy in premanifest and early Huntington's disease. Mov Disord 25:888-895.

CHAPTER 4

Proactive selective response suppression is implemented via the basal ganglia: functional evidence for the Indirect Pathway in humans

ABSTRACT

In the welter of everyday life, people can stop particular response tendencies without affecting others. A key requirement for such selective suppression is that subjects know in advance which responses need stopping. We hypothesized that proactively setting up and implementing selective suppression relies on the basal ganglia, and specifically, regions consistent with the inhibitory Indirect Pathway for which there is scant functional evidence in humans. Consistent with this hypothesis, we show, first, that the degree of proactive motor suppression when preparing to stop selectively (indexed by Transcranial Magnetic Stimulation, TMS) corresponds to striatal, pallidal, and frontal activation (indexed by functional MRI). Second, we demonstrate that greater striatal activation at the time of selective stopping correlates with greater behavioral selectivity. Third, we show that people with striatal and pallidal volume reductions (those with premanifest Huntington's disease) have both absent proactive motor suppression and impaired behavioral selectivity when stopping. Thus, stopping goals are used to proactively set up specific basal ganglia channels that may then be triggered to implement selective suppression. By linking this suppression to the striatum and pallidum, these results provide compelling functional evidence in humans of the basal ganglia's inhibitory Indirect Pathway.

INTRODUCTION

Stopping action can occur in several forms. A simple form of stopping occurs in reaction to an infrequent external signal (Verbruggen and Logan, 2008, Chambers et al., 2009, Boehler et al., 2010). Such *reactive* stopping has broad motor effects, suggesting use of a global inhibitory mechanism (Badry et al., 2009, Majid et al., 2011, Cai et al., 2012, Greenhouse et al., 2012). Some circumstances, however, may demand *selective* stopping targeted at a particular response (Aron and Verbruggen, 2008, Majid et al., 2011). Experimentally, this can be induced by requiring the subject to initiate two responses and then stopping one while continuing the other. For such stopping to be truly *mechanistically* selective, as opposed to nonselectively stopping all responses before re-initiating the one that must continue (cf. Bissett and Logan, 2013), it appears critical that subjects use stopping goals to prepare in advance which response channels might have to be stopped (Claffey et al., 2010, Cai et al., 2011). We refer to this as 'proactive selective stopping.' As this reflects a more ecologically valid form of control than simple reactive stopping (Aron, 2011), understanding its neural correlates could have wider implications, especially for disorders of response control.

Here we hypothesized that proactive selective stopping is implemented via fronto-basal ganglia signaling through the striatum and pallidum. These nodes are involved in two classical basal ganglia pathways: the Direct and Indirect Pathways. The Indirect Pathway is of particular relevance to proactive selective stopping as its net effect upon thalamocortical drive is inhibitory, and it has the appropriate anatomical selectivity (Hazrati and Parent, 1992, Albin et al., 1995). While this pathway features prominently in movement disorders

and cognitive neuroscience alike (Penney and Young, 1983, Vonsattel et al., 1985, Mink, 1996, Jahfari et al., 2011), functional evidence *in humans* is scant. This is because of limitations in imaging resolution, the paucity of behavioral tasks known to engage selective stopping, and the difficulty in showing that a neural substrate in humans is *necessary* for behavior.

With a behavioral paradigm for examining proactive selective stopping, wherein each trial has both a *preparing-to-stop* and an *outright-stopping* phase (Aron and Verbruggen, 2008, Cai et al., 2011, Majid et al., 2011), we investigated the underlying neural mechanisms using three methods. First, we used single-pulse TMS over the motor cortex as a probe of corticomotor excitability. We aimed to replicate our earlier result (Cai et al., 2011) of proactive suppression of response channels when preparing to stop selectively. Second, we used fMRI in the same subjects to test whether a) proactive suppression measured by TMS would correspond to striatal and pallidal fMRI activation (indicating that basal ganglia channels are used to set up proactive suppression); and b) whether these basal ganglia 'suppression channels' would be retriggered when stopping outright. Third, we aimed to evaluate if striatum and pallidum are *necessary* for proactive selective stopping by studying premanifest Huntington's disease (preHD) individuals who have MRI-confirmed damage of these structures, examining whether they are impaired in proactive selective stopping compared to matched controls.

METHODS

Subjects

Experiment 1

Eighteen healthy right-handed subjects (8 males, 10 females, mean age: 21.6±2.4 years) participated in a TMS session and then an fMRI session. All subjects provided written consent in accordance with the Institutional Review Board (IRB) guidelines of the University of California, San Diego (UCSD). They also completed a TMS safety-screening questionnaire (Rossi et al., 2009) and an fMRI safety-screening form. Subjects had no history of neurological or psychiatric disorder.

Experiment 2

Sixteen right-handed HD-positive subjects took part; two subjects were excluded (one was an outlier on behavior, the other was given a diagnosis of manifest HD), leaving a group of 14 premanifest HD subjects (preHD: 4 males, 10 females). Mean CAG repeat length of the mutant HD-gene allele was 43.0±2.8 repeats. Based on this, preHD were predicted to be 11.1±6.0 years from disease onset (Langbehn et al., 2004, Langbehn et al., 2010). There were 15 controls (8 males, 7 females), matched on age (preHD: 43.4±13.4 years; controls: 42.0±12.6 years, $t<1$), education (preHD: 14.1±2.4 years; controls: 15.3±2.4 years, $t_{27}=1.421$, n.s.), the Mini Mental Status Exam (MMSE; preHD: 28.2±2.2 points; controls: 28.5±1.6 points out of 30, $t<1$) (Folstein et al., 1975) and the Montreal Cognitive Assessment (MoCA; preHD: 26.4±2.5 points; controls: 27.0±2.5 points out of 30, $t<1$) (Nasreddine et al., 2005). All subjects provided written consent in accordance with UCSD IRB guidelines and

completed the safety screening form. Subjects were not taking neuropsychiatric drugs and had no neurological condition besides preHD status. At the time of the TMS experiment, the experimenter was blind to the genetic diagnosis of the preHD group.

Selective Stop-Signal Task

Experiment 1 TMS version

We used the Selective Stop-Signal task, adapted from Cai et al. (2011), in which subjects initiated a two-hand response on each trial but tried to stop one of the two responses in the case of an infrequent stop signal (Figure 4.1A). A key characteristic of this task is that each trial consists of two separate phases: a *preparing-to-stop* phase, where subjects must prepare in advance the hand that might need to stop, and an *outright-stopping* phase in which the response is made.

After an instruction session and two practice blocks, subjects performed twelve blocks proper. Each block had 48 trials. On each trial, subjects prepared by placing index and little fingers of each hand on four buttons. The two index fingers made up 'inner' responses, while the two little fingers made up 'outer' responses. Trials began with a cue (i.e. 'Maybe Stop Right'/MSR, 'Maybe Stop Left'/MSL, or 'Null') written in white on a black background for 500ms. The MSR and MSL cues (20 trials each per block) instructed subjects to prepare to stop a particular hand in the case of a stop signal later in the trial. The Null trials (8 per block) indicated that no response would be necessary and provided a TMS baseline.

After the cue, the screen then turned blank for an average of 4s before go-signal onset (range 1.5 – 7s). Single-pulse TMS was delivered over the motor cortex representation of the right hand on every trial during this Cue-Go stimulus interval, 1s after the cue offset (Figure 4.1B). This served to index the corticomotor excitability of the right hand motor representation at a given moment (see below for more details). This early 1s stimulation time was of particular interest because it was the very time-point at which we had previously identified proactive hand suppression in a task paradigm with a fixed 1.5s Cue-Go stimulus interval (Cai et al., 2011). We aimed to replicate those findings, albeit using a slower task design where the Cue-Go stimulus interval was extended and jittered. This was an important design consideration for the subsequent fMRI session.

After the preparatory period, an imperative Go stimulus was presented on MSR and MSL trials. This consisted in four horizontally arranged circles with two circles colored blue, indicating either a bimanual 'inner' or 'outer' finger response (equal probabilities). Failure to respond with both hands simultaneously (defined as > 70ms difference in response times) resulted in a "Decoupled" warning presented for 1s. The inter-trial interval (ITI) was a fixed 1s. On Go trials (50% of trials, 10 MSR, 10 MSL per block), the circles remained until a response was made or 1s had passed. On Stop trials (25% of trials, 5 MSR, 5 MSL per block), a red X appeared in the center of the screen after a short stop-signal delay (SSD) and remained until the end of the trial. Subjects were required to stop the response of the hand previously cued at the beginning of the trial while quickly continuing with the other hand.

Note that some trials were so-called 'Partial trials' (25% of trials, 5 MSR, 5 MSL per block), in which the screen remained blank until the end of the trial. These trials, requiring

stopping preparation without a subsequent response, were important to statistically isolate the neural contribution of the preparation phase in the fMRI session (Ollinger et al., 2001) but were also used in the TMS session for task consistency.

The SSD dynamically varied throughout the experiment – increasing or decreasing by 50ms with every successful or failed stop, respectively, leading to an approximate probability of stopping of 50%. The stop signal reaction time (SSRT) was calculated using the integration method (Verbruggen and Logan, 2009). Additional behavioral measures included the accuracy and rate of decoupling on Go trials, the probability of stopping successfully on Stop trials, the stopping direction error rate (how many times the subject stopped the incorrect hand), median Go RT, median RT on failed Stop trials, and median RT of the unstopped continuing hand on Stop trials (the Continuing RT).

The Stopping Interference Effect indexes the selectivity of stopping (Aron and Verbruggen, 2008). We estimated this effect as the median RT of the continuing hand (when the other hand is stopped) minus the median RT of that same hand on analogous Go trials. These analogous Go trials were determined by rank-ordering the Go RTs and then averaging those RTs longer than the *n*th one, where *n* is obtained by multiplying the number Go RTs in the distribution by the probability of failing to stop on Stop trials. This method provides a more accurate estimate of the Stopping Interference Effect as it accounts for the fact that the Go process on successful Stop trials will be slower than that of all Go trials (Verbruggen and Logan, 2009).

Experiment 1 fMRI version

There were three short practice blocks outside the scanner, and then four blocks within the scanner. Task details were similar to the TMS procedure with a few differences. Each scanner block was made up of 48 trials with four equiprobable cues (MSR, MSL, 'Maybe Stop Both'/MSB, and 'Just Go'/JG). There was no Null cue, but the JG condition served as a comparable baseline by assuring subjects that no stop signal would occur on that trial. MSR and MSL were *selective* stopping cues, while MSB was a *nonselective* stopping cue indicating that subjects should stop both hand responses in the case of a stop-signal. We have previously shown that stopping in the MSB condition has a physiological profile akin to simple reactive stopping for which proactive selective preparation would be unlikely (cf. Majid et al., 2011). Thus the MSB served as an additional control condition.

For the MSR, MSL, and MSB conditions, 50% of trials were Go trials (6 trials per condition per block), 25% were Stop trials (3 trials per condition per block), and 25% were Partial trials (3 trials per condition per block). For the JG condition, 75% of trials were Go trials (9 trials per block) and 25% were Partial trials (3 trials per block). The inter-trial interval was jittered from 1s to 5s (mean 3s).

Experiment 2 TMS version

There were 3 practice blocks followed by 8 blocks proper of the TMS task. There were a few differences compared to TMS in Experiment 1. Each block was made up of 30 trials with five equiprobable cues (MSR, MSL, MSB, JG, and the baseline Null – 6 trials per condition). In addition to the Null baseline, JG and MSB conditions served as additional

control conditions for which proactive selective motor suppression was not expected (cf. Majid et al., 2011). Cues were presented for 500ms. After cue offset, the screen remained blank for a *fixed* 1.5s period until the go-signal, and TMS was always delivered 1s after cue offset (exactly 500ms before the go-signal) on each trial. These timing parameters matched those of Cai et al. (2011) for which proactive suppression was demonstrated at the group level, since fMRI design considerations were not relevant for Experiment 2. Accordingly, there were also no Partial trials. Stop trials thus occurred on 33% of all MSR, MSL, and MSB trials (2 per block per condition).

TMS

EMG Recordings

The subjects sat about 50cm in front of a 19-inch monitor with their hands placed on a four-keypad response devise (two vertical keypads for index finger responses flanked by two horizontal keypads for little finger responses). Surface electromyography (EMG) was recorded using a pair of 10-mm silver electrodes from the first dorsal interosseous (FDI) of the right hand, optimal on account of this muscle's role in the right hand index response. A ground electrode was placed over the radial wrist protuberance of the right hand.

A Glass QP511 Quad AC Amplifier System (Glass Technologies, West Warwick, RI) amplified the EMG signal using a 30 Hz to 1kHz band-pass filter and a 60 Hz notch filter. A CED Micro 1401 mk II acquisition system sampled the data at a frequency of 2 kHz. Data were recorded using CED Signal v4 (Cambridge Electronic Design, Cambridge, UK).

TMS delivery

Transcranial Magnetic Stimulation was delivered with a MagStim 200-2 system (Magstim, Whitland, UK) and a figure-of-eight coil (7 cm diameter). The study began with a thresholding procedure in which subjects sat with their hand resting upon the table. The coil was initially placed approximately 5cm left and 2 cm anterior to the vertex to find the cortical representation of the right FDI muscle. With single-pulse stimulation, the coil was incrementally repositioned and the stimulation intensity was incrementally increased until a reliable motor evoked potential (MEP) was obtained in the right FDI. The amplitude of this MEP served as an index of the excitability of the corticomotor representation of the right hand at a particular point in time.

The lowest stimulation level required to elicit MEP amplitudes of at least 0.05 mV in at least 5 of 10 trials was determined as the resting motor threshold (Rossini et al., 1994). The exact location of stimulation was marked on the scalp for future reference. The experimental stimulation intensity for use throughout the study was determined as the stimulation level that consistently elicited MEP amplitudes that were approximately half the size of the subject's maximum MEP amplitude. This ensured that both increases and decreases in corticomotor excitability could be optimally identified, for subject responses to TMS theoretically fell on the steepest limb of the subject's stimulation-response curve (Devanne et al., 1997). The mean experimental stimulation intensity as a percentage of maximum simulator output was 51.2±8.1% for Experiment 1 and 48.5±9.1% for Experiment 2.

Analysis

Peak-to-peak MEP amplitude was determined using custom MATLAB software. Trials were excluded if the root mean square of EMG activity in the 100ms before TMS delivery was greater than 10μV to ensure no preliminary hand activation. MEP amplitudes for each condition (MSR, MSL, or Null, with the addition of MSB or JG in Experiment 2) were then trimmed to ensure distribution normality (by removing the upper and lower 10% of values) (Wilcox, 2001, Stinear and Byblow, 2004) and averaged. Percent Hand Modulation, a measure of right hand motor excitability change compared to the Null baseline 1s after cue offset, was determined for all non-Null conditions using the following formula: (Condition MEP - Null MEP)/Null MEP * 100%. Negative Percent Hand Modulation on MSR trials indicates *proactive motor suppression* of the hand that might need to stop later in the trial. The same analysis was run on the root mean square EMG measure to ensure that there were *no* significant group or conditional differences before TMS was delivered.

Functional MRI

Task optimization

Custom software implemented in SPM2 (http://www.fil.ion.ucl.ac.uk/spm/) simulated the optimal trial event order, Cue-Go stimulus interval lengths, and inter-trial interval lengths for each scan before the fMRI session. This kept the correlation between different trial regressors below 33%, so that we could separate the BOLD response in *preparing-to-stop* and *outright-stopping* phases.

Data acquisition

We used a 3T GE MR750 scanner equipped with an eight-channel head coil at the UCSD Keck Center for Functional MRI. A T_1-weighted sequence with $1mm^3$ resolution was used to acquire anatomical images (TR=8.092, TE=3.164ms, TI=600ms, 178 slices, flip angle = 8˚). 209 functional T_2*-weighted echoplanar images (EPI) were acquired for each of the four scanning runs with a 4mm slice thickness (TR=2000ms, TE=32ms, flip angle = 90˚, image matrix = 64x64, FOV = 220mm x 220mm, voxel size = 4mm x 3.44mm x 3.44mm). The first four volumes were discarded to allow for T_1 equilibrium effects. A single fieldmap image was obtained (TR=500, TE=8.5ms, flip angle = 45˚, same FOV as EPI) to correct for gradient distortions using custom software.

Preprocessing, general linear modeling and analysis

The data were processed using FSL software (www.fmrib.ox.ac.uk/fsl). The functional images were realigned to correct for small head movements (Jenkinson et al., 2002). A 5mm full-width half-maximum Gaussian kernel was then used to spatially smooth the data, which was subsequently high-pass filtered using a 100s cutoff. EPI images were first registered to the T_1 structural image and then nonlinearly registered to a standard 2mm MNI152 template using 12 degrees of freedom (Jenkinson and Smith, 2001).

For each scan of each subject, data were fitted with two different models, basic or parametric. In the basic model, MSR and MSL conditions were merged into a single *selective* stopping condition (MSR+L), in addition to the MSB and JG conditions. Fourteen separate events were modeled overall. For the *preparing-to-stop* phase, each condition (MSR+L,

MSB, and JG) was modeled as a separate event for 500ms beginning at the preparatory cue onset. For the *outright-stopping* phase, the following events were modeled for 1s beginning at the Go stimulus onset: 'Go' (correct response on Go trials, all three conditions), 'Stop' (successful inhibition on Stop trials, MSR+L and MSB only), 'Fail' (unsuccessful inhibition on Stop trials, MSR+L and MSB only), 'Partial' (partial trials, all three conditions), and a nuisance event for all other occurrences. The parametric model was the same as the basic model with the addition of a regressor for the Continuing RT on successfully inhibited MSR+L stop trials (Stop_RT_param). Since this regressor was demeaned, it was statistically identical to a trial-by-trial regressor of the Stopping Interference Effect, where the Continuing RT of a particular successful Stop trial is subtracted by the subject's average Go RT. Go RT for an individual subject was stable throughout the fMRI experiment, and this regressor did not differ appreciably from that of a *more local estimate* of the Stopping Interference Effect, where the Continuing RT for a particular successful Stop trial was subtracted by the average Go RT of the three correct Go trials before and after the Stop trial.

For *preparing to stop* we contrasted MSR+L > JG Preparation using the basic model. For *outright stopping* we contrasted MSR+L (Stop > Go) using the basic model and MSR+L Stop_RT_param > null using the parametric model.

Analysis was performed using the FSL tool FEAT (fMRI Expert Analysis Tool). For each subject, a higher-level fixed effects analysis was used to combine contrasts from the four different scanner runs. FMRIB's Local Analysis of Mixed Effects (FLAME) tool with automatic outlier deweighting was used for a mixed-effects group average (one sample t-tests).

FLAME was also used in a group-wise regression of individual Percent Hand Modulation measures and subject activation. A basal ganglia mask in MNI152 standard space, and derived from the Harvard/Oxford Atlas in FSL, was used for some analyses. This included all of the caudate, putamen, and pallidum.

Structural MRI analysis for Experiment 2

Nine of the 14 preHD subjects (2 males, 7 females) had taken part in an earlier study (2.6±0.2years prior) that included structural imaging (Majid et al., 2011b). In that study there were also 22 matched controls. Here we re-analyzed the data derived from automated volumetric segmentation, using FreeSurfer (Fischl et al., 2002, Fischl et al., 2004), of T_1-weighted images (from that study's second visit). We analyzed data from seven subcortical structures (viz. accumbens, amygdala, caudate, hippocampus, pallidum, putamen, and thalamus). Bilateral structural volumes were summed and normalized to each subject's total intracranial volume. Group difference statistics were corrected for multiple comparisons using the strict Bonferroni method.

The 9 preHD subjects who had taken part in the imaging study did not differ significantly from the 5 who did not with regards to any measure, whether age (46.0±15.8 vs. 38.8±6.9 years old, $t<1$) or mutant CAG repeat length (42.8±3.2 vs. 43.4±2.3 repeats, $t<1$).

RESULTS

Experiment 1: TMS and fMRI in young volunteers

In the TMS session, Go RT was 611±90ms, the probability of stopping was 50.3±5.8%, the speed of stopping (Stop Signal Reaction Time, SSRT) was 282±61ms, and the Stopping Interference Effect was 68±63ms (Table 4.1).

As a likely consequence of having lengthened the task timing parameters to match the fMRI session, proactive right hand suppression on MSR trials (i.e. negative MSR Percent Hand Modulation) was *not* now seen at the group level while it had been in Cai et al. (2011), which used a fixed and much shorter cue-stimulus interval. Instead there was very high variability across subjects, ranging from -33.4% to 42.7% even after the removal of a statistical outlier (group mean: 4.4±20.6%; n=17). Conveniently, however, this variability allowed us to relate TMS-measured physiology with fMRI-measured brain activation (see below).

All subjects later took part in an fMRI session (mean delay 21.4 days, SD=20.9 days). The MSR and MSL conditions were combined into a single selective MSR+L condition to increase statistical power. For this condition, Go RT was 614±81ms, the probability of stopping was 53.0±11.8%, SSRT was 251±44ms, and the Stopping Interference Effect was 60±56ms. These values compare very favorably with those of the TMS session (Table 4.1).

Preparing-to-stop phase

We hypothesized that the striatum and pallidum would be active in the MSR+L condition. At the overall group level, we contrasted MSR+L (preparation for selective

stopping) with JG baseline (preparation without any possible stopping). Consistent with our hypothesis, there was widespread activation in the bilateral putamen and pallidum, as well as premotor cortex, parietal cortex, occipital cortex, and left thalamus ($Z>2.3$, $p<0.05$ whole brain cluster correction) (Figure 4.2A, Table 4.2).

We then investigated whether this *preparing-to-stop* activation correlated with the TMS-derived proactive suppression (n=17 after the removal of the abovementioned statistical outlier). We hypothesized that subjects who were more able to suppress the right hand in the *preparing-to-stop* phase (i.e., with more negative MSR Percent Hand Modulation) would also show greater activation of striatum and pallidum in the analogous *preparing-to-stop* phase of the fMRI session. Consistent with our hypothesis, a group-wise regression analysis revealed greater activation in the left putamen and pallidum, as well as the left thalamus, supramarginal gyrus, pre-supplementary motor cortex (preSMA), and paracingulate gyrus in subjects who better suppressed the stopping hand ($Z>2.0$, $p<0.05$ whole brain cluster correction) (Figure 4.2B, Table 4.2).

Notably, the above results reveal that the subgroup of subjects who did not have TMS-measured proactive hand suppression also did not have striatum and pallidum activation (see Figure 4.2B, lower left for descriptive plot of left putamen activation). We speculate that proactive suppression simply occurred *later* in the trial for these subjects (in both TMS and fMRI sessions). With a median split, we divided subjects into “early suppressor” (n=9) and “early non-suppressor” (n=8) groups based on the MSR Percent Hand Modulation measure. We then generated peristimulus plots for signal change after the onset of the selective stopping cue (MSR or MSL) for each group at the left putamen ROI of

Figure 4.2B, lower left. The plots indeed show that the rise in activation in the "early non-suppressor" group occurs later, even though both groups peak around the same time (Figure 4.2B, lower right). This delayed activation but eventual catch-up in "early non-suppressors" suggests that they may in fact be "late suppressors" for whom proactive hand suppression was missed in the TMS task, and it explains in part why stopping behavior may not have differed between groups.

We also included an MSB condition in the fMRI session as an additional control (as it does not require selective stopping). For the contrast of MSB > JG, there was only limited left premotor and parietal activation ($Z>2.3$, $p<0.05$ whole brain cluster correction) (Figure 4.3A, Table 4.2), consistent with the fact that neither condition should engage regions for proactive selective suppression. For the MSR+L > MSB contrast there was bilateral dorsal caudate and thalamus activation, as well as the bilateral premotor and parietal cortices ($Z>2.3$, $p<0.05$ whole brain cluster correction) (Figure 4.3B, Table 4.2), consistent, again, with a striatal role in preparing to stop selectively.

Outright-stopping phase

We hypothesized that when the stop-signal occurs, the basal ganglia should again be activated to implement stopping that is selectively targeted at a particular response tendency. To examine this we contrasted successful Stop trials with Go trials in the MSR+L condition (MSR+L Stop > Go). There was activation of the basal ganglia, including bilateral ventral caudate and putamen, as well as thalamus, bilateral inferior frontal cortex (IFC), preSMA, orbitofrontal cortex, insular cortex, premotor cortex, and paracingulate cortex

(Z>2.3, p<0.05 whole brain cluster correction) (Figure 4.4A, Table 4.3). Notably, this outright-stopping activation partially overlapped with activation in the MSR+L > JG preparation contrast, and also with the parametric preparation contrast (i.e. where MSR+L > JG preparation correlated with proactive hand suppression from the TMS study). The regions of overlap for the latter were: left caudate (-10 8 8), putamen (-16 8 -2), pallidum (-12 4 0), insula (-34 18 0), and the midline preSMA (2 18 51).

Next, we examined if the striatal activation during selective stopping was related to behavioral selectivity (operationalized as a minimal RT delay for the continuing hand movement, i.e. a small Stopping Interference Effect). For each subject, activity on MSR+L successful Stop trials was regressed against the continuing hand RT on those trials and then a group analysis was performed. We found that the greater the selectivity of stopping (smaller Stopping Interference Effect), the greater the activity in the bilateral dorsal head of caudate (Z>2.3, p<0.05 cluster corrected over a whole basal ganglia mask) (Figure 4.4B, Table 4.3). This activation was unlikely due simply to the faster speed of the movement made on selective Stop trials; an analogous analysis in which activity on Go trials was regressed against RT on those trials did not reveal activity in the caudate even at a reduced cluster threshold (Z>1.8, p<0.05 cluster corrected over a whole basal ganglia mask). Also, although this activation was more dorsal than the activation in the MSR+L Stop > Go contrast, it overlapped considerably with the MSR+L > MSB preparation contrast (right caudate: 14 10 16; left caudate: -12 2 16).

Outright stopping in the MSB condition again served as a control condition. Activation in the MSB Stop > Go contrast was only significant in the right inferior frontal

cortex (rIFC), orbitofrontal cortex, and insular cortex (Figure 4.4C, Table 4.3). This activation of right frontal cortex is consistent with many studies implicating this region in simple reactive stopping (Aron et al., 2004, Chamberlain et al., 2006, Chikazoe, 2010).

Experiment 2: TMS in preHD vs. controls

The physiological and fMRI results of Experiment 1 show that the striatum and pallidum are active for proactive selective stopping. If these basal ganglia regions are *necessary* for this function, then damage to them in premanifest Huntington's disease should impair proactive selective stopping.

Indeed, the preHD group was behaviorally impaired in the selectivity of stopping, as there was an elevated Stopping Interference Effect (preHD: 467±330ms; controls: 221±183ms; t_{27}=2.508, p<.05). As Go RT was also longer in preHD (preHD: 1100±285ms; controls: 863±209ms; t_{27}=2.566, p<.05) we calculated a normalized measure of stopping selectivity by dividing the Stopping Interference Effect by Go RT for each subject. This normalized Stopping Interference Effect was also significantly elevated in preHD (preHD: 42.4±29.5%; controls: 25.4±17.3%, t_{27}=1.913, p<.05) (Figure 4.5A, Table 4.1). Neither the probability of stopping nor SSRT differed significantly between groups.

Experiment 2 timing parameters matched those of our earlier report wherein proactive suppression *was* demonstrated at the group level (Cai et al., 2011). Strikingly, proactive suppression following the MSR cue, determined using single-pulse TMS to index motor excitability in the preparing-to-stop phase, was absent in preHD but present in controls (Percent Hand Modulation; preHD: 6.5±15.7%, one-sample t_{13}=1.564, n.s.; controls:

-7.8±11.9%, one-sample t_{14}=2.524, p<.05; group difference, t_{27}=2.770, p<.01) (Figure 4.5C, Table 4.1). This difference was unlikely due to measurement error in the preHD group, as variability in hand modulation was similar for both preHD and control groups.

Importantly, right hand modulation did not differ from zero for any group on MSL trials for which stopping preparation of the right hand was not necessary (preHD: 6.5±18.3%, t_{13}=1.320, n.s.; controls: 3.5±24.3%, t<1; group difference, t<1). Neither did right hand modulation differ for zero for any group on JG trials for which stopping preparation is not necessary (preHD: 18.1±44.4%, t_{13}=1.524, n.s.; controls: 2.9±13.4%, t<1; group difference, t_{27}=1.267, n.s.) or on MSB trials also not requiring preparation for selective stopping (preHD: 9.8±23.7%, t_{13}=1.555, n.s.; controls: 0.5±10.2%, t<1; group difference, t_{27}=1.405, n.s.).

Notably, structural MRI confirmed basal ganglia damage in the preHD group. In an earlier imaging study (2.6±.2 years prior) (Majid et al., 2011b) nine of the current fourteen preHD subjects had received T1 scans. Here, we compare volumes of seven subcortical regions (accumbens, amygdala, caudate, hippocampus, pallidum, putamen, and thalamus) in these nine current subjects vs. the 22 controls in that study. Region by Group ANOVA showed a significant interaction ($F_{4.196,29}$=2.414, p<.05 with Huynh-Feldt correction), as well as significant effects for Region ($F_{6,29}$=1447, p<.001) and Group ($F_{1,29}$=5.981, p=.021). The subset of nine preHD had smaller volumes in the putamen (Percent Intracranial Volume; preHD: 0.59±.06%; controls: 0.67±.06%; t_{29}=3.135; p<.007) and pallidum (preHD: 0.20±.02%; controls: 0.23±.02% of ICV; t_{29}=3.054; p<.007) but not in the other five subcortical regions (Figure 4.5D, Table 4.4). These differences were significant even after strict Bonferroni

correction for seven multiple comparisons. While it is likely that there was progressive atrophy during this period to other structures, these were likely other areas of the striatum such as the caudate and accumbens, rather than other subcortical regions (see Stoffers et al., 2010, van den Bogaard et al., 2010, Aylward et al., 2011).

Discussion

We investigated the neural correlates of proactive selective stopping, a complex yet crucial everyday behavior that requires selective control of one's actions through advance planning. In Experiment 1, single-pulse TMS of the right hand indexed the top-down effect of stopping goals in suppressing motor channels of the hand that might have to stop. Importantly, those subjects who suppressed the relevant hand early in the trial had greater functional activation in the striatum, pallidum, and preSMA locked to the cue in the subsequent fMRI session. In the *outright-stopping* phase, fMRI again revealed striatal and pallidal activation for selective stopping, and moreover, that the degree of striatal activation correlated with the degree of behavioral stopping selectivity. Finally, we repeated a version of the TMS study in a preHD group (with basal ganglia volume reductions) and matched controls. Consistent with the putative importance of the striatum and pallidum to proactive selective stopping, TMS revealed proactive hand suppression in controls but not the preHD group, and the latter were also behaviorally impaired at selective stopping.

Proactive selective suppression engages striatum, pallidum, and preSMA

The top-down influence of stopping goals on motor channels consistently leads to proactive motor suppression in healthy subjects, shown in a similar paradigm (Cai et al., 2011) and indeed replicated in the current Experiment 2 control subjects. Yet Experiment 1 did not show this at the group level. We suppose the high inter-subject variability in proactive suppression was due to the much slower task design (needed for fMRI), which now meant that some subjects probably only implemented proactive suppression close to the go-signal, or even after it, rather than close to the cue. The fMRI peristimulus analysis further supported this interpretation of a timing difference.

Notably, preSMA activation correlated with the degree of proactive hand suppression measured by TMS. This suggests that the preSMA may have a top-down influence over the basal ganglia to 'set up' inhibitory response channels later triggered by the stop-signal. Such a role for the preSMA is consistent with the many studies that have implicated it in proactive stopping (Coxon et al., 2009, Chen et al., 2010, Stuphorn and Emeric, 2012, Swann et al., 2012, Zandbelt et al., 2012). The preSMA is also connected to both the rIFC (Johansen-Berg, 2010, Coxon et al., 2012, King et al., 2012, Swann et al., 2012), a node important for outright stopping (Aron et al., 2004, Chikazoe et al., 2007), and the striatum (Parthasarathy et al., 1992, Inase et al., 1999). Several studies specifically implicate the preSMA and striatum in the speed-accuracy trade-off (Forstmann et al., 2010, Forstmann et al., 2011), a form of proactive control.

As fMRI findings are merely correlational, we sought to establish that the striatum and pallidum are *necessary* for proactive selective stopping by studying preHD subjects (Experiment 2). In preHD, there are frank basal ganglia volume reductions, particularly for

the striatum and pallidum (Aylward et al., 2004, Hobbs et al., 2009, Tabrizi et al., 2009, Paulsen et al., 2010, Majid et al., 2011a, Majid et al., 2011b). In the current study, nine of the fourteen preHD subjects had confirmed volume reductions in the putamen and pallidum from an earlier study (Majid et al., 2011b), and this is likely true of the whole group.

Consistent with our predictions, the preHD group showed no proactive hand suppression (indexed by TMS) vs. controls and had an elongated Stopping Interference Effect (even when scaling for general slowing). These specific impairments occurred in the context of otherwise satisfactory task performance and cognitive examination scores similar to controls. Such preHD impairments may relate to difficulties in translating declarative working memory goals into a striatally-mediated proactive influence over motor channels.

Outright selective stopping

We hypothesized that the network of brain regions implicated in preparing to stop could serve as a 'proactive inhibitory set' (Aron, 2011), which can be triggered when stopping is later needed. Consistent with this, basal ganglia and preSMA activation recurred when outright stopping was required. Moreover, there was rIFC activation, not seen in any preparatory contrast. Whether the rIFC is important for proactive response control, and for which kinds of response control, is still unclear. Similar to the current findings, some other studies question whether rIFC is activated proactively (e.g. Zandbelt et al., 2012), whereas others do show a rIFC role in, for example, anticipation-related slowing (Jahfari et al., 2010, Swann et al., 2012).

Here we also show that when stopping selectively, the degree of behavioral selectivity correlated with the degree of striatal activation on a subject-by-subject basis. Notably, the dorsal caudate focus of this activation coincided with regions activated when contrasting preparation for selective vs. nonselective stopping. This reinforces the notion that these regions are important for the *selectivity* of stopping. This result also suggests that stopping in this paradigm is *mechanistically selective*, as opposed to merely stopping all and then restarting one response – which might the case for other behavioral paradigms which purport to measure behaviorally selective stopping but do not allow for advanced preparation (cf. Bissett and Logan, 2013). Two other considerations bear on this. First, the activation in the abovementioned dorsal caudate was related to the selectivity of stopping but not to merely hand movement when going. Second, the Stopping Interference Effect in Experiment 1 was a mere 60ms on average, with many subjects having a value close to zero, implying almost perfectly selective stopping.

Our findings point to some heterogeneity in the striatum. While a more dorsal caudate region was implicated in the *selective* aspect of stopping (see above), a more ventral striatal region was implicated in motor suppression (i.e. related to proactive hand suppression in advance of stopping and for outright stopping, compare figures 2B and 4A).

Human evidence for the Indirect Pathway

We propose that striatal and pallidal activation in this study is a functional index of Indirect Pathway involvement in mechanistically selective stopping. First, we linked striatal activation to a form of selective motor suppression, as do neurophysiological studies in

primates (Ford and Everling, 2009, Watanabe and Munoz, 2010) and rodents (Bryden et al., 2012). Second, we find selective stopping impairments in a population thought to primarily have Indirect Pathway degeneration in the early stage of disease (Vonsattel et al., 1985, Albin et al., 1995, Starr et al., 2008). Indeed, hyperkinetic (disinhibitory) symptoms in early-stage HD are classically thought to arise from an impaired ability to stop specific movements (Penney and Young, 1983). Third, this form of behaviorally selective stopping has been associated with longer SSRT compared to simple nonselective stopping (Aron and Verbruggen, 2008, Claffey et al., 2010), which is consistent with delays expected from the greater number of synapses in the Indirect Pathway vs. the Hyperdirect Pathway that is implicated in simple reactive stopping (Magill et al., 2004, Aron and Poldrack, 2006, Ray et al., 2009).

We acknowledge, however, that more definitive proof for the Indirect Pathway is required. This could include (i) high resolution imaging of nodes believed specific to this pathway (e.g. external Globus Pallidus) (Mattfeld et al., 2011) during selective stopping; (ii) D2 receptor imaging (Black et al., 1997) to quantify Indirect Pathway integrity in relation to individual variation in selective stopping behavior/physiology; and (iii) parallel task development with neurophysiology in rodents and monkeys, as has been done for simple stopping (Boucher et al., 2007, Leventhal et al., 2012, Stuphorn and Emeric, 2012).

Implications

The results have timely practical implications, allowing for further study of the Indirect Pathway *in humans* and connecting these studies to the burgeoning, sophisticated

studies of basal ganglia pathways using optogenetics in mice (Kravitz et al., 2012) and neurophysiology in rodents (Leventhal et al., 2012) and monkeys (Kim et al., 2012). Furthermore, the development of functional indices of the putative Indirect Pathway could have clinical import for neurodegenerative disorders such as Huntington's disease, where there is an urgent need for biomarkers for subtle functional changes before there is major irreversible cell loss (Ross and Tabrizi, 2011).

The results have theoretical implications too. While it has been argued that a major role for striatum is to weight particular response channels in advance of action (i.e. a proactive 'response set,' see Robbins and Brown, 1990, Hikosaka et al., 2006), the current data argue the striatum can also be used to set up a proactive *inhibitory* set. Specifically we propose that frontal cortical regions such as the preSMA drive the implementation of inhibitory response channels in the striatum and that these are then triggered subsequently when stopping is needed. These results also support a psychological distinction between declarative vs. procedural working memory (instantiated here as proactive suppression) (cf. Oberauer, 2009). This fits with recent theories regarding the striatal role in working memory (Scimeca and Badre, 2012) by showing that declarative working memory in the cortex could be 'translated' into a procedural working memory plan in the striatum.

Summary

We show that subjects use their goals to stop particular response tendencies by proactively suppressing those response channels. We further show that this corresponds to

striatal and pallidal activation and that damage to these structures affects selective response suppression.

ACKNOWLEDGEMENTS

This chapter, in full, was submitted for publication and may appear in Majid, Cai, Corey-Bloom, and Aron, *Journal of Neurosciences*, 2013. We thank Jody Goldstein and Cait Casey for subject recruitment, Rogier Mars for providing fMRI optimization scripts, Yu-Chin Chiu for comments on the manuscript, and NIH, the Alfred P Sloan Foundation, and CHDI for financial support. The dissertation author was the primary investigator and author of this paper.

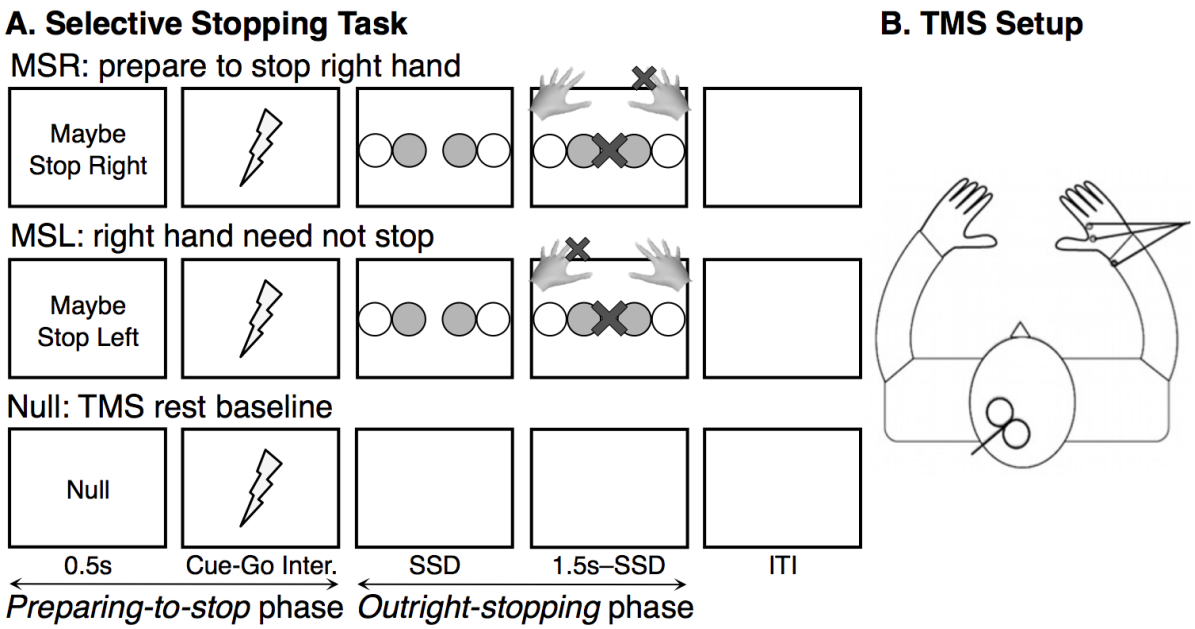

Figure 4.1: *Selective stopping task design*. A. *Task Design:* Each trial began with a preparatory cue (0.5s). 'Maybe Stop Right' (MSR) and 'Maybe Stop Left' (MSL) indicated which hand might have to stop in the case of an uninformative Stop-signal. After a delay (Exp. 1: 4s jittered; Exp. 2: 1.5s fixed), a Go signal (two blue circles) appeared, prompting a bimanual response with either the inner (index) or outer (pinky) fingers together. On a third of trials, a Stop signal (red X) then appeared after a dynamically varied stop-signal delay (SSD), requiring the subject to stop the previously cued hand while continuing the other. The Null cue indicated a no-action rest trial and served as the TMS baseline. In the fMRI paradigm, this baseline was replaced by the 'Just Go' (JG) cue, which indicated that no Stop signal would follow a Go signal.
B. *TMS Setup:* TMS was delivered over the left motor representation of the right hand, producing a motor evoked potential (MEP) recorded by electromyography (EMG). TMS was always delivered 1s after the offset of the stopping cue (represented by lightning bolts).

Table 4.1: *Behavior and TMS*

	Experiment 1 (n=18)		*Experiment 2*	
Behavior (selective stop condition)	*TMS task*	*fMRI task*	*Controls (n=15)*	*PreHD (n=14)*
Go accuracy (%)	91.3±5.1	87.2±4.7	91.8±5.0	86.2±10.6
Go Reaction Time (RT, ms)	611±90	614±81	863±209	1100±285*
Go decoupling rate (%)	7.6±4.8	3.9±4.2	6.2±3.3	11.5±10.4
Stop probability (%)	50.3±5.8	53.0±11.8	57.0±7.8	62.8±8.1
Stopping Direction Errors (%)	3.5±3.8	5.6±7.6	2.0±2.8	3.4±3.5
Continuing hand RT on stops (ms)	755±89	739±81	1186±360	1702±55**
Stopping Interference Effect (ms)	68±63	60±56	221±183	467±330*
Failed Stopping RT (ms)	559±76	551±71	720±159	949±498
Stop Signal Delay (SSD, ms)	310±61	337±60	543±142	630±143
Stop Signal RT (SSRT, ms)	282±61	277±52	292±94	405±290
TMS				
Resting Motor Thresh. (% of max)	46.2±7.8	N/A	41.2±6.9	47.3±9.8
Stimulation Level (% of max)	51.2±8.1	N/A	45.5±7.2	52.4±9.8
MSR MEP (mV)	0.54±.36	N/A	0.77±.44	0.81±.37
MSL MEP (mV)	0.55±.33	N/A	0.86±.50	0.81±.40
Null MEP (mV)	0.53±.37	N/A	0.85±.47	0.78±.39
MSR MEP Modulation (%)	4.4±20.6	N/A	-7.8±11.9	6.1±15.2**
MSL MEP Modulation (%)	16.9±37.2	N/A	3.5±24.3	6.2±17.7

Values given as average ± standard deviation. MEP: mean motor evoked potential amplitude (trimmed) for a given condition. MEP Modulation (%) is calculated as follows: (MSR or MSL MEP – Null MEP)/(Null MEP)*100%. For Experiment 2, asterisks represent significant differences between preHD and controls at the $p<.05$ (*) and $p<.01$ (**) levels.

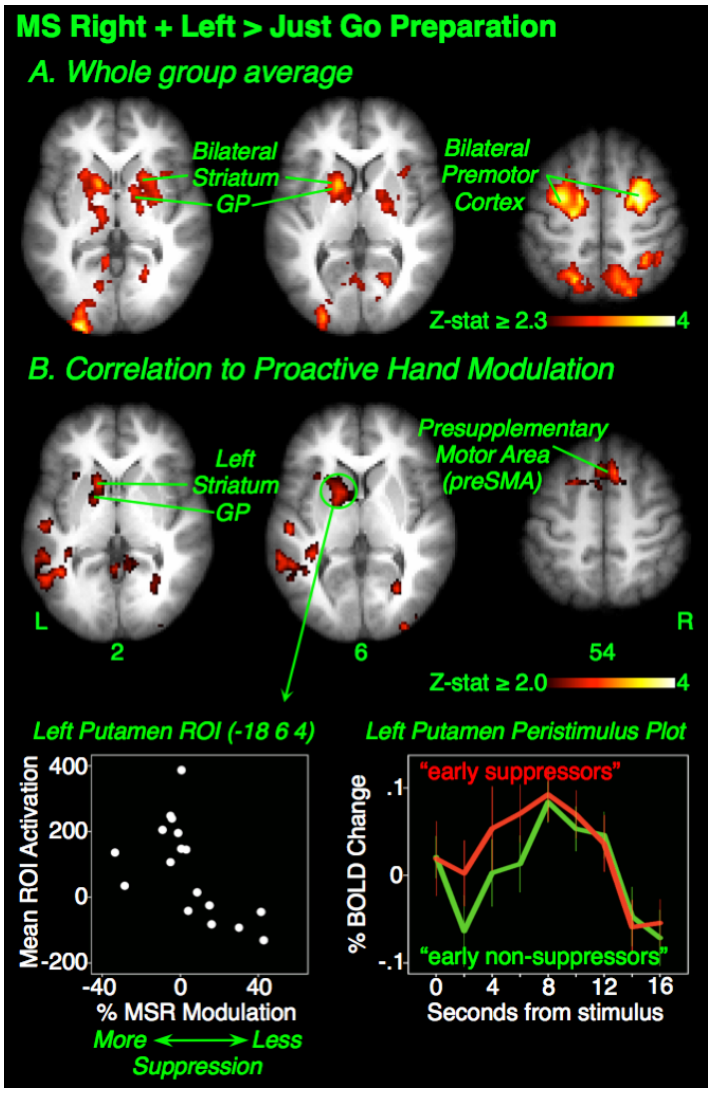

Figure 4.2: *Experiment 1: Preparing to stop selectively and motor suppression*. A. *Maybe Stop Right + Left > Just Go preparatory activation*: In the whole group, preparation to stop selectivity activated bilateral striatum, globus pallidus, and premotor cortex (not shown). B. *Group-wise regression of fMRI activation against TMS proactive suppression*: In the TMS session, Percent Hand Modulation indexed the degree of top-down influence of the Maybe Stop Right stopping goal on right hand motor channels compared to Null. This was calculated as follows: (Maybe Stop Right MEP – Null MEP)/Null MEP * 100%. Activation in the left putamen, pallidum, and preSMA was greater in subjects who more readily suppressed the right hand when cued. *Lower left inset*: Subject MSR Percent Hand Modulation plotted against mean activation in a left putamen ROI (4mm radius) for descriptive purposes. Greater activation is seen in subjects with greater suppression. *Lower right inset*: For the same left putamen ROI, peristimulus plots are shown for those subjects who showed proactive hand suppression at 1s after cue offset ("early suppressors," n=9), vs. those who did not ("early non-suppressors," n=8).

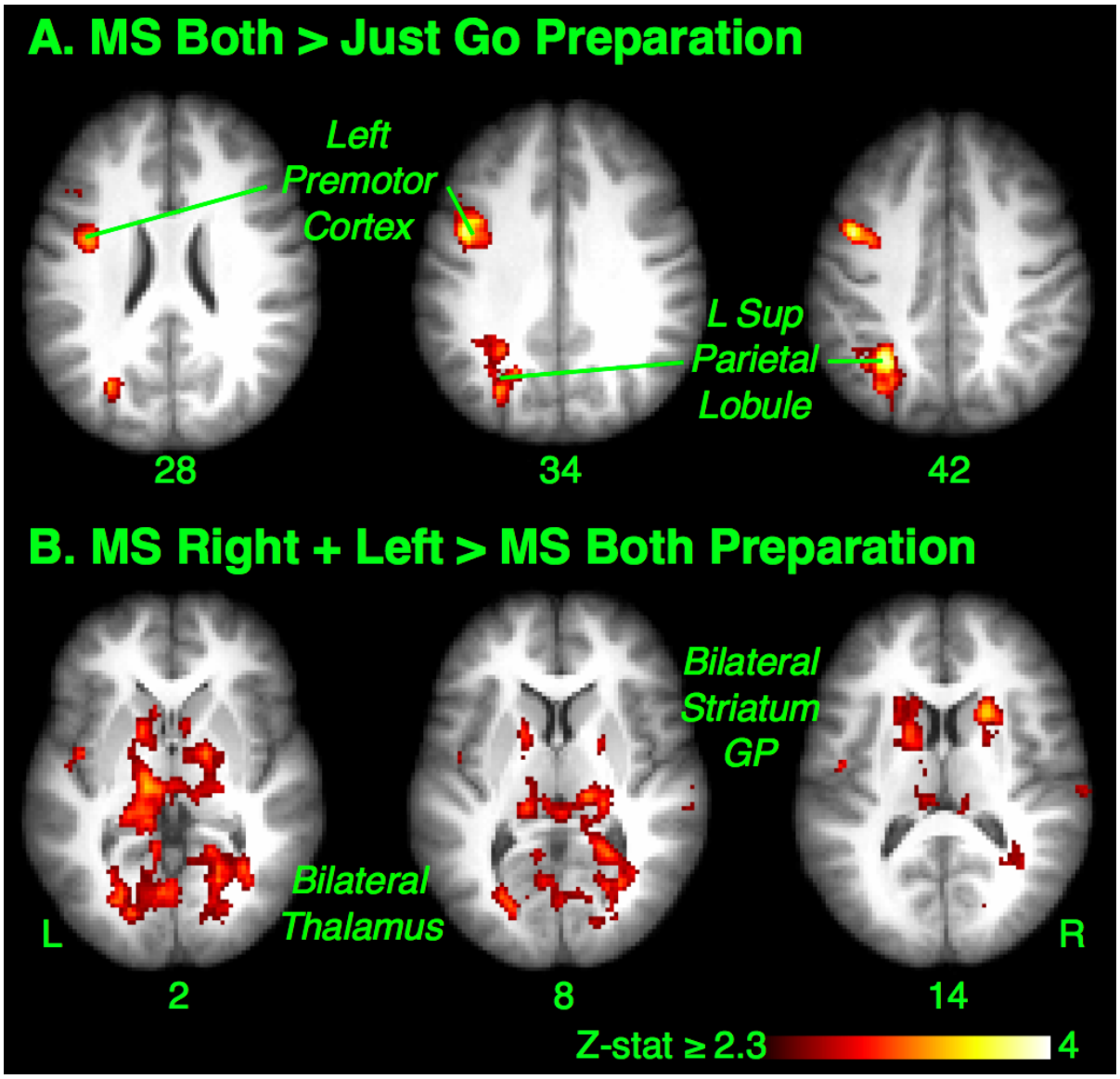

Figure 4.3: *Experiment 1: Preparing to stop nonselectively*. A. *Maybe Stop Both > Just Go preparatory activation*: There was activation of left premotor and parietal regions. B. *Maybe Stop Right + Left > Maybe Stop Both preparatory activation*: There was activation of bilateral dorsal caudate and thalamus, as well as bilateral premotor and parietal regions (not shown).

Table 4.2: *Experiment 1 activation coordinates for the Preparing-to-Stop phase*

Contrast	Region	Side	x	y	z	Size (vox.)
MS+L > JG preparation	Premotor Cortex	L	-44	-8	34	5242
	Premotor Cortex	R	26	-6	44	
	Superior Frontal Gyrus	R	22	0	48	
	Premotor Cortex	L	-50	2	36	
	Supplementary Motor Cort.	L	-10	6	44	
	Superior Parietal Lobule	R	32	-48	40	4659
	Supramarginal Gyrus	L	-42	-44	42	
	Occipital Pole	L	-16	-100	-4	3459
	Putamen	R	22	8	-10	
	Pallidum	L	-22	-2	-4	1237
	Putamen	L	-18	6	4	
	Thalamus	L	-12	-20	-2	
Correlation of MS+L > JG preparation against degree of proactive suppression in TMS task (n=17 after exclusion of a TMS outlier)	Post. Supramarginal Gyrus	L	-54	-48	20	6828
	Putamen	L	-18	6	4	962
	Pallidum	L	-18	2	4	
	Thalamus	L	-18	-24	16	
	PreSMA	R	6	20	52	947
	Paracingulate Gyrus	L	-4	18	46	
MSB > JG preparation	Superior Parietal Lobule	L	-32	-56	40	804
	Premotor Cortex	L	-46	2	36	772
MS+L > MSB preparation	Premotor Cortex	R	28	-8	54	20781
	Premotor Cortex	L	-32	-14	42	
	Caudate	L	-12	4	14	
	Caudate	R	16	14	14	
	Thalamus	L	-14	-24	0	
	Thalamus	R	12	-24	4	

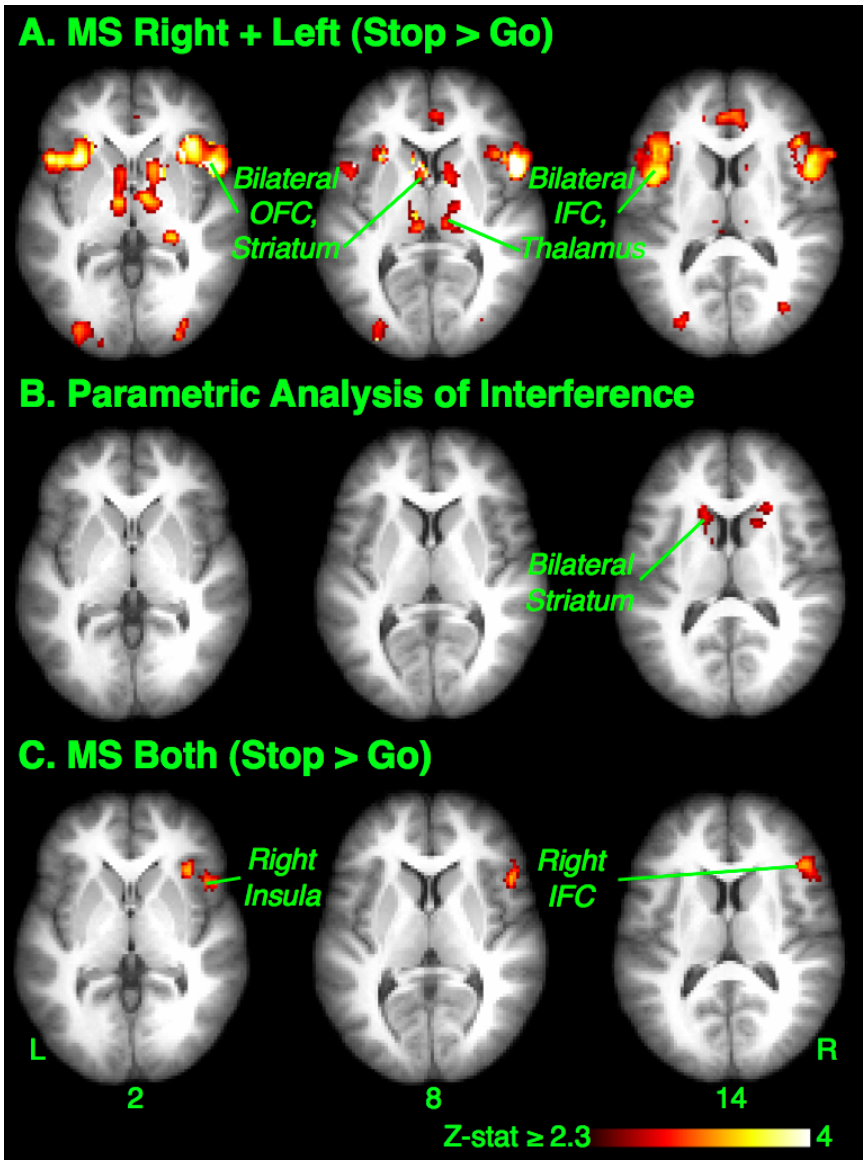

Figure 4.4: *Experiment 1: Outright-Stopping phase*
A. *Maybe Stop Right + Left (Stop > Go)*: When stopping needed to be selective, the comparison of successful Stop to Go trials showed wide activation, including the bilateral orbitofrontal cortex (OFC), striatum, inferior frontal cortex (IFC), and thalamus. Premotor and supplementary motor cortices were also active (not shown).
B. *Parametric Analysis – greater striatal activation with more selective stopping*: Activation on successful MSR+L Stop trials scaled parametrically with reduced stopping interference (i.e. faster continuing hand responses and greater selectivity). The bilateral head of caudate was identified (Cluster correction over the whole basal ganglia mask).
C. *Maybe Stop Both (Stop > Go)*: In the control condition where stopping did not need to be selective, comparison of successful Stop to Go trials showed restricted activation limited to the right inferior frontal cortex (rIFC), orbitofrontal cortex (OFC), and insular cortex.

Table 4.3: *Experiment 1 Activation coordinates for the Outright-Stopping phase*

Contrast	Region	Side	x	y	z	Size (vox.)
MSR+L (Stop > Go)	Insular Cortex	R	38	20	-8	8286
	Paracingulate Gyrus	R	8	20	42	
	PreSMA	R	4	20	50	
	Premotor Cortex	R	38	4	28	
	Inferior Frontal Cortex	R	52	10	6	
	Orbitofrontal Cortex	L	-32	22	-10	4871
	Insular Cortex	L	-34	18	-6	
	Occipital Fusiform Gyrus	L	-28	-88	-12	4167
	Angular Gyrus	R	36	-50	36	3116
	Caudate	R	10	6	2	1623
	Caudate	L	-12	8	4	
	Accumbens	R	12	12	-6	
	Pallidum	R	14	6	2	
	Putamen	R	16	10	0	
	Occipital Fusiform Gyrus	R	22	-88	-10	1263
Parametric analysis of MSR+L Stop Trials and Interference RT	Caudate	L	-12	4	18	330
	Caudate	R	14	14	14	219
MSB (Stop > Go)	Orbitofrontal Cortex	R	34	18	-18	908
	Inferior Frontal Gyrus	R	48	20	4	
	Insular Cortex	R	34	24	0	

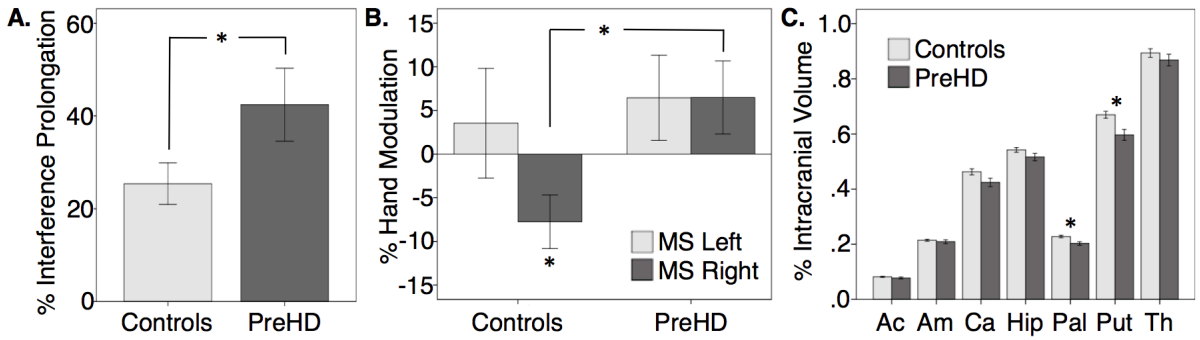

Figure 4.5: *Experiment 2: preHD vs. controls*
A. *Less selective stopping:* When stopping one hand, the preHD group took longer to continue with the other hand even when scaling for Go RT. Percent Interference Prolongation was calculated as: Interference (ms)/MSR+L Go RT (ms) * 100%.
B. *TMS suppression differences*: Proactive selective suppression in Experiment 2 on MSR trials (when the right hand must prepare to stop) was identified only in controls (negative hand modulation to the null baseline), whereas no such suppression occurred in preHD. On MSL trials, when the right hand need not stop, right hand excitability did not differ significantly from the null baseline in either group. Percent Hand Modulation was calculated as such: (Maybe Stop MEP - Null MEP)/Null MEP * 100%.
C. *Subcortical volume differences:* Smaller brain volumes in 9 of the 14 preHD subjects who took part in a structural imaging study 2.6 years prior. Compared to the 22 controls in that study, the preHD subjects showed reduced volumes (normalized as a percentage of individual intracranial volume) in the putamen and pallidum after Bonferroni correction. Abbreviations: Ac, accumbens; Am, amygdala; Ca, caudate; Hip, hippocampus; Pal, pallidum; Put, putamen; and Th, thalamus.

Table 4.4: *PreHD volumetric data*

Volumetric data (% ICV)	Controls (n=22)	PreHD (n=9)	t_{29}	*p*
Accumbens	0.08±.01	0.08±.01	<1	n.s.
Amygdala	0.21±.02	0.21±.02	<1	n.s.
Caudate	0.46±.05	0.42±.05	1.781	.085
Hippocampus	0.54±.04	0.52±.04	1.525	n.s.
Pallidum	0.23±.02	0.20±.02**	2.932	.007**
Putamen	0.67±.06	0.60±.06**	3.009	.005**
Thalamus	0.89±.07	0.87±.06	<1	n.s.

**Significant after strict Bonferroni correction for 7 comparisons. Volumetric data given as the sum of bilateral structures normalized as a percentage of individual Intracranial Volume (%ICV). Data from second visit described in Majid et al. (2011b), which included 9 of the 14 preHD subjects studied here compared to 22 matched controls.

References

Albin RL, Young AB, Penney JB (1995) The functional anatomy of disorders of the basal ganglia. Trends Neurosci 18:63-64.

Aron AR (2011) From Reactive to Proactive and Selective Control: Developing a Richer Model for Stopping Inappropriate Responses. Biol Psychiatry.

Aron AR, Poldrack RA (2006) Cortical and subcortical contributions to Stop signal response inhibition: role of the subthalamic nucleus. J Neurosci 26:2424-2433.

Aron AR, Robbins TW, Poldrack RA (2004) Inhibition and the right inferior frontal cortex. Trends Cogn Sci (Regul Ed) 8:170-177.

Aron AR, Verbruggen F (2008) Stop the presses: dissociating a selective from a global mechanism for stopping. Psychol Sci 19:1146-1153.

Aylward EH, Nopoulos PC, Ross CA, Langbehn DR, Pierson RK, Mills JA, Johnson HJ, Magnotta VA, Juhl AR, Paulsen JS, PREDICT-HD Investigators, Coordinators of the Huntington Study Group (2011) Longitudinal change in regional brain volumes in prodromal Huntington disease. J Neurol Neurosurg Psychiatry 82:405-410.

Aylward EH, Sparks BF, Field KM, Yallapragada V, Shpritz BD, Rosenblatt A, Brandt J, Gourley LM, Liang K, Zhou H, Margolis RL, Ross CA (2004) Onset and rate of striatal atrophy in preclinical Huntington disease. Neurology 63:66-72.

Badry R, Mima T, Aso T, Nakatsuka M, Abe M, Fathi D, Foly N, Nagiub H, Nagamine T, Fukuyama H (2009) Suppression of human cortico-motoneuronal excitability during the Stop-signal task. Clin Neurophysiol 120:1717-1723.

Bissett PG, Logan GD (2013) Selective Stopping? Maybe Not. J Exp Psychol Gen.

Black KJ, Gado MH, Perlmutter JS (1997) PET measurement of dopamine D2 receptor-mediated changes in striatopallidal function. J Neurosci 17:3168-3177.

Boehler CN, Appelbaum LG, Krebs RM, Hopf JM, Woldorff MG (2010) Pinning down response inhibition in the brain--conjunction analyses of the Stop-signal task. Neuroimage 52:1621-1632.

Boucher L, Palmeri TJ, Logan GD, Schall JD (2007) Inhibitory control in mind and brain: an interactive race model of countermanding saccades. Psychol Rev 114:376-397.

Bryden DW, Burton AC, Kashtelyan V, Barnett BR, Roesch MR (2012) Response inhibition signals and miscoding of direction in dorsomedial striatum. Front Integr Neurosci 6:69.

Cai W, Oldenkamp C, Aron AR (2011) A proactive mechanism for selective suppression of response tendencies. J Neurosci 31:5965-5969.

Cai W, Oldenkamp CL, Aron AR (2012) Stopping speech suppresses the task-irrelevant hand. Brain Lang 120:412-415.

Chamberlain SR, Fineberg NA, Blackwell AD, Robbins TW, Sahakian BJ (2006) Motor inhibition and cognitive flexibility in obsessive-compulsive disorder and trichotillomania. Am J Psychiatry 163:1282-1284.

Chambers CD, Garavan H, Bellgrove MA (2009) Insights into the neural basis of response inhibition from cognitive and clinical neuroscience. Neurosci Biobehav Rev 33:631-646.

Chen X, Scangos KW, Stuphorn V (2010) Supplementary motor area exerts proactive and reactive control of arm movements. J Neurosci 30:14657-14675.

Chikazoe J (2010) Localizing performance of go/no-go tasks to prefrontal cortical subregions. Current Opinion in Psychiatry.

Chikazoe J, Konishi S, Asari T, Jimura K, Miyashita Y (2007) Activation of right inferior frontal gyrus during response inhibition across response modalities. J Cogn Neurosci 19:69-80.

Claffey MP, Sheldon S, Stinear CM, Verbruggen F, Aron AR (2010) Having a goal to stop action is associated with advance control of specific motor representations. Neuropsychologia 48:541-548.

Coxon JP, Stinear CM, Byblow WD (2009) Stop and go: the neural basis of selective movement prevention. J Cogn Neurosci 21:1193-1203.

Coxon JP, Van Impe A, Wenderoth N, Swinnen SP (2012) Aging and inhibitory control of action: cortico-subthalamic connection strength predicts stopping performance. J Neurosci 32:8401-8412.

Devanne H, Lavoie BA, Capaday C (1997) Input-output properties and gain changes in the human corticospinal pathway. Exp Brain Res 114:329-338.

Fischl B, Salat D, Busa E, Albert M, Dieterich M, Haselgrove C, van der Kouwe A, Killiany R, Kennedy D, Klaveness S, Montillo A, Makris N, Rosen B, Dale A (2002) Whole brain segmentation: automated labeling of neuroanatomical structures in the human brain. Neuron 33:341-355.

Fischl B, Salat DH, van der Kouwe AJW, Makris N, Ségonne F, Quinn BT, Dale AM (2004) Sequence-independent segmentation of magnetic resonance images. Neuroimage 23 Suppl 1:S69-84.

Folstein M, Folstein S, McHugh P (1975) "Mini-mental state". A practical method for grading the cognitive state of patients for the clinician. J Psychiatr Res 12:189-198.

Ford KA, Everling S (2009) Neural activity in primate caudate nucleus associated with pro- and antisaccades. J Neurophysiol 102:2334-2341.

Forstmann BU, Anwander A, Schäfer A, Neumann J, Brown S, Wagenmakers E-J, Bogacz R, Turner R (2010) Cortico-striatal connections predict control over speed and accuracy in perceptual decision making. Proc Natl Acad Sci USA 107:15916-15920.

Forstmann BU, Tittgemeyer M, Wagenmakers EJ, Derrfuss J, Imperati D, Brown S (2011) The speed-accuracy tradeoff in the elderly brain: a structural model-based approach. J Neurosci 31:17242-17249.

Greenhouse I, Oldenkamp CL, Aron AR (2012) Stopping a response has global or nonglobal effects on the motor system depending on preparation. J Neurophysiol 107:384-392.

Hazrati LN, Parent A (1992) The striatopallidal projection displays a high degree of anatomical specificity in the primate. Brain Res 592:213-227.

Hikosaka O, Nakamura K, Nakahara H (2006) Basal ganglia orient eyes to reward. J Neurophysiol 95:567-584.

Hobbs NZ, Henley SMD, Wild EJ, Leung KK, Frost C, Barker RA, Scahill RI, Barnes J, Tabrizi SJ, Fox NC (2009) Automated quantification of caudate atrophy by local registration of serial MRI: evaluation and application in Huntington's disease. Neuroimage 47:1659-1665.

Inase M, Tokuno H, Nambu A, Akazawa T, Takada M (1999) Corticostriatal and corticosubthalamic input zones from the presupplementary motor area in the macaque monkey: comparison with the input zones from the supplementary motor area. Brain Res 833:191-201.

Jahfari S, Stinear CM, Claffey M, Verbruggen F, Aron AR (2010) Responding with restraint: what are the neurocognitive mechanisms? J Cogn Neurosci 22:1479-1492.

Jahfari S, Waldorp L, van den Wildenberg WP, Scholte HS, Ridderinkhof KR, Forstmann BU (2011) Effective connectivity reveals important roles for both the hyperdirect (fronto-subthalamic) and the indirect (fronto-striatal-pallidal) fronto-basal ganglia pathways during response inhibition. J Neurosci 31:6891-6899.

Jenkinson M, Bannister P, Brady M, Smith S (2002) Improved optimization for the robust and accurate linear registration and motion correction of brain images. Neuroimage 17:825-841.

Jenkinson M, Smith S (2001) A global optimisation method for robust affine registration of brain images. Med Image Anal 5:143-156.

Johansen-Berg H (2010) Behavioural relevance of variation in white matter microstructure. Current Opinion in Neurology 23:351-358.

Kim S, Cai X, Hwang J, Lee D (2012) Prefrontal and striatal activity related to values of objects and locations. Front Neurosci 6:108.

King AV, Linke J, Gass A, Hennerici MG, Tost H, Poupon C, Wessa M (2012) Microstructure of a three-way anatomical network predicts individual differences in response inhibition: a tractography study. Neuroimage 59:1949-1959.

Kravitz AV, Tye LD, Kreitzer AC (2012) Distinct roles for direct and indirect pathway striatal neurons in reinforcement. Nat Neurosci 15:816-818.

Langbehn DR, Brinkman RR, Falush D, Paulsen JS, Hayden MR, Investigators of the Huntington's Disease Collaborative Group (2004) A new model for prediction of the age of onset and penetrance for Huntington's disease based on CAG length. Clin Genet 65:267-277.

Langbehn DR, Hayden MR, Paulsen JS, PREDICT-HD Investigators of the Huntington's Disease Collaborative Group (2010) CAG-repeat length and the age of onset in Huntington disease (HD): a review and validation study of statistical approaches. Am J Med Genet B Neuropsychiatr Genet 153B:397-408.

Leventhal DK, Gage GJ, Schmidt R, Pettibone JR, Case AC, Berke JD (2012) Basal ganglia beta oscillations accompany cue utilization. Neuron 73:523-536.

Magill PJ, Sharott A, Bevan MD, Brown P, Bolam JP (2004) Synchronous unit activity and local field potentials evoked in the subthalamic nucleus by cortical stimulation. J Neurophysiol 92:700-714.

Majid DS, Aron AR, Thompson WK, Sheldon S, Hamza S, Stoffers D, Holland D, Goldstein J, Corey-Bloom J, Dale AM (2011b) Basal ganglia atrophy in prodromal Huntington's disease is detectable over one year with automatic segmentation. Mov Disord.

Majid DS, Cai W, George JS, Verbruggen F, Aron AR (2011) Transcranial magnetic stimulation reveals dissociable mechanisms for global versus selective corticomotor suppression underlying the stopping of action. Cereb Cortex 22:363-371.

Majid DS, Stoffers D, Sheldon S, Hamza S, Thompson WK, Goldstein J, Corey-Bloom J, Aron AR (2011a) Automated structural imaging analysis detects premanifest Huntington's disease neurodegeneration within 1 year. Mov Disord.

Mattfeld AT, Gluck MA, Stark CE (2011) Functional specialization within the striatum along both the dorsal/ventral and anterior/posterior axes during associative learning via reward and punishment. Learn Mem 18:703-711.

Mink JW (1996) The basal ganglia: focused selection and inhibition of competing motor programs. Prog Neurobiol 50:381-425.

Nasreddine ZS, Phillips NA, Bedirian V, Charbonneau S, Whitehead V, Collin I, Cummings JL, Chertkow H (2005) The Montreal Cognitive Assessment, MoCA: a brief screening tool for mild cognitive impairment. J Am Geriatr Soc 53:695-699.

Oberauer K (2009) Design for a Working Memory. Psychology of Learning and Motivation: Advances in Research and Theory, Vol 51 51:45-100.

Ollinger J, Corbetta M, Shulman GL (2001) Separating processes within a trial in event-related function MRI. Neuroimage 13:218-229.

Parthasarathy HB, Schall JD, Graybiel AM (1992) Distributed but convergent ordering of corticostriatal projections: analysis of the frontal eye field and the supplementary eye field in the macaque monkey. J Neurosci 12:4468-4488.

Paulsen JS, Nopoulos PC, Aylward E, Ross CA, Johnson H, Magnotta VA, Juhl A, Pierson RK, Mills J, Langbehn D, Nance M, PREDICT-HD Investigators and Coordinators of the Huntington's Study Group (HSG) (2010) Striatal and white matter predictors of estimated diagnosis for Huntington disease. Brain research bulletin.

Penney JB, Jr., Young AB (1983) Speculations on the functional anatomy of basal ganglia disorders. Annu Rev Neurosci 6:73-94.

Ray NJ, Jenkinson N, Brittain J, Holland P, Joint C, Nandi D, Bain PG, Yousif N, Green A, Stein JS, Aziz TZ (2009) The role of the subthalamic nucleus in response inhibition: evidence from deep brain stimulation for Parkinson's disease. Neuropsychologia 47:2828-2834.

Robbins TW, Brown VJ (1990) The role of the striatum in the mental chronometry of action: a theoretical review. Rev Neurosci 2:181-214.

Ross CA, Tabrizi SJ (2011) Huntington's disease: from molecular pathogenesis to clinical treatment. Lancet Neurol 10:83-98.

Rossi S, Hallett M, Rossini PM, Pascual-Leone A (2009) Safety, ethical considerations, and application guidelines for the use of transcranial magnetic stimulation in clinical practice and research. Clin Neurophysiol 120:2008-2039.

Rossini PM, Barker AT, Berardelli A, Caramia MD, Caruso G, Cracco RQ, Dimitrijevic MR, Hallett M, Katayama Y, Lucking CH (1994) Non-invasive electrical and magnetic stimulation of the brain, spinal cord and roots: basic principles and procedures for routine clinical application. Report of an IFCN committee. Electroencephalogr Clin Neurophysiol 91:79-92.

Scimeca JM, Badre D (2012) Striatal contributions to declarative memory retrieval. Neuron 75:380-392.

Starr PA, Kang GA, Heath S, Shimamoto S, Turner RS (2008) Pallidal neuronal discharge in Huntington's disease: support for selective loss of striatal cells originating the indirect pathway. Exp Neurol 211:227-233.

Stinear CM, Byblow WD (2004) Impaired modulation of intracortical inhibition in focal hand dystonia. Cereb Cortex 14:555-561.

Stoffers D, Sheldon S, Kuperman JM, Goldstein J, Corey-Bloom J, Aron AR (2010) Contrasting gray and white matter changes in preclinical Huntington disease: an MRI study. Neurology 74:1208-1216.

Stuphorn V, Emeric EE (2012) Proactive and reactive control by the medial frontal cortex. Front Neuroeng 5:9.

Swann NC, Cai W, Conner CR, Pieters TA, Claffey MP, George JS, Aron AR, Tandon N (2012) Roles for the pre-supplementary motor area and the right inferior frontal gyrus in stopping action: electrophysiological responses and functional and structural connectivity. Neuroimage 59:2860-2870.

Tabrizi SJ, Langbehn DR, Leavitt BR, Roos RA, Durr A, Craufurd D, Kennard C, Hicks SL, Fox NC, Scahill RI, Borowsky B, Tobin AJ, Rosas HD, Johnson H, Reilmann R, Landwehrmeyer B, Stout JC, TRACK-HD Investigators (2009) Biological and clinical manifestations of Huntington's disease in the longitudinal TRACK-HD study: cross-sectional analysis of baseline data. Lancet Neurol 8:791-801.

van den Bogaard SJA, Dumas EM, Acharya TP, Johnson H, Langbehn DR, Scahill RI, Tabrizi SJ, van Buchem MA, van der Grond J, Roos RAC, TRACK-HD Investigative Group (2010) Early atrophy of pallidum and accumbens nucleus in Huntington's disease. J Neurol.

Verbruggen F, Logan GD (2008) Response inhibition in the stop-signal paradigm. Trends Cogn Sci (Regul Ed) 12:418-424.

Verbruggen F, Logan GD (2009) Models of response inhibition in the stop-signal and stop-change paradigms. Neurosci Biobehav Rev 33:647-661.

Vonsattel JP, Myers RH, Stevens TJ, Ferrante RJ, Bird ED, Richardson EP, Jr. (1985) Neuropathological classification of Huntington's disease. J Neuropathol Exp Neurol 44:559-577.

Watanabe M, Munoz DP (2010) Saccade suppression by electrical microstimulation in monkey caudate nucleus. J Neurosci 30:2700-2709.

Wilcox RR (2001) Fundamentals of modern statistical methods : substantially improving power and accuracy. New York: Springer.

Zandbelt BB, Bloemendaal M, Neggers SF, Kahn RS, Vink M (2012) Expectations and violations: Delineating the neural network of proactive inhibitory control. Hum Brain Mapp.

CHAPTER 5

Training motor suppression through real-time feedback

ABSTRACT

We present a novel procedure by which selective motor suppression of particular muscles on the right hand can be trained using trial-by-trial feedback of corticomotor excitability. We focused on training the selective control of two right hand muscles in particular, namely the dorsal interosseous (FDI) muscle of the index and the abductor digiti minimi (ADM) muscle of the pinky. With single-pulse transcranial magnetic stimulation of the left motor cortex representation of right hand, we obtain a measure of corticomotor excitability for both muscles simultaneously. In Experiment 1, we show conclusive evidence that subjects cued to suppress a particular finger can improve in this ability over the course of practice. In Experiment 2, this procedure is applied towards training motor suppression in the context of selective response inhibition.

INTRODUCTION

Response inhibition, the ability to hold back from an action, is an essential aspect of everyday behavior and a key executive function. Behavioral measures of response inhibition, determined in tasks such as the Stop-Signal or Go/No-Go task, are impaired in a number of conditions including Attention Deficit Hyperactivity Disorder (Murphy, 2002, Aron et al., 2003, Lijffijt et al., 2005) or Obsessive Compulsive Disorder (Chamberlain et al.,

2006, Menzies et al., 2007). On account of this, the possibility of improving response inhibition ability through training has great potential as a form of therapy.

Although a number of studies have shown improvements with training for other executive functions such as working memory (Klingberg et al., 2002, Klingberg et al., 2005, Thorell et al., 2009, Johnstone et al., 2010), efforts towards improving response inhibition through training, however, have been met with mixed results. For instance, while training working memory ability was found to cause a generalized benefit in other working memory tasks, training response inhibition (with a Go/No-Go or Stop-Signal task) was found to cause only limited improvements in the training task itself, without any transfer of the benefits to other response inhibition tasks (Thorell et al., 2009, Johnstone et al., 2010, Manuel et al., 2010, Guerrieri et al., 2012). Training effects reported in other studies can be accounted for by age-related changes in response inhibition (Dowsett and Livesey, 2000), for it is well-established that this ability improves through early development and reduces in old age (Williams et al., 1999, Carver et al., 2001, Bedard et al., 2002). These changes are likely more a function of changes in underlying brain development rather than training effects *per se* (Tamm et al., 2002, Coxon et al., 2012).

Although there is a limited "transfer" effect of response inhibition training on improving general behavior, such as in reducing caloric intake (Guerrieri et al., 2012), some studies have reported positive results when inhibitory signals are presented closely paired with the behavior of interest (i.e. presenting a NoGo signal with images of beer may reduce appetitive drive for alcohol) (Houben, 2011, Houben et al., 2011, Veling et al., 2011). Others have shown evidence that motor slowing associated with response inhibition training can

reduce gambling behavior even after two hours (Verbruggen et al., 2012). Nonetheless, efforts to train simple forms of response inhibition directly may be more difficult, as behavioral measures such as Stop-Signal Reaction Time (SSRT, the speed of stopping) are known to be relatively stable over long periods of time (Logan and Cowan, 1984) and not affected by extensive training (Cohen and Poldrack, 2008).

The relative invariance of behavioral measures of stopping such as SSRT may be due to constraints of anatomy. Converging evidence suggests that simple response inhibition is executed by signaling via the Hyperdirect Pathway connecting the cortex to the Subthalamic Nucleus (Aron and Poldrack, 2006, Aron et al., 2007, Coxon et al., 2012, King et al., 2012), which in turn can lead to rapid suppression of thalamocortical excitation to the motor cortex (Nambu et al., 2002). Although this rapid system may not allow for further improvements in stopping time, recent evidence suggests that more complex forms of stopping (those that require (proactive) advanced planning for selective response inhibition) may rely on signaling through the striatum (Majid et al., *under review*), and this may allow for a greater capacity for plastic change (Graybiel, 2005). Thus, targeting *proactive selective* stopping behavior may lead to a more fruitful method to training response inhibition.

A key and possibly trainable phenomenon associated with proactive selective stopping behavior is *proactive selective motor suppression*. This phenomenon, identified with single-pulse transcranial magnetic stimulation (TMS) to probe corticomotor excitability, is a top-down suppressive influence of response inhibition goals upon motor effectors that might have to stop in the future (Claffey et al., 2010, Cai et al., 2011, Majid et al., *under review*). Furthermore, training selective motor suppression may directly lead to

improvements in selective response inhibition, since the degree of selective motor suppression when preparing to stop has been found to correlate with improved behavior when selectively stopping, manifested as a reduced Stopping Interference Effect, i.e. the RT prolongation effect of stopping the prepared action on actions that must continue (Cai et al., 2011).

With TMS as a probe of corticomotor excitability, proactive motor suppression can be determined on a trial-by-trial basis and thus can be fed back to a subject to allow for immediate behavioral adjustment and improvement, i.e. real-time biofeedback. Various methods of real-time biofeedback have been used to train control over internal states, including the feedback of heart rate (Manuck et al., 1975) and surface electrical rhythms of the brain (electroencephalogram, EEG) (Nowlis and Kamiya, 1970). Notably, the use of EEG biofeedback may have a positive effect on the control of emotional responses (Allen et al., 2001), musical ability (Egner and Gruzelier, 2003), and attention (Egner and Gruzelier, 2001), possibly even as a therapy for Attention Deficit Disorder (Friel, 2007). Recently, studies have explored biofeedback of functional MRI (fMRI) activation, particularly focused on the motor cortex (Yoo and Jolesz, 2002, Weiskopf et al., 2003, deCharms et al., 2004, deCharms, 2008) but also on the amygdala (Posse et al., 2003), auditory cortex (Yoo et al., 2007), insular cortex (Caria et al., 2007), right inferior frontal gyrus (Rota et al., 2009), or presupplementary motor cortex (Subramanian et al., 2011). These studies have shown some benefit in reducing pain symptoms (deCharms et al., 2005) or reducing symptoms in Parkinson's disease (Subramanian et al., 2011)

To our knowledge, no study has explored the potential of single-pulse TMS of the motor cortex and electromyography (EMG) of the resulting motor evoked potential (MEP) as a means of biofeedback. Yet such a method may be superior to the biofeedback methods discussed above. When TMS is delivered over the left motor cortex representation of the right hand, the resulting MEP can serve as an instantaneous measure of right hand corticomotor excitability – a temporally- and spatially-specific measure that cannot be obtained using EEG or fMRI. We investigate here whether individuals can learn to suppress hand corticomotor excitability by trial-by-trial feedback, and if so, whether this improved ability will lead to positive effects on selective response inhibition behavior.

EXPERIMENT 1 METHODS

Real-time TMS/EMG procedure

Subjects sat in front of a 19-inch monitor with their right hand resting on a table. Surface electromyography (EMG) was recorded using a pair of 10mm silver electrodes for two separate muscles on the right hand: 1) the first dorsal interosseous (FDI) used to abduct the *index* finger and 2) the abductor digiti minimi (ADM) used to abduct the little finger or *pinky*. Additional ground electrodes were placed on the radial and ulnar wrist protuberances for the FDI and ADM, respectively. Since single-pulse TMS was delivered in a way that produces motor evoked potentials in both muscles simultaneously, this recording procedure allowed investigation into whether inhibitory control can be *selective* at a given trial (Figure 5.1).

A Class QP511 Quad AC Amplifier System (Glass Technologies, West Warwick, RI) amplified the EMG signal from two separate lines (corresponding to the index and pinky muscles) using a 30Hz to 1kHz band-pass filter and a 60Hz notch filter. T-shaped coaxial junctions were then used to split the amplifier output into a signal directed to a recording computer and a signal directed to the presentation computer. Data directed to the *recording* computer was sent first to a CED Micro 1401 mk II acquisition system that sampled the data at a frequency of 2 kHz. This acquisition system then transmitted the data to the recording computer where CED Signal v4 (Cambridge Electronic Design, Cambridge, UK) was used to read and store full EMG data in two separate channels (corresponding to each muscle) over a 500ms period on each trial.

Particularly important for the *real-time* feedback methodology, data sent to the *presentation* computer (viewed by the subject) were relayed via a USB-1208FS data acquisition device. Data entered the device through analog input terminals configured for single-ended measurements (namely, “CH0 IN” and “CH2 IN”). Two additional analog input terminals (namely, “CH1 IN” and “CH3 IN,” respectively) were grounded by connecting them to analog ground terminals (named “AGND”). The acquisition device was connected to the presentation computer via a USB 2.0 port, and the signal was received using Matlab code provided in the Psychophysics Toolbox (i.e. Psychtoolbox, see Brainard, 1997, Kleiner et al., 2007), the *DaqAInScan.m* function in particular. With regards this function, the two analog input terminals corresponded to “channels” 8 and 10, respectively. The sampling rate was 2000/s. The default voltage range of the signal was ±10V (a gain of 2x), whereas the voltage

range of the CED Signal program was ±2V, so the voltage measurement obtained on the presentation computer needed to be divided by 5 in order to be comparable.

TMS was delivered with a MagStim 200-2 system (Magstim, Whitland, UK) and a figure-of-eight coil (7cm diameter). The study began with a thresholding procedure in which subjects sat with their right hands resting upon the table. The coil was initially approximated 5cm left and 2cm anterior to the vertex to find the cortical representation of the right hand. With single-pulse stimulation, the coil was incrementally repositioned and the stimulus intensity was incrementally increased until a reliable motor evoked potential (MEP) was obtained in both the right FDI and ADM. The amplitude of this MEP served as an index of the excitability of the corticomotor representation of each muscle at a particular point in time.

The lowest stimulation level required to elicit MEP amplitudes of at least 0.05 mV in at least 5 of 10 trials in *both* recorded muscles served as the resting motor threshold (Rossini et al., 1994). The exact location of stimulation was marked directly on the scalp for future reference. Experimental stimulation intensity for use throughout the study was determined as 110% of resting motor threshold.

Real-time feedback-training task

A real-time feedback-training task was used to train subjects to better exert *selective* motor control over muscles involved in either the right index (FDI) or pinky (ADM) movement. Each block consisted of 36 trials.

The first 12 trials of these served as important baseline trials by which to normalize MEP amplitude in the subsequent part of the block. For these 12 trials, subjects saw the "Null" cue for 500ms, indicating that they should remain at rest during the rest of the trial. A blank screen then followed for an additional 1s before TMS was delivered. EMG traces for the two muscles were recorded in the presentation computer for both a 100ms period before TMS delivery (pre-TMS EMG) and a 25ms period after TMS delivery, which included the MEP. The screen remained blank for another 500ms after TMS delivery. If the root-mean-square for one of the pre-trigger EMG traces exceeded 0.01mV, a 1s warning was then delivered to prevent subjects from prematurely activating any muscle, and the trial was excluded from any subsequent analysis. The inter-trial interval was 2s. After all 12 Null trials, the mean MEP amplitude for each muscle was calculated to serve as a resting baseline.

The remaining 24 trials began with a 500ms cue that either instructed subjects to "Suppress Index" or "Suppress Pinky" (12 each, randomly presented). Subjects were told to experiment with mental strategies by which the motor excitability of the cued finger may be reduced, learning through trial-and-error. As was the case for the Null trials, the screen became blank for 1s and TMS was delivered. Pre-TMS EMG (100ms) and the MEP (25ms) traces were recorded for both muscles. The screen remained blank for another 500ms before feedback was delivered (Figure 5.1).

Feedback was presented for 1s. Subjects saw two feedback bars, associated with the index (FDI) and pinky (ADM). The bar associated with the cued muscle was colored red, and the bar associated with the non-cued muscle was colored blue. The bar height for a

particular muscle, either the FDI or ADM, was calculated as follows: *log(trial MEP) – log(mean Null MEP)*. Thus suppression on a given trial with respect to the mean Null baseline would be presented as a (negative) downward pointing bar. If the cued (red) bar was downward pointing (suppressed below baseline) and more negative than the non-cued (blue) bar (suppressed selectively), a "Good Job" message was fed back to the subject in the center of the screen (between the two bars). A "Try Again" message was delivered if this was not the case. A warning was delivered instead of feedback if the root-mean-square of the pre-TMS trace exceeded 0.01mV (Figure 5.1).

TMS analysis

After the training session, peak-to-peak amplitude was determined using custom MATLAB software. All trials for which the root-mean-square of the pre-TMS trace exceeded 0.01mV were excluded to ensure that the effect of preliminary activation on the subsequent MEP did not bias the results. The distribution of MEP amplitudes following each cue ("Suppress Index," "Suppress Pinky," and "Null") for either the FDI (index) and ADM (pinky) were then trimmed to ensure distribution normality (by removing the upper and lower 10% of values) (Wilcox, 2001) and averaged. MEP modulation of either of these muscles on a "Suppress" cue was calculated as the percentage change of the mean "Suppress" cue MEP from the mean "Null" MEP [("Suppress" cue MEP – "Null" MEP)/"Null" MEP *100%]. Negative modulation indicated suppression.

Four measures were thus calculated: 1) FDI modulation on "Suppress Index" trials (Cued Index Modulation), 2) FDI modulation on "Suppress Pinky" trials (Uncued Index

Modulation), 3) ADM modulation on “Suppress Index” trials (Uncued Pinky Modulation), and 4) ADM modulation on “Suppress Pinky” trials (Cued Pinky Modulation).

EXPERIMENT 1 RESULTS

Subjects

Fourteen healthy right-handed subjects (4 males, 10 females, mean age: 20.9±4.1 years) participated in 10 blocks of the suppression-training task described above. All subjects provided written consent in accordance with the Institutional Review Board (IRB) guidelines of the University of California, San Diego (UCSD). They also completed a TMS safety-screening questionnaire (Rossi et al., 2009). Mean resting motor threshold to elicit an MEP was 44.3±8.7% of maximum stimulator output. The experimental stimulation intensity used for the training blocks was 49.3±8.7%.

Subjects were encouraged to use a variety of strategies to suppress the cued finger. These strategies included imagining preventing a movement with the cued finger, imagining the cued finger as numb or on ice, or “thinking away” from the cued finger by imagining alternative movements (i.e. using other fingers). Subjects were told to evaluate each method through trial-and-error after receiving the feedback and to settle on the method that worked the best.

TMS Results

Subjects stated that they tried employing a number of mental strategies to bring about motor suppression. These included imagining the cued muscle “going numb” or

"going on ice." However, all subjects confirmed that the mental strategy that seemed to work best was to *think away* from the cued muscle. Subjects reported imagining movement with the pinky during the "Suppress Index" cue and imagining movement with the index during the "Suppress Pinky" cue.

The 10 blocks of the experiment were divided into two halves. In the in first half (Early Training), subjects suppressed neither the index nor the pinky muscles significantly below baseline when cued (Cued Index Modulation: -16.9±51.7%, t_{13}=1.223, n.s.; Cued Pinky Modulation: 9.9±53.6, t_{13}<1). As predicted, the excitability of neither hand muscle differed from baseline when not cued (Uncued Index Modulation: 29.3±94.2%, t_{13}=1.164, n.s.; Uncued Pinky Modulation: 55.4±149.5%, t_{8}=1.386, n.s.). Cued vs. Uncued Modulation differed only slightly for the Index (t_{13}=2.119, p=.054) and not for the Pinky (t_{13}=1.520, n.s.), suggesting that subjects had not yet developed full ability to modulate finger excitability based on the task demands (Figure 5.2, Table 5.1).

With practice, these profiles changed, as manifest in the second half of the training session (Late Training). Subjects now significantly suppressed the cued index finger (Cued Index Modulation: -36.1±36.6%, t_{13}=3.690, p=.003) and the cued pinky (Cued Pinky Modulation: -20.8±33.6%, t_{13}=2.312, p=.038). Again, finger excitability did not differ from baseline when not cued (Uncued Index Modulation: 31.1±87.0%, t_{13}=1.339, n.s.; Uncued Pinky Modulation: 70.3±152.2%, t_{13}=1.727, n.s.). Selective control, the difference in the modulation of a particular muscle when cued vs. uncued, was apparent for both the Index (t_{13}=3.634, p=.003) and the Pinky (t_{13}=2.555, p=.024) (Figure 5.2, Table 5.1).

Repeated-measures ANOVA with three factors (Session Half [Early vs. Late] X Recorded Muscle [Index vs. Pinky] X Cued State) was used to investigate the change in MEP over time for the cued vs. uncued measures for each muscle. There was a significant effect for Cued State ($F_{1,13}$=7.711, p=.016), suggesting that subjects were able to modulate finger excitability for a particular muscle when cued. There was no effect for Recorded Muscle ($F_{1,13}$=2.767, n.s.) or Session Half ($F_{1,13}$=2.767, n.s.), however. Cued State X Session Half interaction trended towards significance ($F_{1,13}$=3.969, p=.068), suggesting that modulation ability changed over the course of training. On closer inspection with planned comparisons, repeated-measures T-tests showed that practice slightly improved suppression of the index when the index was cued (t_{13}=1.983, p=.069) but had no effect when the index was not cued (t_{13}<1). Likewise, practice improved suppression of the pinky when the pinky was cued (t_{13}=2.892, p=.013) but had no effect when the pinky was not cued (t_{13}<1) (Figure 5.2, Table 5.1).

Experiment 1 Summary

The results of Experiment 1 show that with real-time feedback of motor evoked potential amplitude from TMS, subjects are able to progressively learn to suppress a particular cued right hand finger, either the index or the pinky. In the early half of the training session, subjects did not demonstrate selective control over finger muscles, and MEPs for a particular muscle did not significantly differ whether or not the muscle was cued for suppression. There was, however, a trend-line effect of selective control for the index

finger; index MEPs were slightly reduced when cued for suppression compared to when not cued.

Subjects conveyed that the most effective method they used to suppress a finger was to actually think about the other finger. Surprisingly, this did in fact lead to significant suppression of both the cued index and pinky compared to baseline rather than significant activation of the other finger. Furthermore, each finger showed evidence of selective control, and the muscle was more suppressed when cued compared to when not cued. Between the two training halves, subjects became better at suppressing the cued pinky. The same effect for the index was at trend-line significance, possibly because subjects started off with better selective control of the index even in the first half of training.

EXPERIMENT 2 METHODS

Task Modifications

Experiment 2 investigated whether training of selective motor suppression, as shown in Experiment 1, could be behaviorally beneficial with regards to selective stopping. This required three main modifications: 1) the proactive selective stopping task was modified for responses on a single hand, 2) the training session had an additional Go movement response so as to be similar to the selective stopping task, and 3) a sham-feedback control group was included.

Modification 1: Selective Stopping Task

Subjects took part in a proactive selective stopping task both before and after eight blocks of the suppression-training task (Figure 5.3B). In this proactive selective stopping task, subjects initiated a two-finger response using *both* the index and pinky fingers, either of the right or left hand. Before the Go stimulus, a "Suppress" cue ("Suppress Index" or "Suppress Pinky") informed subjects which of the finger responses they might have to stop in the case of a rare stop signal (33% of trials). Thus the task requires proactive preparation for selective stopping of either the index or pinky.

Each block of the proactive selective stopping task was designed to be similar in timing and structure of the suppression-training task. Thus, each block consisted of 36 trials (12 initial "Null" trials and 24 "Suppress" trials). The "Null" trials served as a resting baseline. Each cue was presented for 500ms followed by a blank screen for 1s. TMS was then delivered. EMG traces were recorded both before the TMS pulse for 100ms or at the time of the MEP. If the root-mean-square for one of the pre-TMS EMG traces exceeded 0.01mV, a 1 second warning was delivered at the end of the trial.

Subjects placed both fingers (index and pinky) of the left and right hands on four separate response boxes. On "Suppress" trials, the screen remained blank for 500ms after TMS delivery. The Go stimulus then appeared. This consisted of four circles arranged in a row, with either the two leftmost or two rightmost circles colored blue to indicate a left hand or right hand response, respectively (equal probabilities). Failure to respond with both fingers simultaneously (defined as >70ms difference in response times) resulted in a "Decoupled" warning presented for 1s at the end of the trial.

On Go trials (67% of trials, 9 “Suppress Index” and 9 “Suppress Pinky” trials per block), the circles remained until a response was made or 1s had passed. On Stop trials (33% of trials, 3 “Suppress Index” and 3 “Suppress Pinky” trials per block), a red X appeared in the center of the screen after a short stop-signal delay (SSD) and remained until the end of the trial. Subjects tried to stop the response of the figure cued for suppression at the beginning of the trial with continuing the response of the other finger.

The SSD dynamically varied throughout the experiment – increasing or decreasing by 50ms with every successful or failed stop, respectively, leading to p(stop) ~ 50%. The stop signal reaction time (SSRT) was calculated using the integration method (Verbruggen and Logan, 2009). Additional behavior measures included the accuracy and decoupling rate on Go trials, the probability of stopping successfully on Stop trials, the stopping direction error rate (how many times the subject stopped the incorrect finger), the median RT on failed Stop trials, and the median RT of the unstopped continuing finger on Stop trials (the Continuing RT).

The Stopping Interference Effect indexes the selectivity of stopping (Aron and Verbruggen, 2008). We estimated this effect as the median RT of the continuing finger (when the other finger is stopped) minus the median RT of that same finger on analogous Go trials. These analogous Go trials were determined by rank-ordering the Go RTs and then averaging those RTs longer than the *n*th one, where *n* is obtained by multiplying the number Go RTs in the distribution by the probability of failing to stop on Stop trials. This method provides a more accurate estimate of the Stopping Interference Effect as it

accounts for the fact that the Go process on successful Stop trials will be slower than that of all Go trials (Verbruggen and Logan, 2009).

No MEP Feedback was delivered after each trial. However, subjects were warned against prematurely activating any finger or decoupling for 1s after the Go signal offset. The inter-trial interval was 1.7s.

Modification 2: Go response in training task.

The Suppression-Training task was the same as in Experiment 1 except with one key difference. In order to train subjects to selectively suppress a right hand finger shortly before having to make a two-finger Go response (as is desired for the proactive selective task), the suppression-training task now included a Go response 500ms after TMS delivery on trials in which "Suppression" was cued. The Go stimulus was a horizontal array of four circles cuing either a left (leftmost circles blue) or right (rightmost circles blue) response. A "Decoupled" warning again was delivered if subjects did not respond with both fingers simultaneously. The circles remained on the screen until a response was made or 1s had passed. The real-time feedback, just as in Experiment 1, then appeared on the screen immediately after the Go response (Figure 5.3C).

Modification 3: Sham-feedback Control group.

Subjects were randomly assigned to either a real-feedback group, for which the TMS feedback was a correct representation of the real MEP, or a sham-feedback group. Each individual in the sham-feedback group received the same TMS feedback as another

individual in the real-feedback group. Thus, both groups saw the same degree of positive "Good Job" feedback. After the first subject (who necessarily received real feedback), both the experimenter and the subject were oblivious to the group assignment.

Overall Structure

All subjects engaged in 18 total blocks of the task. Blocks 1 and 2 were of the proactive selective stopping task, to serve as a behavioral baseline. Blocks 3 and 4 were of the basic training task of Experiment 1, without any Go response. This served to introduce subjects to the suppression task. The next eight blocks, blocks 5-12, were of the modified training task with the additional Go component. The remaining 6 blocks, blocks 13-18, returned to the proactive selective stopping task in order to investigate whether training could be behaviorally beneficial (Figure 5.3A).

EXPERIMENT 2 RESULTS

Subjects

After the exclusion of one behavioral outlier, twenty healthy subjects participated in Experiment 2, randomly assigned to a real-feedback group (n=12, 10 males, 2 females, all right handed, mean age: 22.4±4.3 years) and a sham-feedback group (n=8, 2 males, 6 females, 2 left handed, mean age: 24.4±12.1 years). Age did not differ between subject groups (t_{18}<1). All subjects provided written consent in accordance with the Institutional Review Board (IRB) guidelines of the University of California, San Diego (UCSD). They also completed a TMS safety-screening questionnaire (Rossi et al., 2009). Groups did not differ in

mean resting motor threshold as a percentage of maximum stimulator output (Real-Feedback: 41.7±8.7%; Sham-Feedback: 43.6±9.7%, t_{18}<1) or in experimental stimulation intensity (Real-Feedback: 45.6±9.0%; Sham-Feedback: 48.1±9.8%, t_{18}<1).

Training Session

Subjects took part in eight blocks of the suppression-training task after two pre-training behavioral blocks and before six post-training behavioral blocks. Cued vs. Uncued Modulation was determined for the Index and Pinky in both the first and last four blocks to assess longitudinal change (Early vs. Late training) (Figure 5.4, Table 5.2). Thus for each finger muscle, ANOVA was run with three factors (Cue, Group, and Session Half). There were no significant interactions between factors. Contrary to prediction, there was no effect of Group (Index: F<1; Pinky: F<1). However, there were effects of Session Half on both Index and Pinky Modulation (Index: $F_{1,18}$=6.666, p=.019; Pinky: $F_{1,18}$=6.248, p=.022) and of Cue on Index Modulation (Index: $F_{1,18}$=6.832, p=.018; Pinky: $F_{1,18}$=2.272, p=.15). On closer inspection with planned paired-sample *t*-tests, only the real-feedback group showed reduced Index Modulation between the two training halves (t_{11}=2.433, p=.033) whereas the sham-feedback group did not (t_7=1.779, n.s.) (Figure 5.4, Table 5.2). In the last half of training, only the real-feedback group showed a difference in cued vs. uncued Index Modulation (t_{11}=2.854, p=.016) whereas the sham-feedback group did not (t_7=1.533, n.s.) (Figure 5.4, Table 5.2). Still, neither Index nor Pinky Modulation was negative in the latter half of the training paradigm for either of the two groups, and no other significant differences were identified.

Pre-training behavioral blocks

Subjects took part in two blocks of the proactive-selective stopping task before suppression-training task. Groups did not differ in Go RT (Real-Feedback: 662±114ms; Sham-Feedback: 660±203ms, t_{18}<1) or Go Accuracy (Real-Feedback: 78.2±12.0%; Sham-Feedback: 68.6±19.5%, t_{18}=1.360, n.s.). Groups also did not differ in the probability of stopping (Real-Feedback: 64.2±19.4%; Sham-Feedback: 72.0±15.4%, t_{18}=1.360, n.s.), Stopping Interference Effect (Real-Feedback: 187±245ms; Sham-Feedback: 174±159ms, t_{18}<1), mean Stop Signal Delay (SSD) (Real-Feedback: 238±33ms; Sham-Feedback: 240±31ms, t_{18}<1), and Stop Signal Reaction Time (SSRT) (Real-Feedback: 301±58ms; Sham-Feedback: 327±97ms, t_{18}<1). The groups were thus matched at baseline. However, we caution that due to the low number of trials, SSRT calculations may not be reliable.

Index and Pinky Modulation were calculated and analyzed with a two-factor ANOVA (Cue X Group). There was no Cue by Group interaction for either finger (Index: $F_{1,18}$=1.970, n.s.; Pinky: $F_{1,18}$=2.525, n.s.), and there was no effect of Group (Index: $F_{1,18}$=3.530, n.s.; Pinky: $F_{1,18}$=1.704, n.s.). This again suggests that the groups were matched at baseline. There was a significant effect of Cue on Index Modulation ($F_{1,18}$=9.982, p=.005) and Pinky Modulation ($F_{1,18}$=4.864, p=.041) (Figure 5.5, Table 5.3). However, planned paired-sample *t*-tests of cued vs. uncued finger modulation for each group separately showed no significant differences.

One major observation was that finger modulation was significantly elevated for both the index and pinky, whether cued or uncued, in both the Real- and Sham-feedback

group (all t>2, p<.05). This may suggest generalized excitability during these first two blocks of the behavioral task and may confound the subsequent results.

Post-training behavioral blocks.

Subjects then completed and additional six blocks of the proactive-selective stopping task after the suppression-training task. Just as in the pre-training blocks, Go RT (Real-Feedback: 663±124ms; Sham-Feedback: 615±137ms, t_{18}<1) or Go Accuracy (Real-Feedback: 87.5±7.0%; Sham-Feedback: 85.8±9.9%, t_{18}<1.). Groups also did not differ in the probability of stopping (Real-Feedback: 56.7±12.3%; Sham-Feedback: 53.3±13.8%, t_{18}<1), Stopping Interference Effect (Real-Feedback: 177±149ms; Sham-Feedback: 82±136ms, t_{18}=1.458, n.s.), mean Stop Signal Delay (SSD) (Real-Feedback: 349±112ms; Sham-Feedback: 339±99ms, t_{18}<1), and Stop Signal Reaction Time (SSRT) (Real-Feedback: 249±69ms; Sham-Feedback: 275±52ms, t_{18}<1).

Cued vs. Uncued Modulation was calculated for both the index and pinky, and values were analyzed in a two-factor ANOVA (Cue X Group). Once again, there was no Cue by Group interaction for either finger (Index: F<1; Pinky: F<1), and there was no effect of Group (Index: F<1.; Pinky: F<1). However, there was a significant effect of Cue on Index Modulation (F=5.363, p=.033) and Pinky Modulation (F=6.454, p=.021) (Figure 5.5, Table 5.3). Still, planned paired-sample t-tests of cued vs. uncued finger modulation for each group separately showed no significant differences.

Change between sessions

Repeated Measures ANOVA was run for all behavioral measures between the two sessions. There was no interaction between Group and Session or any significant effect of Group for any behavioral measures. Though Go RT did not differ between sessions (F<1), Go Accuracy did increase between sessions ($F_{1,1}$=26.603, p<.001). Reflecting the stabilization of the stopping staircase, the stopping probability did decrease to ~50% ($F_{1,1}$=9.130, p=.007) due to a lengthening SSD ($F_{1,1}$=27.699, p<.001). However, there was no change in the Stopping Interference Effect ($F_{1,1}$=1.660, p=.214).

When comparing change between the pre-training and post-training blocks, a 3-factor ANOVA (Cue X Group X Session) was run. There were no significant interactions. However, there was a significant effect of Cue (Index: F=9.886, p=.006; Pinky: F=9.762, p=.006) and a significant effect of Session (Index: F=20.485, p<.001; Pinky: F=18.683, p<.001). Closer inspection with planned paired-sample *t*-tests showed that both the Real- and Sham-feedback groups had decreases between sessions for Cued Index Modulation (Real-feedback: t_{11}=3.270, p=.007; Sham-feedback: t_7=2.907, p=.023) and Cued Pinky Modulation (Real-feedback: t_{11}=2.451, p=.032; Sham-feedback: t_7=5.146, p=.001) (Figure 5.5, Table 5.3). This is likely because finger modulation was elevated across the board for all measures in the pre-training behavioral task, whereas finger modulation did not differ from baseline for any measure in the post-training behavioral task.

Relationship between proactive suppression and interference

Greater proactive suppression before the onset of a successful selective stopping trial has been found to correlate with smaller Stopping Interference on that trial (Cai et al., 2011), suggesting that proactive suppression allows for greater selectivity when stopping. We thus investigated the following two hypotheses using data from the post-training behavioral blocks: 1) proactive right *index* suppression before successfully stopping that finger will relate to faster completion of the continuing (right pinky) response on that trial, and 2) proactive right *pinky* suppression before successfully stopping that finger will relate to faster completion of the continuing (right index) response on that trial.

Only subjects who had four or more right-hand successful Stop trials for a particular condition ("Suppress Index" or "Suppress Pinky") were included in the analysis. For each subject, the MEP of the cued finger on Stop trials was regressed to the RT of the Continuing (uncued) finger response. We predicted a *positive* correlation, since smaller MEPs (more proactive suppression) would predict faster Continuing RTs (less Stopping Interference). Pearson's R-value was determined for each subject for both the "Suppress Index" and "Suppress Pinky" conditions. The group-wise distribution of R-values was then compared for difference from zero (indicating no correlation) in one-sample T-tests.

Though R-values were not positive across the group in the "Suppress Index" condition (t<1), they were significantly different from zero in the "Suppress Pinky" condition (R=0.30±.45, t_{15}=2.616, p=.019). This suggests that greater suppression of the right pinky before successfully stopping that pinky correlates to greater stopping selectivity on a subject-by-subject basis.

Experiment 2 Summary

Subjects engaged first in two blocks of a proactive selective stopping task, then eight blocks of a feedback-driven suppression-training task, and then six blocks of a proactive stopping task. The suppression-training task was a shorter and modified form from that of Experiment 1, with the addition of a Go response component. Possibly on account of these differences, subjects neither in the Real- nor Sham-feedback group showed clear evidence of below-baseline suppression of the cued finger. There is however a small suggestion that real-feedback training did allow for better selective control whereas sham-feedback training did not. Only in the Real-feedback group was Cued Index Modulation in late training more negative than Cued Index Modulation in early training (indicating improvement with practice) and more negative than Uncued Index Modulation in late training (indicating some selective control). However, the training session in large part did not accomplish the intended goal of greater suppression, as had been the case in Experiment 1.

Results from the proactive selective behavioral task pre- and post-training were also largely inconclusive. There were no improvements in behavioral measures, such as a reduction in the Stopping Interference Effect, in either the Real- or Sham-feedback groups. Furthermore, TMS results may have been confounded by a generalized elevation of all modulation measures in the first two pre-behavioral blocks. Yet despite this, when focusing on the post-behavioral blocks alone, there was some evidence that greater proactive motor suppression (of the pinky in particular) before successful stop trials related to a reduced Stopping Interference Effect on those trials.

DISCUSSION

Experiment 1

In Experiment 1, we establish that individuals are able to gain greater control of the motor excitability of specific muscles with the aid of the real-time feedback of motor evoked potentials from single-pulse Transcranial Magnetic Stimulation (TMS). Subjects were asked to use some mental strategy to *suppress* the motor excitability of a particular muscle below that of a baseline. Importantly, single-pulse TMS over the right hand representation of the left motor cortex resulted in motor evoked potentials in two separate right hand muscles, allowing for an investigation as to whether such suppression could be done selectively. Indeed, although subjects showed little control over right hand excitability in the early half of the training session, this selective control did improve. By the second half of the training session, subjects effectively could use mental strategies to train selective suppression of whichever finger was cued.

Training the use of motor imagery has been used as an encouraging therapeutic method in conditions such as stroke (Dijkerman et al., 2004, Cramer et al., 2007, Dunsky et al., 2008), spinal chord injury (Stevens and Stoykov, 2003), and Parkinson's disease (Subramanian et al., 2011). Such mental motor imagery has been found to robustly activate non-primary motor areas in healthy individuals but also some weak activation in M1 (Sharma et al., 2006). Whereas all these studies have used motor imagery to increase activation of M1 in cases when motor activity is impaired, our study addresses a novel goal, training M1 *suppression* for benefit in inhibitory control.

Though subjects began the training session with a number of possible strategies to choose from, all eventually settled upon *thinking away* from the cued muscle as the most effective strategy, whether this was through imagining movement of the uncued finger (e.g. imagining motion of the index when the pinky was cued for suppression and vice versa) or on some other finger of the same hand (e.g. the thumb when suppressing the index). Since such motor imagery is likely to activate the M1 representations of these alternative muscles, one mechanistic possibility is that this activation in turn inhibits the M1 representation of the cued finger, leading to effective suppression through a form of *motor surround inhibition* (Hallett, 2003, Sohn and Hallett, 2004b). At which level of the motor cortex that that this process occurs, however, is not fully clear. Surround inhibition is a well-documented organizational principle of the sensory system (Hubel and Wiesel, 1968) and was originally thought to be a function of cortico-cortical inhibition local to the cortex (Gilbert and Wiesel, 1983). Analogously, cortico-cortical inhibition has also been suggested in the motor cortex (Kujirai et al., 1993, Hanajima et al., 1996) and could underlie the suppression seen here. Further work in sensory systems, however, has suggested that the actual locus of surround inhibition may be in lower level thalamic structures that in turn reduce excitatory drive to cortical sensory regions (Ozeki et al., 2004, Smith, 2006). Similarly, surround inhibition of the motor cortex has been thought to be a function of the influence of inhibitory basal ganglia pathways, such as the Indirect Pathway, in reducing thalamocortical drive to the cortex (Mink, 2003).

Another consideration lends further support to the possibility that the motor suppression we see here is driven by the basal ganglia. The basal ganglia has been long

implicated in feedback-driven learning with regards to tasks such as categorical classification (Doya, 2000, Packard and Knowlton, 2002, Aron et al., 2004, Shohamy et al., 2004a, Seger, 2008). Midbrain dopamine signaling, in response to reward and punishment, is believed to underlie this form of learning (Shohamy et al., 2008) and impairments occur in Parkinson's disease where dopaminergic signaling is impaired (Frank et al., 2004, Shohamy et al., 2004b).

These findings may have a particular impact in leading to new therapeutic techniques in neurological disorders where motor inhibition is impaired. One prime example is the case of Focal Hand Dystonia, for which there is impairments in motor surround inhibition (Sohn and Hallett, 2004a) and impaired modulation of intracortical inhibition (Stinear and Byblow, 2004). Furthermore, focal hand dystonia, and other forms of dystonias such as musician's dystonia and writer's cramp, are all thought to be circuit disorders of the basal ganglia (DeLong and Wichmann, 2007) in which the excitatory direct pathway is overactive, surpassing signaling of the indirect pathway and leading to an overall reduction in basal ganglia inhibitory output to the thalamus (Starr et al., 2005). Real-time feedback training of selective motor suppression could thus be a tool in retraining motor inhibition through the basal ganglia.

Experiment 2

Experiment 2 addressed whether training of motor suppression could indeed lead to behavioral advantages in selective stopping. A number of studies have shown that preparation for selective stopping leads to proactive motor suppression of the effector that

might have to stop (Claffey et al., 2010, Cai et al., 2011, Majid et al., *under review*). Converging evidence from neuroimaging and the study of premanifest Huntington's disease suggests that striatal and pallidal signaling underlies the phenomenon, and the basal ganglia's classical Indirect Pathway may be a likely candidate for such an inhibitory mechanism (Majid et al., *under review*). Although a number of alternative possibilities exist, the same basal ganglia mechanism may drive the training of selective motor suppression that was identified in Experiment 1, as argued above. If so, training selective motor suppression may lead to behavioral benefits in selective stopping, since task-related proactive selective motor suppression has been found to relate to greater behavioral selectivity when subjects actually do stop successfully (Cai et al., 2011).

The results from Experiment 2, however, were not fully conclusive. Subjects engaged in the feedback-training task did not show clear suppression of cued finger by the end of training or during the post-training behavioral session. A number of factors may bear on this. Firstly, due to timing constraints, the length of the feedback-training session was reduced compared to that of Experiment 1. In addition, the feedback-training task was modified to include an additional response component to increase similarity to the behavioral task. However, this additional response component may have increased the difficulty for subjects training selective finger suppression, whether or not they were in the Real- or Sham-feedback group. Nonetheless, the feedback-training results from Experiment 2 do suggest that subjects receiving real-feedback were slightly more proficient in selective motor control compared to those receiving sham-feedback, though direct group comparisons were not significant.

Secondly, the TMS results from the selective stopping behavioral task were in part confounded by a generalized motor excitability both fingers in the two pre-behavioral blocks, regardless of whether the fingers were cued or not. It is likely that this effect may have been minimized if subjects could take part in more blocks of the behavioral task, which would also yield a more reliable measure of behavior, but constraints as to the total time available for subject involvement limited this possibility.

Thirdly, the implementation of the proactive selective stopping task used here required that subjects initiate responses with two fingers of a single hand, stopping one in the case of a Stop signal. This differed from those previously used (Aron and Verbruggen, 2008, Claffey et al., 2010, Cai et al., 2011, Majid et al., *under review*) where subjects rather initiated responses with *two separate hands*. It is likely that this task difference required additional coordination and increased task difficulty; this may have been reflected in the large Stopping Interference Effect identified in this study compared to the studies cited above (in particular, due to use of the same method of calculating the Stopping Interference Effect, cf. Majid et al., *under review*). However, investigation of the post-training behavioral blocks of Experiment 2 did show evidence of a relationship between proactive motor suppression of the pinky and the Stopping Interference Effect on trials when the right pinky was successfully stopped. This finding in part replicates the finding of Cai et al. (2011) and reiterates that motor suppression training may still have future potential in leading to behavioral improvements in selective stopping. Thus, future endeavors that improve on the task paradigm of Experiment 2 by increasing the length of the feedback-training and behavioral sessions may yield more conclusive results than those of Experiment 2.

ACKNOWLEDGMENTS

I thank Jan Wessel for assistance in methodological development in this chapter.

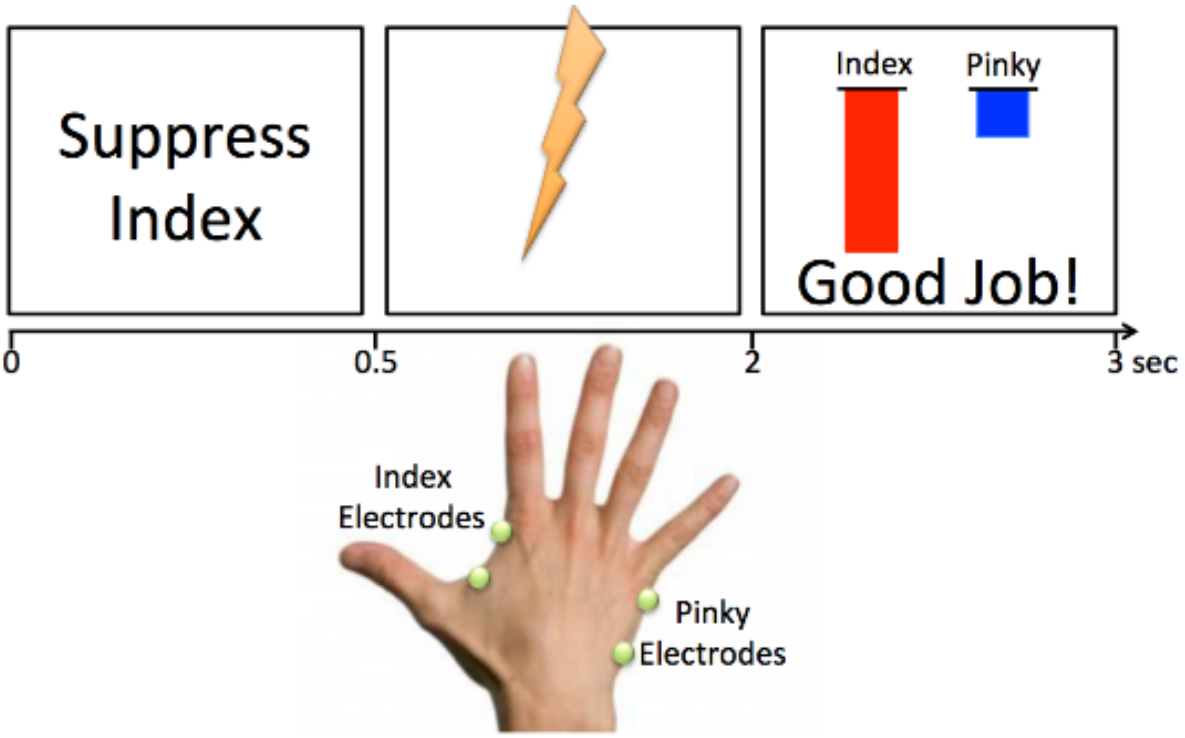

Figure 5.1: *Feedback-driven suppression training task*. (top) Subjects first see a suppression cue for 500ms followed by a blank screen. TMS is delivered 1s after cue-offset and the MEP is recorded from both the Index and Pinky (see bottom panel for location of electrodes on the FDI [index] and ADM [pinky] muscles). After an additional 500ms, feedback is delivered in the form of two bars using the following formula for each muscle respectively: *log(trial MEP) – log(mean Null MEP)*. If the bar associated with the cued muscle (presented in red) is suppressed compared to baseline (red bar pointing negatively) and the other muscle (red bar more negative than blue bar), a "Good Job!" feedback is delivered. In any other case, the subject is told to "Try Again."

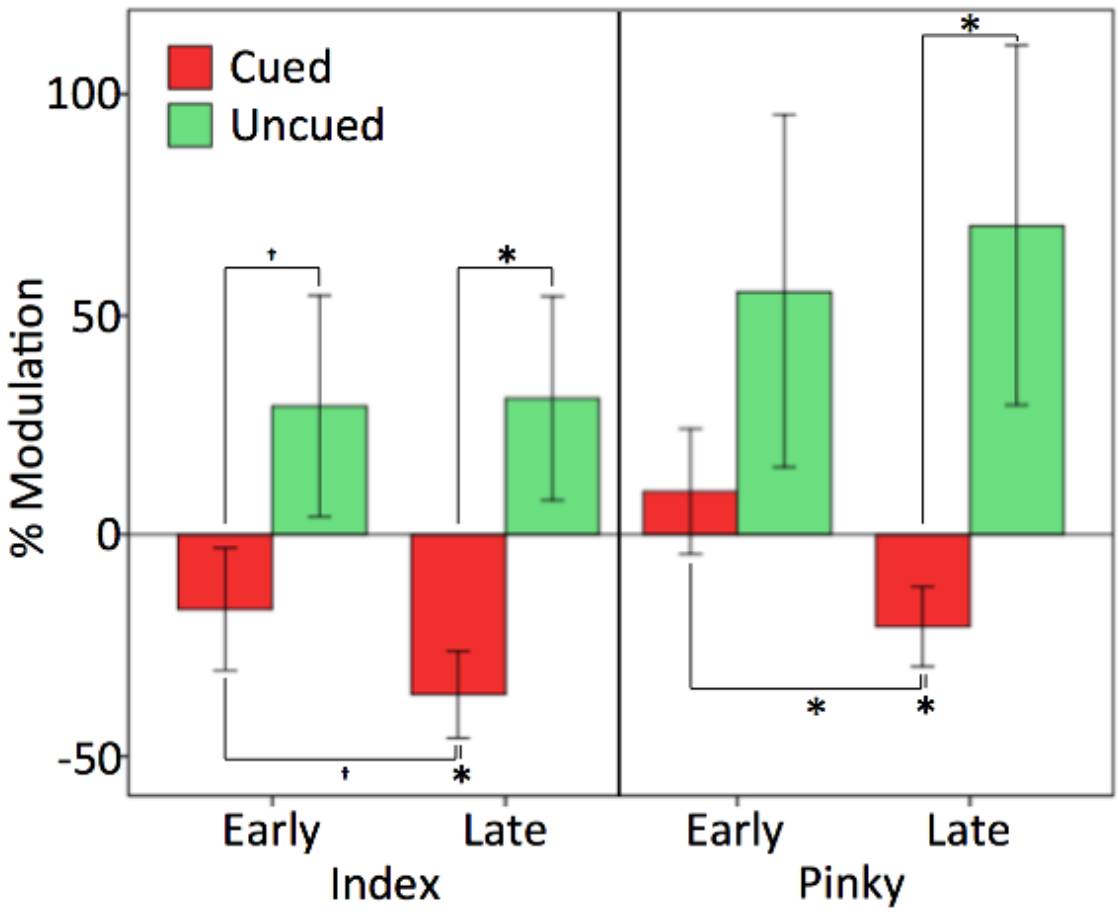

Figure 5.2: *Experiment 1 finger modulation for the Index (left) and Pinky (right)*. Bars represent Percent MEP Modulation compared to the Null baseline, calculated as the percentage change of the mean "Suppress" cue MEP from the mean "Null" MEP [("Suppress" cue MEP – "Null" MEP)/"Null" MEP *100%]. Negative modulation indicated suppression. * represents significant differences or difference from baseline at p<.05. † represents differences with trend-line significant at p<.10

Table 5.1: *Experiment 1 finger modulation for early and late training*

	First 5 blocks (early training)		Last 5 blocks (late training)	
	Cued	Uncued	Cued	Uncued
Index	-16.9 ± 51.7 %	29.3 ± 94.2 %	-36.1 ± 36.6 % *	31.1 ± 87.0 %
Pinky	9.9 ± 53.6 %	55.4 ± 149.5 %	-20.8 ± 20.8 % *	70.3 ± 152.2 %

Values represent Percent MEP Modulation compared to the Null baseline, calculated as the percentage change of the mean “Suppress” cue MEP from the mean “Null” MEP [(“Suppress” cue MEP – “Null” MEP)/”Null” MEP *100%]. Negative modulation indicated suppression. * represents significant difference from baseline at $p<.05$.

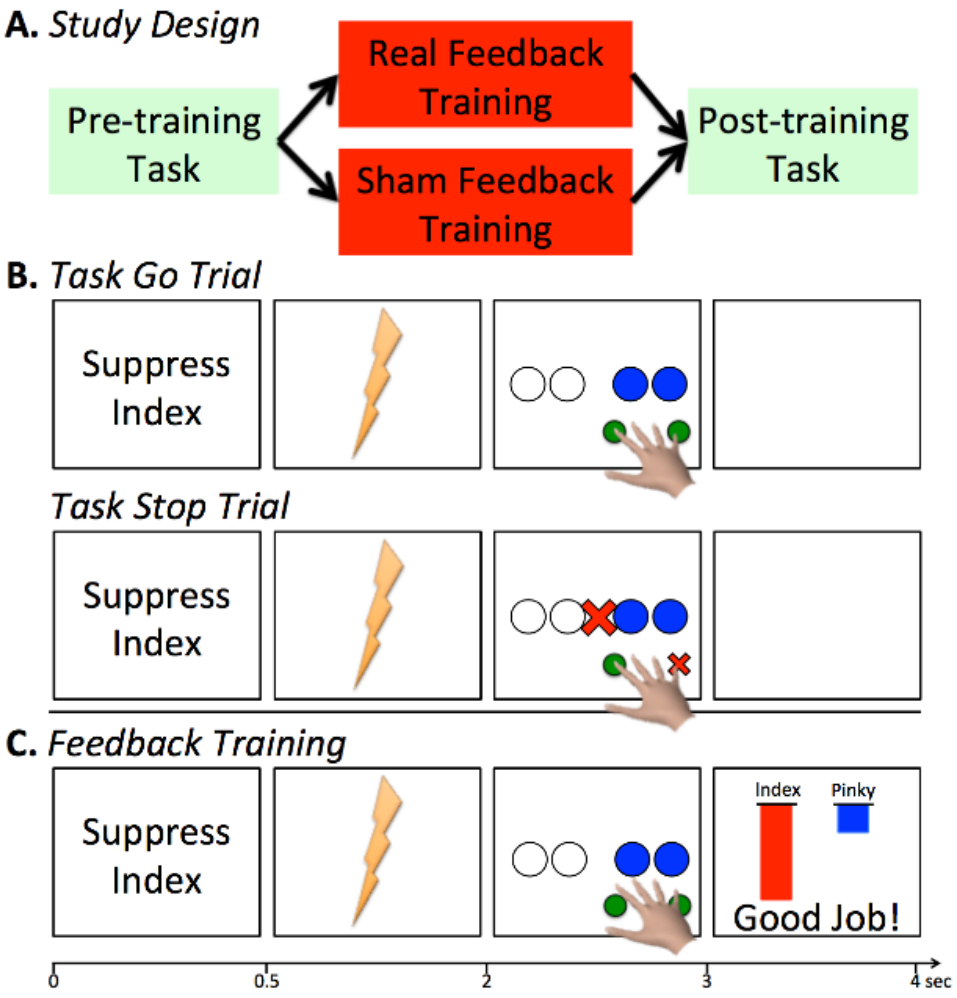

Figure 5.3: *Experiment 2 modifications*. (A) Study design. All subjects engaged in two blocks of the pre-training task before the training session. Subjects were randomly assigned to a real-feedback group or a sham-feedback group (whose feedback corresponded to that of a subject in the real-feedback group. After eight blocks of the feedback training task, all subjects completed another six blocks of the behavioral task. (B) Proactive Selective Stop-Signal task. Each trial began with a preparatory cue (0.5s, 'Suppress Index' or 'Suppress Pinky') that indicated which finger might have to stop in the case of an uninformative Stop-signal. After a delay, a Go signal (two blue circles) appeared, prompting a two-finger response with either the left or right hand. On a third of trials, a Stop signal (red X) then appeared after a dynamically varied stop-signal delay (SSD), requiring the subject to stop the previously cued finger while continuing the other. C. Feedback training task. The training task was the same as that used in Experiment 1 except for the addition of a Go response after TMS delivery but before feedback. This was to ensure that the feedback-training task is similar to the proactive selective stop-signal task. Sham-feedback subjects received feedback identical to that of another subject in the real-feedback group, randomly assigned.

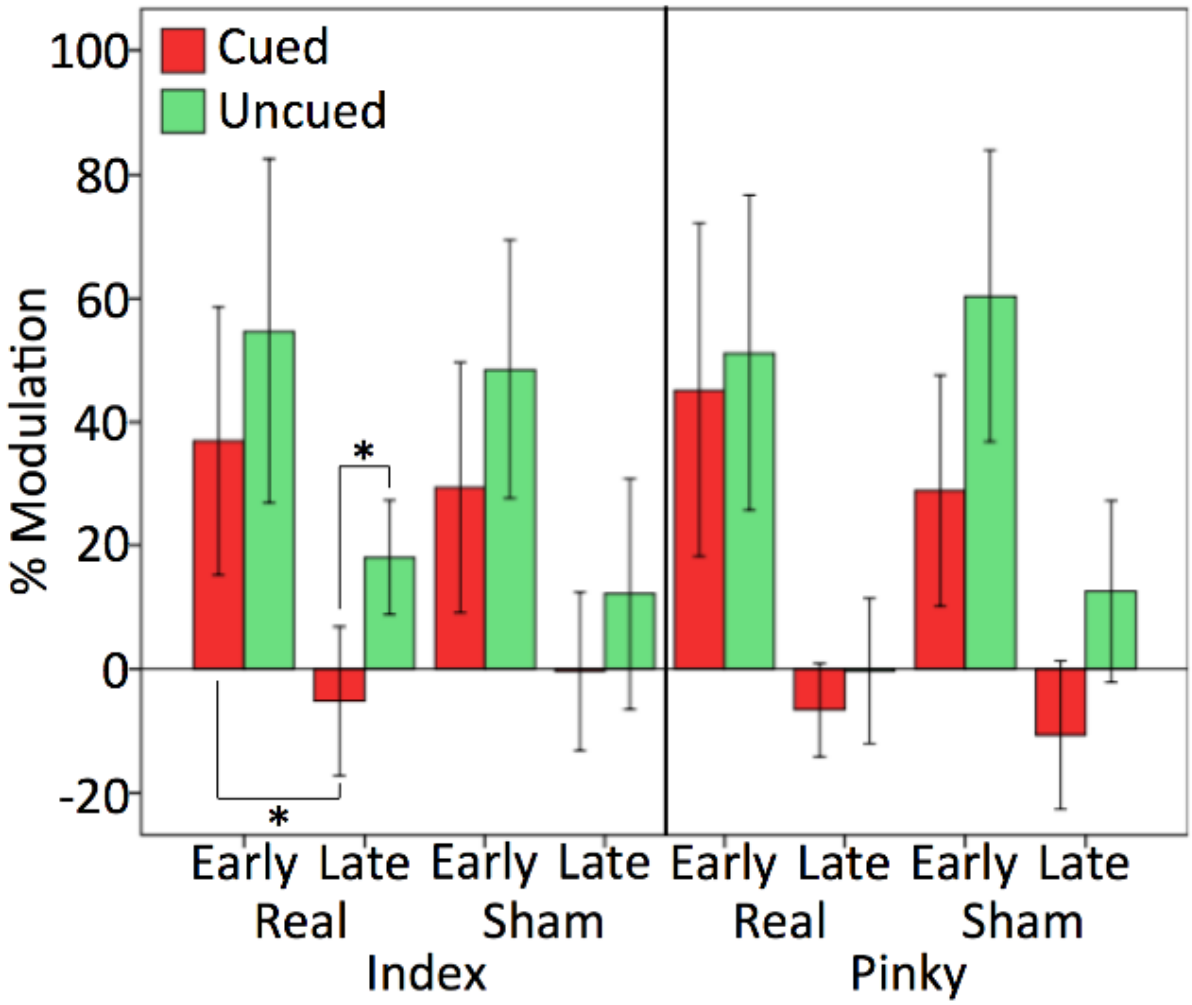

Figure 5.4: *Experiment 2 finger modulation in early and late feedback training*. Bars represent Percent MEP Modulation compared to the Null baseline, calculated as the percentage change of the mean "Suppress" cue MEP from the mean "Null" MEP [("Suppress" cue MEP – "Null" MEP)/"Null" MEP *100%]. Negative modulation indicated suppression. * represents significant differences at p<.05.

Table 5.2: *Experiment 2 finger modulation during early and late feedback training*

		Real-Feedback		Sham-Feedback	
		Cued	Uncued	Cued	Uncued
Index	Early	36.9 ± 75.3 %	54.7 ± 96.5 %	29.4 ± 57.6 %	48.5 ± 59.2 %
	Late	-5.2 ± 51.5 %	18.0 ± 32.4 %	-0.4 ± 35.9 %	12.1 ± 52.8 %
Pinky	Early	45.2 ± 93.5 %	51.2 ± 88.5 %	28.9 ± 53.1 %	60.4 ± 66.6 %
	Late	-6.4 ± 26.0 %	-0.3 ± 40.5 %	-10.6 ± 33.9 %	12.5 ± 52.8 %

Values represent Percent MEP Modulation compared to the Null baseline, calculated as the percentage change of the mean “Suppress” cue MEP from the mean “Null” MEP [(“Suppress” cue MEP – “Null” MEP)/”Null” MEP *100%]. Negative modulation indicated suppression.

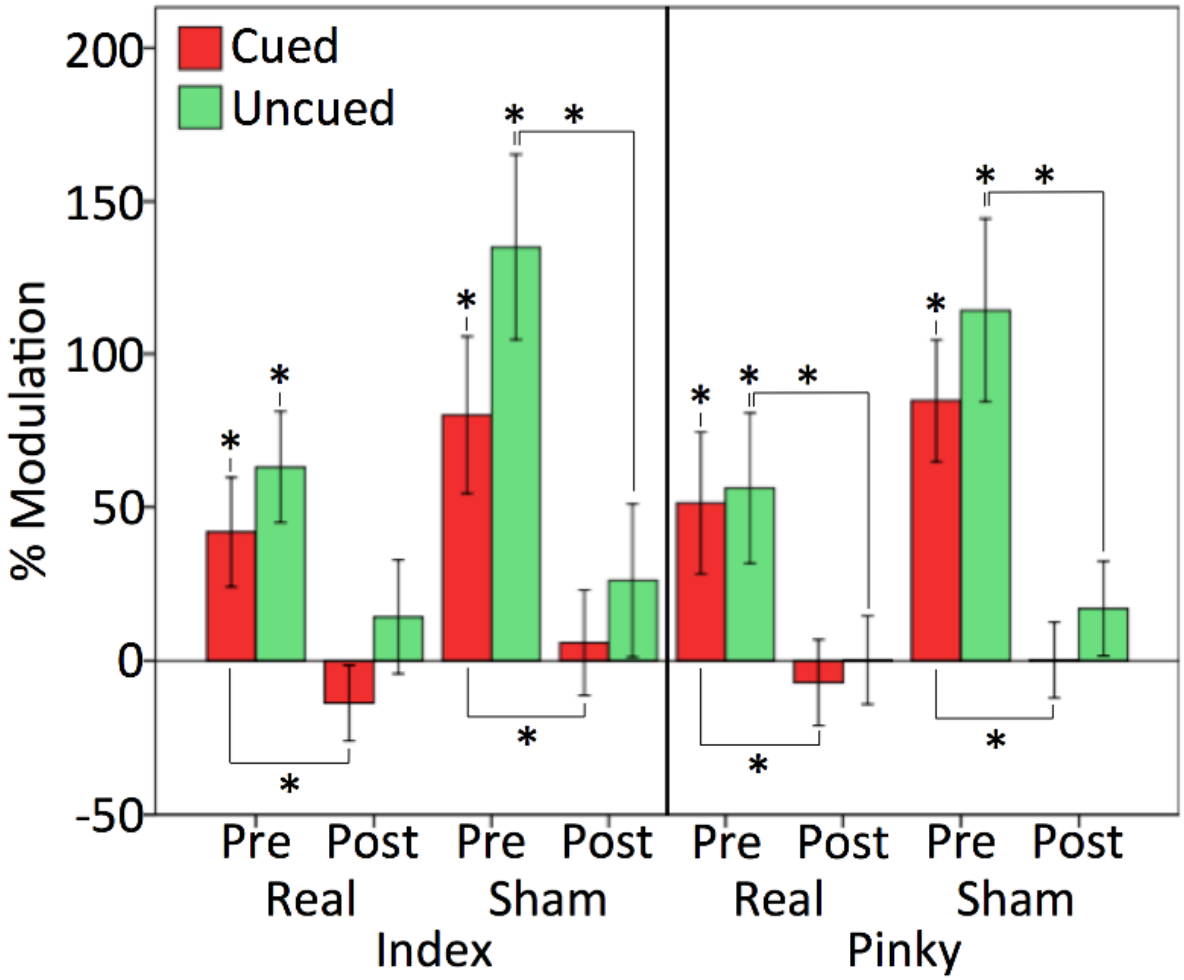

Figure 5.5: *Experiment 2 finger modulation in pre- and post-training behavioral blocks*. Bars represent Percent MEP Modulation compared to the Null baseline, calculated as the percentage change of the mean "Suppress" cue MEP from the mean "Null" MEP [("Suppress" cue MEP – "Null" MEP)/"Null" MEP *100%]. Negative modulation indicated suppression. * represents significant differences or difference from baseline at p<.05.

Table 5.3: *Experiment 2 finger modulation during pre- and post-training behavioral task*

		Real-Feedback		Sham-Feedback	
		Cued	Uncued	Cued	Uncued
Index	Pre	41.8 ± 61.7 % *	63.0 ± 62.7 % *	80.0 ± 72.5 % *	135.0 ± 86.0 % *
	Post	-13.8 ± 42.7 %	14.2 ± 64.0 %	5.9 ± 48.5 %	26.1 ± 70.4 %
Pinky	Pre	51.3 ± 80.1 % *	56.2 ± 85.0 % *	84.6 ± 56.3 % *	144.4 ± 85.0 % *
	Post	-7.1 ± 48.4 %	0.2 ± 49.7 %	0.4 ± 34.7 %	17.0 ± 43.5 %

Values represent Percent MEP Modulation compared to the Null baseline, calculated as the percentage change of the mean “Suppress” cue MEP from the mean “Null” MEP [(“Suppress” cue MEP – “Null” MEP)/”Null” MEP *100%]. Negative modulation indicated suppression. * represents significant difference from baseline at $p<.05$.

References

Allen JJ, Harmon-Jones E, Cavender JH (2001) Manipulation of frontal EEG asymmetry through biofeedback alters self-reported emotional responses and facial EMG. Psychophysiology 38:685-693.

Aron AR, Behrens TE, Smith S, Frank MJ, Poldrack RA (2007) Triangulating a cognitive control network using diffusion-weighted magnetic resonance imaging (MRI) and functional MRI. J Neurosci 27:3743-3752.

Aron AR, Dowson JH, Sahakian BJ, Robbins TW (2003) Methylphenidate improves response inhibition in adults with attention-deficit/hyperactivity disorder. Biol Psychiatry 54:1465-1468.

Aron AR, Poldrack RA (2006) Cortical and subcortical contributions to Stop signal response inhibition: role of the subthalamic nucleus. J Neurosci 26:2424-2433.

Aron AR, Shohamy D, Clark J, Myers C, Gluck MA, Poldrack RA (2004) Human midbrain sensitivity to cognitive feedback and uncertainty during classification learning. J Neurophysiol 92:1144-1152.

Aron AR, Verbruggen F (2008) Stop the presses: dissociating a selective from a global mechanism for stopping. Psychol Sci 19:1146-1153.

Bedard AC, Nichols S, Barbosa JA, Schachar R, Logan GD, Tannock R (2002) The development of selective inhibitory control across the life span. Developmental neuropsychology 21:93-111.

Brainard DH (1997) The Psychophysics Toolbox. Spatial vision 10:433-436.

Cai W, Oldenkamp C, Aron AR (2011) A proactive mechanism for selective suppression of response tendencies. J Neurosci 31:5965-5969.

Caria A, Veit R, Sitaram R, Lotze M, Weiskopf N, Grodd W, Birbaumer N (2007) Regulation of anterior insular cortex activity using real-time fMRI. Neuroimage 35:1238-1246.

Carver AC, Livesey DJ, Charles M (2001) Age related changes in inhibitory control as measured by stop signal task performance. The International journal of neuroscience 107:43-61.

Chamberlain SR, Fineberg NA, Blackwell AD, Robbins TW, Sahakian BJ (2006) Motor inhibition and cognitive flexibility in obsessive-compulsive disorder and trichotillomania. Am J Psychiatry 163:1282-1284.

Claffey MP, Sheldon S, Stinear CM, Verbruggen F, Aron AR (2010) Having a goal to stop action is associated with advance control of specific motor representations. Neuropsychologia 48:541-548.

Cohen JR, Poldrack RA (2008) Automaticity in motor sequence learning does not impair response inhibition. Psychon Bull Rev 15:108-115.

Coxon JP, Van Impe A, Wenderoth N, Swinnen SP (2012) Aging and inhibitory control of action: cortico-subthalamic connection strength predicts stopping performance. J Neurosci 32:8401-8412.

Cramer SC, Orr EL, Cohen MJ, Lacourse MG (2007) Effects of motor imagery training after chronic, complete spinal cord injury. Exp Brain Res 177:233-242.

deCharms RC (2008) Applications of real-time fMRI. Nat Rev Neurosci 9:720-729.

deCharms RC, Christoff K, Glover GH, Pauly JM, Whitfield S, Gabrieli JD (2004) Learned regulation of spatially localized brain activation using real-time fMRI. Neuroimage 21:436-443.

deCharms RC, Maeda F, Glover GH, Ludlow D, Pauly JM, Soneji D, Gabrieli JD, Mackey SC (2005) Control over brain activation and pain learned by using real-time functional MRI. Proc Natl Acad Sci U S A 102:18626-18631.

DeLong MR, Wichmann T (2007) Circuits and circuit disorders of the basal ganglia. Arch Neurol 64:20-24.

Dijkerman HC, Ietswaart M, Johnston M, MacWalter RS (2004) Does motor imagery training improve hand function in chronic stroke patients? A pilot study. Clinical rehabilitation 18:538-549.

Dowsett SM, Livesey DJ (2000) The development of inhibitory control in preschool children: effects of "executive skills" training. Developmental psychobiology 36:161-174.

Doya K (2000) Complementary roles of basal ganglia and cerebellum in learning and motor control. Curr Opin Neurobiol 10:732-739.

Dunsky A, Dickstein R, Marcovitz E, Levy S, Deutsch JE (2008) Home-based motor imagery training for gait rehabilitation of people with chronic poststroke hemiparesis. Arch Phys Med Rehabil 89:1580-1588.

Egner T, Gruzelier JH (2001) Learned self-regulation of EEG frequency components affects attention and event-related brain potentials in humans. Neuroreport 12:4155-4159.

Egner T, Gruzelier JH (2003) Ecological validity of neurofeedback: modulation of slow wave EEG enhances musical performance. Neuroreport 14:1221-1224.

Frank MJ, Seeberger LC, O'Reilly R C (2004) By carrot or by stick: cognitive reinforcement learning in parkinsonism. Science 306:1940-1943.

Friel PN (2007) EEG biofeedback in the treatment of attention deficit hyperactivity disorder. Alternative medicine review : a journal of clinical therapeutic 12:146-151.

Gilbert CD, Wiesel TN (1983) Clustered intrinsic connections in cat visual cortex. J Neurosci 3:1116-1133.

Graybiel AM (2005) The basal ganglia: learning new tricks and loving it. Curr Opin Neurobiol 15:638-644.

Guerrieri R, Nederkoorn C, Jansen A (2012) Disinhibition is easier learned than inhibition. The effects of (dis)inhibition training on food intake. Appetite 59:96-99.

Hallett M (2003) Surround inhibition. Supplements to Clinical neurophysiology 56:153-159.

Hanajima R, Ugawa Y, Terao Y, Ogata K, Kanazawa I (1996) Ipsilateral cortico-cortical inhibition of the motor cortex in various neurological disorders. J Neurol Sci 140:109-116.

Houben K (2011) Overcoming the urge to splurge: influencing eating behavior by manipulating inhibitory control. Journal of behavior therapy and experimental psychiatry 42:384-388.

Houben K, Nederkoorn C, Wiers RW, Jansen A (2011) Resisting temptation: decreasing alcohol-related affect and drinking behavior by training response inhibition. Drug and alcohol dependence 116:132-136.

Hubel DH, Wiesel TN (1968) Receptive fields and functional architecture of monkey striate cortex. J Physiol 195:215-243.

Johnstone SJ, Roodenrys S, Phillips E, Watt AJ, Mantz S (2010) A pilot study of combined working memory and inhibition training for children with AD/HD. Attention deficit and hyperactivity disorders 2:31-42.

King AV, Linke J, Gass A, Hennerici MG, Tost H, Poupon C, Wessa M (2012) Microstructure of a three-way anatomical network predicts individual differences in response inhibition: a tractography study. Neuroimage 59:1949-1959.

Kleiner M, Brainard DH, Pelli D (2007) What's new in Psychtoolbox-3. Perception 36.

Klingberg T, Fernell E, Olesen PJ, Johnson M, Gustafsson P, Dahlstrom K, Gillberg CG, Forssberg H, Westerberg H (2005) Computerized training of working memory in children with ADHD--a randomized, controlled trial. J Am Acad Child Adolesc Psychiatry 44:177-186.

Klingberg T, Forssberg H, Westerberg H (2002) Training of working memory in children with ADHD. J Clin Exp Neuropsychol 24:781-791.

Kujirai T, Caramia MD, Rothwell JC, Day BL, Thompson PD, Ferbert A, Wroe S, Asselman P, Marsden CD (1993) Corticocortical inhibition in human motor cortex. J Physiol (Lond) 471:501-519.

Lijffijt M, Kenemans JL, Verbaten MN, van Engeland H (2005) A meta-analytic review of stopping performance in attention-deficit/hyperactivity disorder: deficient inhibitory motor control? Journal of abnormal psychology 114:216-222.

Logan GD, Cowan WB (1984) On the ability to inhibit thought and action: a theory of an act of control. Psychol Rev 91:295-327.

Majid A, Cai W, Corey-Bloom J, Aron AR (*under review*) Proactive selective response suppression is implemented via the basal ganglia: functional evidence for the Indirect Pathway. J Neurosci.

Manuck SB, Levenson RW, Hinrichsen JJ, Gryll SL (1975) Role of feedback in voluntary control of heart rate. Perceptual and motor skills 40:747-752.

Manuel AL, Grivel J, Bernasconi F, Murray MM, Spierer L (2010) Brain dynamics underlying training-induced improvement in suppressing inappropriate action. J Neurosci 30:13670-13678.

Menzies L, Achard S, Chamberlain SR, Fineberg N, Chen C-H, del Campo N, Sahakian BJ, Robbins TW, Bullmore E (2007) Neurocognitive endophenotypes of obsessive-compulsive disorder. Brain 130:3223-3236.

Mink JW (2003) The Basal Ganglia and involuntary movements: impaired inhibition of competing motor patterns. Arch Neurol 60:1365-1368.

Murphy P (2002) Inhibitory control in adults with Attention-Deficit/Hyperactivity Disorder. Journal of attention disorders 6:1-4.

Nambu A, Tokuno H, Takada M (2002) Functional significance of the cortico-subthalamo-pallidal 'hyperdirect' pathway. Neurosci Res 43:111-117.

Nowlis DP, Kamiya J (1970) The control of electroencephalographic alpha rhythms through auditory feedback and the associated mental activity. Psychophysiology 6:476-484.

Ozeki H, Sadakane O, Akasaki T, Naito T, Shimegi S, Sato H (2004) Relationship between excitation and inhibition underlying size tuning and contextual response modulation in the cat primary visual cortex. J Neurosci 24:1428-1438.

Packard MG, Knowlton BJ (2002) Learning and memory functions of the Basal Ganglia. Annu Rev Neurosci 25:563-593.

Posse S, Fitzgerald D, Gao K, Habel U, Rosenberg D, Moore GJ, Schneider F (2003) Real-time fMRI of temporolimbic regions detects amygdala activation during single-trial self-induced sadness. Neuroimage 18:760-768.

Rossi S, Hallett M, Rossini PM, Pascual-Leone A (2009) Safety, ethical considerations, and application guidelines for the use of transcranial magnetic stimulation in clinical practice and research. Clin Neurophysiol 120:2008-2039.

Rossini PM, Barker AT, Berardelli A, Caramia MD, Caruso G, Cracco RQ, Dimitrijevic MR, Hallett M, Katayama Y, Lucking CH (1994) Non-invasive electrical and magnetic stimulation of the brain, spinal cord and roots: basic principles and procedures for routine clinical application. Report of an IFCN committee. Electroencephalogr Clin Neurophysiol 91:79-92.

Rota G, Sitaram R, Veit R, Erb M, Weiskopf N, Dogil G, Birbaumer N (2009) Self-regulation of regional cortical activity using real-time fMRI: the right inferior frontal gyrus and linguistic processing. Hum Brain Mapp 30:1605-1614.

Seger CA (2008) How do the basal ganglia contribute to categorization? Their roles in generalization, response selection, and learning via feedback. Neurosci Biobehav Rev 32:265-278.

Sharma N, Pomeroy VM, Baron JC (2006) Motor imagery: a backdoor to the motor system after stroke? Stroke; a journal of cerebral circulation 37:1941-1952.

Shohamy D, Myers CE, Grossman S, Sage J, Gluck MA, Poldrack RA (2004a) Cortico-striatal contributions to feedback-based learning: converging data from neuroimaging and neuropsychology. Brain 127:851-859.

Shohamy D, Myers CE, Kalanithi J, Gluck MA (2008) Basal ganglia and dopamine contributions to probabilistic category learning. Neurosci Biobehav Rev 32:219-236.

Shohamy D, Myers CE, Onlaor S, Gluck MA (2004b) Role of the basal ganglia in category learning: how do patients with Parkinson's disease learn? Behav Neurosci 118:676-686.

Smith MA (2006) Surround suppression in the early visual system. J Neurosci 26:3624-3625.

Sohn YH, Hallett M (2004a) Disturbed surround inhibition in focal hand dystonia. Ann Neurol 56:595-599.

Sohn YH, Hallett M (2004b) Surround inhibition in human motor system. Exp Brain Res 158:397-404.

Starr PA, Rau GM, Davis V, Marks WJ, Jr., Ostrem JL, Simmons D, Lindsey N, Turner RS (2005) Spontaneous pallidal neuronal activity in human dystonia: comparison with Parkinson's disease and normal macaque. J Neurophysiol 93:3165-3176.

Stevens JA, Stoykov ME (2003) Using motor imagery in the rehabilitation of hemiparesis. Arch Phys Med Rehabil 84:1090-1092.

Stinear CM, Byblow WD (2004) Impaired modulation of intracortical inhibition in focal hand dystonia. Cereb Cortex 14:555-561.

Subramanian L, Hindle JV, Johnston S, Roberts MV, Husain M, Goebel R, Linden D (2011) Real-time functional magnetic resonance imaging neurofeedback for treatment of Parkinson's disease. J Neurosci 31:16309-16317.

Tamm L, Menon V, Reiss AL (2002) Maturation of brain function associated with response inhibition. J Am Acad Child Adolesc Psychiatry 41:1231-1238.

Thorell LB, Lindqvist S, Bergman Nutley S, Bohlin G, Klingberg T (2009) Training and transfer effects of executive functions in preschool children. Developmental science 12:106-113.

Veling H, Aarts H, Papies EK (2011) Using stop signals to inhibit chronic dieters' responses towards palatable foods. *Behav Res Ther* 49:771-780.

Verbruggen F, Adams R, Chambers CD (2012) Proactive motor control reduces monetary risk taking in gambling. Psychol Sci 23:805-815.

Verbruggen F, Logan GD (2009) Models of response inhibition in the stop-signal and stop-change paradigms. Neurosci Biobehav Rev 33:647-661.

Weiskopf N, Veit R, Erb M, Mathiak K, Grodd W, Goebel R, Birbaumer N (2003) Physiological self-regulation of regional brain activity using real-time functional magnetic resonance imaging (fMRI): methodology and exemplary data. Neuroimage 19:577-586.

Wilcox RR (2001) Fundamentals of modern statistical methods : substantially improving power and accuracy. New York: Springer.

Williams BR, Ponesse JS, Schachar RJ, Logan GD, Tannock R (1999) Development of inhibitory control across the life span. Developmental psychology 35:205-213.

Yoo SS, Jolesz FA (2002) Functional MRI for neurofeedback: feasibility study on a hand motor task. Neuroreport 13:1377-1381.

Yoo SS, Lee JH, O'Leary H, Lee V, Choo SE, Jolesz FA (2007) Functional magnetic resonance imaging-mediated learning of increased activity in auditory areas. Neuroreport 18:1915-1920.

CONCLUSION

Everyday behavior requires that we are able to exert *inhibitory control*, a crucial executive function by which we stop or control our actions in preference for others. Inhibitory control, however, is by no means monolithic and can occur in various ways. At times we may need to suddenly stop all of our actions in response to a surprising event in our environment. At other times we may need to plan in advance so as to selectively stop a particular action without affecting other ongoing actions. The main aim of this dissertation is to explore the neurobiological differences that may underlie these various forms of inhibitory control, with a special attention to the latter case above in which stopping must be selective.

Studies of simple stopping have underscored the importance of cortico-basal ganglia signaling, particularly via the Hyperdirect Signaling Pathway, as a rapid mechanism of stopping (Mink, 1996, Nambu et al., 2002, Aron and Poldrack, 2006, King et al., 2012). Signaling through this pathway is believed to drive basal ganglia inhibition of the thalamus in a fast but nonspecific way (Mink, 1996, Gillies and Willshaw, 1998, Nambu et al., 2002), leading to "global" side-effects of motor suppression in task-irrelevant parts of the body (Badry et al., 2009, Cai et al., 2012, Wessel et al., *under review*). Though this neural mechanism may be useful for inhibitory control in situations where one must stop all of one's actions suddenly, it is unlikely to be the only neural mechanism that exists, since the "global" side-effect would likely be maladaptive in situations when stopping selectivity is required. There may thus be a more *selective* mechanism of stopping (see Aron, 2011), and I

will argue that the basal ganglia's classic *Indirect Pathway* may serve as such an alternative mechanism for selective response inhibition (Mink, 1996).

In chapter 1, I first provide evidence supporting the existence of such an alternative pathway by showing that the global motor suppressive effects of simple stopping (Badry et al., 2009, Cai et al., 2012, Wessel et al., *under review*) are absent when stopping must be behaviorally *selective*, i.e. where a subject must stop one of two actions while continuing the other with limited interference. Single-pulse TMS over the midline leg representation of the motor cortex served as a probe of motor excitability of a task-*irrelevant* effector. As discussed above, stopping that did not need to be selective brought about motor suppression of the leg, suggesting the use of a global mechanism, possible mediated via the Hyperdirect Pathway. However, this involvement of the task-irrelevant leg was absent when subjects stopped selectively. Though we cannot definitively conclude from this that selective stopping requires Indirect Pathway signaling, further considerations support this view. For instance, the speed of stopping, measured using the stop-signal reaction time (SSRT), is longer when stopping must be behaviorally selective compared to when selectivity is not required (Aron and Verbruggen, 2008), and this may reflect differences in signaling time due to the additional synapses in the Indirect Pathway versus the Hyperdirect Pathway (Magill et al., 2004).

In Chapters 2 and 3, I use structural imaging to establish *premanifest* Huntington's disease (PreHD) as a specific striatal and pallidal legion model, despite the absence of overt manifest symptoms during this stage. *Manifest* Huntington's disease, the stage in Huntington's disease in which motor, cognitive, and psychiatric symptoms become

apparent (Young et al., 1986), has a well-known association with cell death in the striatum (Graveland et al., 1985, Halliday et al., 1998). This striatal degeneration, though, must begin long before the manifest phase, since striatal volume is already reduced by approximately 50% in Huntington's disease patients at the time of diagnosis (Aylward et al., 1996, Aylward et al., 2004).

PreHD subjects underwent structural imaging at two visits one year apart and the longitudinal volumetric change was determined with two main methods. The first method was SIENA, part of the FMRIB Software Library (FSL), by which a whole-brain measure of longitudinal change was determined (Smith et al., 2002, Smith et al., 2004). The second method was Quarc, a tool to measure the longitudinal volume change in certain subcortical regions (Holland and Dale, 2011). With this latter method, we establish that longitudinal change in specific subcortical regions, namely the caudate, putamen, and pallidum, can serve as a clinically relevant biomarkers to ascertain the efficacy of future drug treatments in premanifest Huntington's disease (Paulsen, 2009). Longitudinal change was not identified in any other subcortical region studied, such as the Thalamus, Hippocampus, Amygdala, or Accumbens. This finding of regional specificity, in conjunction to much prior work suggesting that the striato-external pallidal Indirect Pathway is disproportionately affected in Huntington's disease (Reiner et al., 1988, Albin et al., 1989, Albin et al., 1992, Starr et al., 2008), suggests that regional volumetric differences in preHD may be a specific marker for Indirect Pathway impairments. We hypothesize thus that if the Indirect Pathway is the alternative pathway that is used when stopping must be selective, preHD striatal and

pallidal volumetric differences may lead to specific behavioral and physiological impairments in selective stopping, which I explore in Chapter 4.

A key selective stopping behavioral index that I hypothesize to be impaired in preHD is the Stopping Interference Effect. Two responses are always initiated at the start of each selective stopping trial, and the Stopping Interference Effect refers to the RT prolongation of the response that must continue on stop trials (compared to the RT of the same response when stopping is not necessary). If stopping is completely *selective* at the mechanistic level, stopping one response on stop trials should have no effect on the completion of the other, and the Stopping Interference Effect will be absent. However, a subject for whom the selective stopping mechanism is impaired (as may be the case in preHD) could first rapidly stop all ongoing actions and then re-initiate the action that must continue, leading to a large Stopping Interference Effect (see Bissett and Logan, 2013 for discussion).

What seems necessary for truly *mechanistically* selective stopping is the ability to prepare in advance. In Chapter 4, I investigate the role of the basal ganglia in selective stopping, focusing on this proactive aspect of preparation. This proactive aspect has been shown to lead to early corticomotor suppression of the particular effector that might have to stop using TMS (Claffey et al., 2010, Cai et al., 2011). I obtain a measure of proactive suppression by using single-pulse TMS to compare the corticomotor excitability of the hand that might have to stop later in the trial compared to a baseline. Then, with functional MRI, I show that healthy subjects who are better able to suppress the cued hand selectively also have greater activity in the basal ganglia and other regions during this same period.

Furthermore, activity in the basal ganglia was once again occurred when selective stopping was successfully accomplished.

PreHD individuals, some of whom took part in the work discussed in Chapters 2 and 3 and for whom striatal and pallidal deficiencies were known, returned to take part in the selective stopping task. These individuals did indeed have a larger Stopping Interference Effect compared to controls, as hypothesized. Furthermore, these individuals were not able to suppress the hand that must prepare to stop, but healthy controls were. Taken together with the evidence that the Indirect Pathway is disproportionately affected in Huntington's disease (Reiner et al., 1988, Albin et al., 1989, Albin et al., 1992, Starr et al., 2008), these findings strongly suggest that the striatally mediated Indirect Pathway may underlie mechanistically selective stopping and may be the alternative pathway hypothesized in Chapter 1.

Lastly, in Chapter 5, I present a novel methodology by which selective suppression of corticomotor excitability of the hand can be trained with real-time feedback of the motor evoked potential from TMS delivery. I conduct two experiments using this methodology. In a first experiment, subjects were stimulated at a motor cortex region that has the representations of both the index and pinky muscles of the right hand. The motor evoked potential from TMS delivery for each muscle, normalized to a baseline, was shown to the subjects on a trial-by-trial basis. Cued to suppress the corticomotor excitability of a particular finger over the other, subjects were all able to progressively improve and suppress the motor excitability of a cued muscle selectively. All subjects reported that the most effective way of doing this was to imagine alternative movements, i.e. to *think away*

from the particular movement that was cued. This suggests the use of motor surround inhibition (Sohn and Hallett, 2004b), which could arise from signaling through basal ganglia mediated inhibitory pathways such as the Indirect Pathway (Mink, 2003), amongst other possibilities. However, results for a second experiment, which tried to translate this feedback-driven effect into task behavior, were inconclusive as to whether this training regimen could have positive impacts on selective stopping *behavior*. This is an interesting avenue for further work. Even without translation into a behavioral paradigm, it is likely that the method underlying the frist experiment (i.e. using imaginative strategies to 'suppress' a particular effector) could have application as a therapy for focal hand dystonia, for which impairments in motor suppression is a major symptom (Sohn and Hallett, 2004a).

Does selective stopping necessarily require a proactive mechanism?

A key distinction presented in Chapter 1 was the difference between selective stopping, where one of action must stop while others continue, and non-selective stopping, where all actions can stop. Selective stopping does not cause a global motor side-effect of suppression on task-irrelevant effectors, as does non-selective stopping. Chapter 4 shows that selective stopping is mediated via a *proactive* stopping mechanism, where planning is necessary and leads to suppression of the hand that might have to stop. Non-selective stopping, by contrast, seems to require less proactivity and has no effect on the excitability of the hand. It is not immediately intuitive that a selective mechanism might always need this advanced preparation. As mentioned above, subjects may elect to *not* prepare in advance and instead stop all actions non-selectively when needed. Only then may they re-

initiate the action that must continue. This method of stopping would be ostensibly "selective" but not "proactive."

Indeed, a number of studies have used "selective" stopping paradigms that do not allow for early preparation; rather, what action must be stopped is first presented in the Stop signal itself. For instance, in some tasks, subjects must make a two-finger movement in response to the movement of two bars on a screen. If at any point, one of the two bars stops moving, the subject must inhibit the movement of the corresponding finger (Coxon et al., 2009, Coxon et al., 2012, Macdonald et al., 2012). Note here that subjects in this task have no idea which of the two fingers they might have to inhibit, and thus cannot prepare in advance. Analysis of behavior in these stopping paradigms suggests that there is a large delay in the completion of the alternative (non-stopped) action, i.e. a large Stopping Interference Effect, suggesting that stopping has a global effect on the motor system (Coxon et al., 2009, Macdonald et al., 2012). Consistent with the hypothesis that this motor slowing is a side effect of rapid Hyperdirect Pathway signaling, neuroimaging work further suggests that variability in white matter connections between the cortex and the subthalamic nucleus relates to variability in stopping times (SSRT) in these paradigms (Coxon et al., 2012). It is thus likely that these "selective" stopping paradigms do not engage truly *mechanistically selective* stopping but rather rely on a rapid reactive mechanism with global effects. Only after all actions are stopped do individuals then re-initiate the alternative movement (Bissett and Logan, 2013).

The stopping paradigm used in this dissertation differs from the above paradigms in that subjects must use foreknowledge prepare for selective stopping well in advance

because the stop-signal is completely uninformative. Because the stop-signal is presented in the middle of the screen and does not indicate which of the two actions must be stopped, subjects must depend on the stopping cue presented at the beginning of the trial ("Maybe Stop Left" or "Maybe Stop Right," for instance). Inability to do this leads to Stopping Direction Errors (i.e. stopping the *wrong* uncued action), and subjects who make more Stopping Direction Errors also have been shown to have longer Stopping Interference Effects on trials when they do in fact stop correctly (Claffey et al., 2010). This is consistent with the notion that due to the lack of preparation for selective stopping, these subjects reactively inhibit both responses on a stop trial and then must re-initiate the response that must be continued.

Does non-selective stopping only use a reactive mechanism?

Just as it is conceivable that selective stopping may sometimes engage a non-proactive mechanism, non-selective stopping may sometimes engage a proactive mechanism, as some studies have suggested (Jahfari et al., 2010, Zandbelt and Vink, 2010, Zandbelt et al., 2011, Jahfari et al., 2012, Zandbelt et al., 2012a, Zandbelt et al., 2012b). This may at first seem contrary to the findings in Chapter 4, where there was little evidence of proactive control when non-selective stopping was cued, either with regards to functional activation in the preparing-to-stop phase or motor suppression of the hands relevant for stopping.

It is important to point out that the definition of *proactive* control used in these other studies differs from the proactive control studied in this dissertation and related

studies (Cai et al., 2011). I have used "proactive control" to refer to the suppressive influence that stopping goals have upon motor response channels *in advance of a trial*, which I have shown is associated with activation in the basal ganglia in the *preparing-to-stop* period. By contrast, proactive control in the studies mentioned above (Jahfari et al., 2010, Zandbelt and Vink, 2010, Zandbelt et al., 2011, Jahfari et al., 2012, Zandbelt et al., 2012a, Zandbelt et al., 2012b) refers rather to reaction time slowing on Go trials when the probability of stopping increases. This stopping anticipation-related slowing or "braking" has been seen in a number of studies (Jahfari et al., 2010, Greenhouse et al., 2012, Swann et al., 2012a, Swann et al., 2012b) and has been shown to implicate the striatum (Jahfari et al., 2010, Zandbelt and Vink, 2010, Zandbelt et al., 2011, Zandbelt et al., 2012b), as well as a number of cortical regions including the supplementary motor complex (Zandbelt et al., 2012b), right inferior frontal cortex (Swann et al., 2012a).

There is evidence for such stopping anticipation-related slowing in the work presented in Chapter 4. In the fMRI experiment, Go RT was slower in each condition for which stopping was cued (the non-selective "Maybe Stop Both" condition and the selective "Maybe Stop Left" or "Right" conditions) compared to when stopping was not cued (i.e. "Just Go" condition). Yet despite similar degrees of slowing for both selective and non-selective stopping, brain activation in the *preparing-to-stop* phase (compared to the "Just Go" baseline) was only identified in the selective condition and not in the non-selective condition. It is possible that the neural processes that lead to slowing in the non-selective stopping condition only come on-line until after the end of the *preparing-to-stop* phase, at the start of the stopping trial. Implementation of proactive control even earlier in a non-

selective stopping trial may be behaviorally costly and even unnecessary, since subjects do not need to stop selectively and can rely on stopping with a rapid reactive mechanism without being harmed by the "global" motor side-effects of such a system (Badry et al., 2009, Cai et al., 2012, Wessel et al., *under review*), as demonstrated in Chapter 1.

Brain networks involved in proactive selective stopping

Based on the work in this dissertation, I claim that both preparation and execution of mechanistically selective stopping relies on signaling through the *Indirect Pathway* of the basal ganglia. Two assumptions inform this claim. The first is that of the two classically established signaling pathways through the striatum, the Direct and the Indirect Pathways, the latter is the one particularly associated with a net inhibitory effect on thalamic excitation to the motor cortex (Mink, 1996, Smith et al., 1998). Thus, striatal activation that occurs in the context of motor inhibition is highly suggestive of signaling through this pathway. The second assumption is that the Indirect Pathway is selectively damaged in both manifest and premanifest Huntington's disease (Vonsattel et al., 1985, Reiner et al., 1988, Albin et al., 1989, Albin et al., 1992, Starr et al., 2008) and may explain the hyperkinetic symptoms of the disease (Penney and Young, 1983, Albin et al., 1995). The behavioral and physiological impairments I present in the study of preHD individuals provide additional support for the role of the Indirect Pathway in selective stopping. More definitive evidence however is required, and this is discussed below.

The basal ganglia's Indirect Pathway must however function in an interconnected network involving cortical regions. What are the cortical drivers implicated in preparing and

executing selective stopping? One such cortical driver may be the presupplementary motor cortex (preSMA). Functional activity in this region, like the basal ganglia, correlated across subjects with the degree of proactive motor suppression identified in the TMS task. Indeed, there are known direct connections between the preSMA and the striatum that may subserve this cortical drive (Parthasarathy et al., 1992, Inase et al., 1999). Although one study does suggest that functional connectivity between the preSMA and striatum reduces with greater "proactive" control (i.e. anticipation-related slowing, see discussion above) (Jahfari et al., 2012), other studies using varied methodologies do all implicate the preSMA (and the nearby SMA) in such "proactive" stopping anticipation-related slowing (Coxon et al., 2009, Chen et al., 2010, Stuphorn and Emeric, 2012, Swann et al., 2012a, Zandbelt et al., 2012b).

By contrast, the role of the right Inferior Frontal Cortex (rIFC), long implicated in reactive stopping (Garavan et al., 1999, Aron et al., 2003, Rubia et al., 2003, Chambers et al., 2006), is not so clear-cut. The rIFC was not implicated in any preparation-related contrast in Chapter 4. This is consistent with work suggesting that the rIFC is not involved in proactive control but rather plays a role only when the stop-signal appears (Zandbelt et al., 2012b). Contrary to this, however, other studies do implicate the rIFC in anticipation-related slowing (Jahfari et al., 2010, Swann et al., 2012a), which, as discussed above, could be considered a form of "proactive" control. Nevertheless, investigation using the high temporal specificity of electrocorticography suggests that the rIFC does not become active until after the go-signal cues movement initiation, whereas preSMA activity can begin before the go-signal (Swann et al., 2012a). It is thus likely that the rIFC does not play a role the specific form of

proactive control that is studied in this dissertation – by which stopping goals cause a suppressive influence over motor channels via the basal ganglia *before any response is made*. Rather, the rIFC may become active only after a response is initiated and may lead to response slowing when stopping becomes more likely. This argues for a role for the rIFC in 'braking' response tendencies or stopping them outright, rather than in 'turning on' inhibitory control in advance of the need to brake or stop.

Finally, the evidence presented in Chapter 4 suggests that at the time of stopping, all three regions – preSMA, rIFC, and the basal ganglia including the striatum – become active and are involved in successfully stopping selectively. Basic reactive stopping has been shown to implicate the two cortical nodes, which are connected to the subthalamic nucleus (STN) via a putative Hyperdirect Pathway (Nambu et al., 1997, Inase et al., 1999, Aron et al., 2007, Madsen et al., 2010, Coxon et al., 2012, King et al., 2012). These two cortical nodes may play a similar role in stopping action when outright stopping is selective. However, now they may functionally project to the striatum rather than to the STN (Inase et al., 1999, Wiesendanger et al., 2004). While the projection via the Indirect Pathway may take longer due to the additional synapses involved (Magill et al., 2004), it is believed to have the neural specificity to bring about focal suppression (Mink, 1996) that is not possible when signaling through the Hyperdirect Pathway (Parent and Hazrati, 1995, Gillies and Willshaw, 1998, Nambu et al., 2002). These two observations may account for increases in SSRT associated with selective vs. nonselective stopping (Aron and Verbruggen, 2008, Claffey et al., 2010) and the absence of a global motor suppressive side effect when selective stopping occurs, as presented in Chapter 1.

Need for more definitive proof of the Indirect Pathway

Although the striatal and pallidal evidence presented in Chapter 4 suggests that the Indirect Pathway implements selective stopping, more definitive proof is necessary. One direction for further study could focus on the *external* globus pallidus (GPe), which is a specific node of the Indirect Pathway, as opposed to the striatum (Direct and Indirect Pathways) and the internal globus pallidus (Direct, Indirect, and Hyperdirect Pathways) (Parent and Hazrati, 1995). Thus, task activity that specifically localizes to the GPe – or impairments in task ability that relate closely with GPe damage – can serve as stronger proof implicating the Indirect Pathway. While imaging the GPe has traditionally been a challenge due to its small size and proximity to the internal Globus Pallidus (GPi), new high-resolution imaging techniques are being developed that allow for visualization of the thin white matter lamina that separates the two GP segments (Mattfeld et al., 2011). After the outline of the GPe is determined for each subject, focused registration techniques can greatly increase the fidelity of group-wise ROI analyses in functional imaging (Miller et al., 2005, Yassa and Stark, 2009).

Such high-resolution imaging techniques focused on the GPe are important for the development of biomarkers for premanifest Huntington's disease. In Chapter 3, we showed that GP volumetric change over the course of a single year could serve as sensitive marker of the premanifest Huntington's disease process. This is most likely not due to loss of cells situated in the GP but rather due to the loss of innervating axons originating in the striatum, as histopathology suggests that the number of pallidum cell bodies do not change (Wakai et

al., 1993) (see Douaud et al., 2009 for in vivo evidence). As has been mentioned above, the loss of these incoming axons however is not uniform across the pallidum, and early work in post-mortem brains suggests that there is a preferential loss in projection fibers from the striatum to the GPe (rather than GPi) in early Huntington's disease (Reiner et al., 1988, Albin et al., 1992). Consistent with the selective loss of striatal inhibition on the GPe, recent work using single-unit recordings show GPe activity, but not GPi activity, is specifically elevated in Huntington's disease (Starr et al., 2008). Consequently, GPe volumetric change may be a far more sensitive biomarker of change in premanifest Huntington's disease than change over the entire pallidum. Furthermore, the degree of GPe volume loss may also serve as a far more sensitive marker related to the degree of selective stopping behavioral impairments identified in preHD participants in Chapter 4.

Another way to strengthen the hypothesis that the Indirect Pathway is specifically involved in selective stopping is to study basal ganglia dopamine signaling pathways. In particular, D1 and D2 dopamine receptors have long been considered a histochemical marker of striatal cells projecting to the GPi (Direct Pathway) and GPe (Indirect Pathway), respectively (Gerfen et al., 1990, Graybiel, 1990). Positron Emission Tomography (PET) imaging can thus be used to image radiolabeled ligands selective for the D2 pathway (such as raclopride, see Black et al., 1997) in the striatum during selective stopping task performance. This method however has considerable limitations with regards to temporal specificity and requires separating trials into blocks based on the stopping condition (i.e. separating selective stopping trial blocks from non-selective stopping trial blocks).

The relationship of D2 dopamine signaling and the Indirect Pathway can be exploited further using neuroactive drugs including D2 antagonists such as chlorpromazine and haloperidol (traditionally used as antipsychotic drugs) or agonists (traditionally used as anti-Parkinsonian drugs) (Wang et al., 2004). However, all such modifying drugs are known to be nonspecific with regards to the exact receptor and locus of action and thus may cloud behavioral results.

Another option is studies in animal models that allow for more controlled investigation of basal ganglia pathways, provided that analogous selective stopping tasks can be developed. For instance, basic stop-signal-like tasks have been developed for primates, notably the countermanding task, (Boucher et al., 2007, Leventhal et al., 2012, Stuphorn and Emeric, 2012) or for rodents (Eagle and Baunez, 2010, Bryden et al., 2012). Development of tasks analogous to *proactive selective* stopping in animals may be feasible with more training. For example, a study in rodents required responding with an alternative response after stopping (Bryden et al., 2012). Such a rodent "stop-change" task could in part be tapping into a system analogous to the selective stopping tasks studied in this dissertation, which also requires completion of an alternative movement after stopping. Those authors found that some medium spiny neurons in the rodent dorsomedial striatum had firing that peaked only in response to a stop-signal that led to successful stopping (Bryden et al., 2012).

Future task development in rodents could lead to behavioral paradigms completely analogous to the proactive selective stopping task used in this dissertation. These paradigms could then be coupled with cutting-edge rodent experimental techniques such as

optogenetics, which allows for precise focal stimulation or inhibition of particular neuronal types using light (Deisseroth, 2011). For instance, optogenetics has already been used to stimulate the D2-receptor coupled Indirect Pathway in the striatum of wake behaving mice, revealing clear relationships between this signaling pathway and freezing and transient punishment behavior (Kravitz et al., 2010, Kravitz et al., 2012). There is also great potential for similar developments in rats, and methods have been developed to stimulate striatal dopamine release in a spatially and temporally specific way (Bass et al., 2010)

Can selective motor suppression be trained?

Whether the selective stopping behavior studied here – and stopping behavior in general – can be improved through training is a difficult question. Indeed, inhibitory control may differ considerably from other "executive functions" such as working memory with regards to how easily improvement can occur. For instance, when training working memory ability, children show improvements over time in both the primary tasks on which they were trained as well as working memory tasks on which they were not trained, suggesting that the benefit of working memory training can be *transferred* widely (Klingberg et al., 2002, Klingberg et al., 2005, Thorell et al., 2009, Johnstone et al., 2010). By contrast, these children show only limited improvement when training inhibitory control (Thorell et al., 2009, Johnstone et al., 2010), and this small benefit does not transfer to any other task (Thorell et al., 2009, Manuel et al., 2010, Guerrieri et al., 2012).

The above results may be explained by differences in the neural circuitry that underlie working memory vs. inhibitory control. The separate regions of the prefrontal

cortex to which these functions localize, for instance, may differ with regards to capacity for plasticity (Kuboshima-Amemori and Sawaguchi, 2007, Thorell et al., 2009). Additionally, signaling via the Hyperdirect Pathway in simple stopping is already very rapid (Nambu et al., 2002) and thus may not be amenable to further changes in plasticity. Subject behavior during stopping may already be at its optimal level.

The hypothesis we present here – that proactive selective stopping is mediated via the basal ganglia's Indirect Pathway rather than the Hyperdirect Pathway – opens a number of doors with regards to the possibility of motor training. The basal ganglia are well-known for considerable capacity for plastic change with learning (Graybiel, 2005) especially with regards to feedback-driven learning of category classification (Doya, 2000, Packard and Knowlton, 2002, Aron et al., 2004, Shohamy et al., 2004a, Seger, 2008). Midbrain dopamine signaling, in response to reward and punishment, is believed to underlie this form of learning (Shohamy et al., 2008) and is impaired in Parkinson's disease where dopaminergic signaling is diminished (Frank et al., 2004, Shohamy et al., 2004b).

Chapter 5 shows definitively that selective motor suppression when cued can be trained with real-time feedback over the course of a single session. However, we were unable to show that this inhibitory ability could readily *transfer* to a proactive selective stopping task context. This may have related to a number of factors including the limited training time available or structural differences between the training procedure and the selective stopping task procedure. Nonetheless, though the exact neurobiological etiology of this trained cued motor suppression is not clear, it is likely that feedback training is recruiting the same basal ganglia inhibitory apparatus that underlies proactive motor

suppression when preparing to stop selectively, i.e. the Indirect Pathway. Cued motor suppression in Chapter 5 seems in part driven by motor surround inhibition (Hallett, 2003, Sohn and Hallett, 2004b) – subjects invariably reported *thinking away* from the muscle cued for suppression towards alternative actions. Though surround inhibition in sensory systems have been traditionally hypothesized to be a process local to the cortex (Hubel and Wiesel, 1968, Gilbert and Wiesel, 1983) and a similar process may occur for the motor system (Kujirai et al., 1993, Hanajima et al., 1996), more recent work suggests that this surround inhibition in both motor and sensory systems arises as a bottom-up influence of changes in thalamic drive to the cortex (Mink, 2003, Ozeki et al., 2004, Smith, 2006). The inhibitory Indirect Pathway is believed to be the main cause of focal reductions of thalamocortical drive to the motor cortex (Mink, 2003). Thus, while we could not show that feedback-driven motor suppression learning could transfer to task benefits in selective stopping ability, the methodology remains a highly promising way by which Indirect Pathway function may be targeted and manipulated.

Summary

In the real world, inhibitory control is rarely a simple matter of stopping outright all of our ongoing actions in response to a clear environmental stimulus. This form of stopping, though easily modeled in the laboratory, may be insufficient in explaining the complexity of everyday behavior. This is especially the case when inhibitory control must be *selective*, i.e. when a particular action must be stopped while others must continue without interference. The work discussed in this dissertation provides evidence of a basal ganglia-mediated neural

mechanism, possibly the classical inhibitory Indirect Pathway, that may underlie this selective inhibitory control. In particular, I show that selective inhibition does not yield the "global" motor suppressive side effects that are often associated with simple inhibition (likely mediated via the Hyperdirect Pathway). I also show functional imaging evidence that both preparation for and execution of selective inhibitory control implicates the striatum, suggestive of Indirect Pathway involvement. Additionally, I present corroborating evidence that there is regionally-specific neural degeneration in premanifest Huntington's disease (preHD), which has long been believed to affect the striatally-mediated Indirect Pathway in particular. I show evidence suggesting that this striatally-mediate signaling mechanism may be *necessary* in preparing for and executing selective inhibitory control by showing preHD impairments in these functions. Lastly, I present a novel TMS methodology by which selective inhibitory control might be trained through real-time trial-by-trial feedback, laying the groundwork for future investigation.

References

Albin R, Reiner A, Anderson K, Dure L, Handelin B, Balfour R, Whetsell W, Penney J, Young A (1992) Preferential loss of striato-external pallidal projection neurons in presymptomatic Huntington's disease. Ann Neurol 31:425-430.

Albin RL, Young AB, Penney JB (1989) The functional anatomy of basal ganglia disorders. Trends Neurosci 12:366-375.

Albin RL, Young AB, Penney JB (1995) The functional anatomy of disorders of the basal ganglia. Trends Neurosci 18:63-64.

Aron AR (2011) From Reactive to Proactive and Selective Control: Developing a Richer Model for Stopping Inappropriate Responses. Biol Psychiatry.

Aron AR, Behrens TE, Smith S, Frank MJ, Poldrack RA (2007) Triangulating a cognitive control network using diffusion-weighted magnetic resonance imaging (MRI) and functional MRI. J Neurosci 27:3743-3752.

Aron AR, Fletcher PC, Bullmore ET, Sahakian BJ, Robbins TW (2003) Stop-signal inhibition disrupted by damage to right inferior frontal gyrus in humans. Nat Neurosci 6:115-116.

Aron AR, Poldrack RA (2006) Cortical and subcortical contributions to Stop signal response inhibition: role of the subthalamic nucleus. J Neurosci 26:2424-2433.

Aron AR, Shohamy D, Clark J, Myers C, Gluck MA, Poldrack RA (2004) Human midbrain sensitivity to cognitive feedback and uncertainty during classification learning. J Neurophysiol 92:1144-1152.

Aron AR, Verbruggen F (2008) Stop the presses: dissociating a selective from a global mechanism for stopping. Psychol Sci 19:1146-1153.

Aylward EH, Codori AM, Barta PE, Pearlson GD, Harris GJ, Brandt J (1996) Basal ganglia volume and proximity to onset in presymptomatic Huntington disease. Arch Neurol 53:1293-1296.

Aylward EH, Sparks BF, Field KM, Yallapragada V, Shpritz BD, Rosenblatt A, Brandt J, Gourley LM, Liang K, Zhou H, Margolis RL, Ross CA (2004) Onset and rate of striatal atrophy in preclinical Huntington disease. Neurology 63:66-72.

Badry R, Mima T, Aso T, Nakatsuka M, Abe M, Fathi D, Foly N, Nagiub H, Nagamine T, Fukuyama H (2009) Suppression of human cortico-motoneuronal excitability during the Stop-signal task. Clin Neurophysiol 120:1717-1723.

Bass CE, Grinevich VP, Vance ZB, Sullivan RP, Bonin KD, Budygin EA (2010) Optogenetic control of striatal dopamine release in rats. J Neurochem 114:1344-1352.

Bissett PG, Logan GD (2013) Selective Stopping? Maybe Not. J Exp Psychol Gen.

Black KJ, Gado MH, Perlmutter JS (1997) PET measurement of dopamine D2 receptor-mediated changes in striatopallidal function. J Neurosci 17:3168-3177.

Boucher L, Palmeri TJ, Logan GD, Schall JD (2007) Inhibitory control in mind and brain: an interactive race model of countermanding saccades. Psychol Rev 114:376-397.

Bryden DW, Burton AC, Kashtelyan V, Barnett BR, Roesch MR (2012) Response inhibition signals and miscoding of direction in dorsomedial striatum. Front Integr Neurosci 6:69.

Cai W, Oldenkamp C, Aron AR (2011) A proactive mechanism for selective suppression of response tendencies. J Neurosci 31:5965-5969.

Cai W, Oldenkamp CL, Aron AR (2012) Stopping speech suppresses the task-irrelevant hand. Brain Lang 120:412-415.

Chambers CD, Bellgrove MA, Stokes MG, Henderson TR, Garavan H, Robertson IH, Morris AP, Mattingley JB (2006) Executive "brake failure" following deactivation of human frontal lobe. J Cogn Neurosci 18:444-455.

Chen X, Scangos KW, Stuphorn V (2010) Supplementary motor area exerts proactive and reactive control of arm movements. J Neurosci 30:14657-14675.

Claffey MP, Sheldon S, Stinear CM, Verbruggen F, Aron AR (2010) Having a goal to stop action is associated with advance control of specific motor representations. Neuropsychologia 48:541-548.

Coxon JP, Stinear CM, Byblow WD (2009) Stop and go: the neural basis of selective movement prevention. J Cogn Neurosci 21:1193-1203.

Coxon JP, Van Impe A, Wenderoth N, Swinnen SP (2012) Aging and inhibitory control of action: cortico-subthalamic connection strength predicts stopping performance. J Neurosci 32:8401-8412.

Deisseroth K (2011) Optogenetics. Nature methods 8:26-29.

Douaud G, Behrens TE, Poupon C, Cointepas Y, Jbabdi S, Gaura V, Golestani N, Krystkowiak P, Verny C, Damier P, Bachoud-Lévi A-C, Hantraye P, Remy P (2009) In vivo evidence for the selective subcortical degeneration in Huntington's disease. Neuroimage 46:958-966.

Doya K (2000) Complementary roles of basal ganglia and cerebellum in learning and motor control. Curr Opin Neurobiol 10:732-739.

Eagle DM, Baunez C (2010) Is there an inhibitory-response-control system in the rat? Evidence from anatomical and pharmacological studies of behavioral inhibition. Neurosci Biobehav Rev 34:50-72.

Frank MJ, Seeberger LC, O'Reilly R C (2004) By carrot or by stick: cognitive reinforcement learning in parkinsonism. Science 306:1940-1943.

Garavan H, Ross TJ, Stein EA (1999) Right hemispheric dominance of inhibitory control: an event-related functional MRI study. Proc Natl Acad Sci U S A 96:8301-8306.

Gerfen CR, Engber TM, Mahan LC, Susel Z, Chase TN, Monsma FJ, Jr., Sibley DR (1990) D1 and D2 dopamine receptor-regulated gene expression of striatonigral and striatopallidal neurons. Science 250:1429-1432.

Gilbert CD, Wiesel TN (1983) Clustered intrinsic connections in cat visual cortex. J Neurosci 3:1116-1133.

Gillies AJ, Willshaw DJ (1998) A massively connected subthalamic nucleus leads to the generation of widespread pulses. Proc Biol Sci 265:2101-2109.

Graveland GA, Williams RS, DiFiglia M (1985) Evidence for degenerative and regenerative changes in neostriatal spiny neurons in Huntington's disease. Science 227:770-773.

Graybiel AM (1990) Neurotransmitters and neuromodulators in the basal ganglia. Trends Neurosci 13:244-254.

Graybiel AM (2005) The basal ganglia: learning new tricks and loving it. Curr Opin Neurobiol 15:638-644.

Greenhouse I, Oldenkamp CL, Aron AR (2012) Stopping a response has global or nonglobal effects on the motor system depending on preparation. J Neurophysiol 107:384-392.

Guerrieri R, Nederkoorn C, Jansen A (2012) Disinhibition is easier learned than inhibition. The effects of (dis)inhibition training on food intake. Appetite 59:96-99.

Hallett M (2003) Surround inhibition. Supplements to Clinical neurophysiology 56:153-159.

Halliday GM, McRitchie DA, Macdonald V, Double KL, Trent RJ, McCusker E (1998) Regional specificity of brain atrophy in Huntington's disease. Exp Neurol 154:663-672.

Hanajima R, Ugawa Y, Terao Y, Ogata K, Kanazawa I (1996) Ipsilateral cortico-cortical inhibition of the motor cortex in various neurological disorders. J Neurol Sci 140:109-116.

Holland D, Dale AM (2011) Nonlinear registration of longitudinal images and measurement of change in regions of interest. Med Image Anal.

Hubel DH, Wiesel TN (1968) Receptive fields and functional architecture of monkey striate cortex. J Physiol 195:215-243.

Inase M, Tokuno H, Nambu A, Akazawa T, Takada M (1999) Corticostriatal and corticosubthalamic input zones from the presupplementary motor area in the macaque monkey: comparison with the input zones from the supplementary motor area. Brain Res 833:191-201.

Jahfari S, Stinear CM, Claffey M, Verbruggen F, Aron AR (2010) Responding with restraint: what are the neurocognitive mechanisms? J Cogn Neurosci 22:1479-1492.

Jahfari S, Verbruggen F, Frank MJ, Waldorp LJ, Colzato L, Ridderinkhof KR, Forstmann BU (2012) How preparation changes the need for top-down control of the basal ganglia when inhibiting premature actions. J Neurosci 32:10870-10878.

Johnstone SJ, Roodenrys S, Phillips E, Watt AJ, Mantz S (2010) A pilot study of combined working memory and inhibition training for children with AD/HD. Attention deficit and hyperactivity disorders 2:31-42.

King AV, Linke J, Gass A, Hennerici MG, Tost H, Poupon C, Wessa M (2012) Microstructure of a three-way anatomical network predicts individual differences in response inhibition: a tractography study. Neuroimage 59:1949-1959.

Klingberg T, Fernell E, Olesen PJ, Johnson M, Gustafsson P, Dahlstrom K, Gillberg CG, Forssberg H, Westerberg H (2005) Computerized training of working memory in children with ADHD--a randomized, controlled trial. J Am Acad Child Adolesc Psychiatry 44:177-186.

Klingberg T, Forssberg H, Westerberg H (2002) Training of working memory in children with ADHD. J Clin Exp Neuropsychol 24:781-791.

Kravitz AV, Freeze BS, Parker PR, Kay K, Thwin MT, Deisseroth K, Kreitzer AC (2010) Regulation of parkinsonian motor behaviours by optogenetic control of basal ganglia circuitry. Nature 466:622-626.

Kravitz AV, Tye LD, Kreitzer AC (2012) Distinct roles for direct and indirect pathway striatal neurons in reinforcement. Nat Neurosci 15:816-818.

Kuboshima-Amemori S, Sawaguchi T (2007) Plasticity of the primate prefrontal cortex. Neuroscientist 13:229-240.

Kujirai T, Caramia MD, Rothwell JC, Day BL, Thompson PD, Ferbert A, Wroe S, Asselman P, Marsden CD (1993) Corticocortical inhibition in human motor cortex. J Physiol (Lond) 471:501-519.

Leventhal DK, Gage GJ, Schmidt R, Pettibone JR, Case AC, Berke JD (2012) Basal ganglia beta oscillations accompany cue utilization. Neuron 73:523-536.

Macdonald H, Stinear CM, Byblow WD (2012) Uncoupling Response Inhibition. J Neurophysiol.

Madsen KS, Baaré WFC, Vestergaard M, Skimminge A, Ejersbo LR, Ramsøy TZ, Gerlach C, Akeson P, Paulson OB, Jernigan TL (2010) Response inhibition is associated with white matter microstructure in children. Neuropsychologia 48:854-862.

Magill PJ, Sharott A, Bevan MD, Brown P, Bolam JP (2004) Synchronous unit activity and local field potentials evoked in the subthalamic nucleus by cortical stimulation. J Neurophysiol 92:700-714.

Manuel AL, Grivel J, Bernasconi F, Murray MM, Spierer L (2010) Brain dynamics underlying training-induced improvement in suppressing inappropriate action. J Neurosci 30:13670-13678.

Mattfeld AT, Gluck MA, Stark CE (2011) Functional specialization within the striatum along both the dorsal/ventral and anterior/posterior axes during associative learning via reward and punishment. Learn Mem 18:703-711.

Miller MI, Beg MF, Ceritoglu C, Stark C (2005) Increasing the power of functional maps of the medial temporal lobe by using large deformation diffeomorphic metric mapping. Proc Natl Acad Sci U S A 102:9685-9690.

Mink JW (1996) The basal ganglia: focused selection and inhibition of competing motor programs. Prog Neurobiol 50:381-425.

Mink JW (2003) The Basal Ganglia and involuntary movements: impaired inhibition of competing motor patterns. Arch Neurol 60:1365-1368.

Nambu A, Tokuno H, Inase M, Takada M (1997) Corticosubthalamic input zones from forelimb representations of the dorsal and ventral divisions of the premotor cortex in the macaque monkey: comparison with the input zones from the primary motor cortex and the supplementary motor area. Neurosci Lett 239:13-16.

Nambu A, Tokuno H, Takada M (2002) Functional significance of the cortico-subthalamo-pallidal 'hyperdirect' pathway. Neurosci Res 43:111-117.

Ozeki H, Sadakane O, Akasaki T, Naito T, Shimegi S, Sato H (2004) Relationship between excitation and inhibition underlying size tuning and contextual response modulation in the cat primary visual cortex. J Neurosci 24:1428-1438.

Packard MG, Knowlton BJ (2002) Learning and memory functions of the Basal Ganglia. Annu Rev Neurosci 25:563-593.

Parent A, Hazrati LN (1995) Functional anatomy of the basal ganglia. II. The place of subthalamic nucleus and external pallidum in basal ganglia circuitry. Brain research Brain research reviews 20:128-154.

Parthasarathy HB, Schall JD, Graybiel AM (1992) Distributed but convergent ordering of corticostriatal projections: analysis of the frontal eye field and the supplementary eye field in the macaque monkey. J Neurosci 12:4468-4488.

Paulsen JS (2009) Biomarkers to predict and track diseases. Lancet Neurol 8:776-777.

Penney JB, Jr., Young AB (1983) Speculations on the functional anatomy of basal ganglia disorders. Annu Rev Neurosci 6:73-94.

Reiner A, Albin RL, Anderson KD, D'Amato CJ, Penney JB, Young AB (1988) Differential loss of striatal projection neurons in Huntington disease. Proc Natl Acad Sci U S A 85:5733-5737.

Rubia K, Smith AB, Brammer MJ, Taylor E (2003) Right inferior prefrontal cortex mediates response inhibition while mesial prefrontal cortex is responsible for error detection. Neuroimage 20:351-358.

Seger CA (2008) How do the basal ganglia contribute to categorization? Their roles in generalization, response selection, and learning via feedback. Neurosci Biobehav Rev 32:265-278.

Shohamy D, Myers CE, Grossman S, Sage J, Gluck MA, Poldrack RA (2004a) Cortico-striatal contributions to feedback-based learning: converging data from neuroimaging and neuropsychology. Brain 127:851-859.

Shohamy D, Myers CE, Kalanithi J, Gluck MA (2008) Basal ganglia and dopamine contributions to probabilistic category learning. Neurosci Biobehav Rev 32:219-236.

Shohamy D, Myers CE, Onlaor S, Gluck MA (2004b) Role of the basal ganglia in category learning: how do patients with Parkinson's disease learn? Behav Neurosci 118:676-686.

Smith MA (2006) Surround suppression in the early visual system. J Neurosci 26:3624-3625.

Smith S, Jenkinson M, Woolrich M, Beckmann C, Behrens T, Johansen-Berg H, Bannister P, De Luca M, Drobnjak I, Flitney D, Niazy R, Saunders J, Vickers J, Zhang Y, De Stefano N, Brady J, Matthews P (2004) Advances in functional and structural MR image analysis and implementation as FSL. Neuroimage 23 Suppl 1:S208-219.

Smith SM, Zhang Y, Jenkinson M, Chen J, Matthews PM, Federico A, De Stefano N (2002) Accurate, robust, and automated longitudinal and cross-sectional brain change analysis. Neuroimage 17:479-489.

Smith Y, Bevan MD, Shink E, Bolam JP (1998) Microcircuitry of the direct and indirect pathways of the basal ganglia. Neuroscience 86:353-387.

Sohn YH, Hallett M (2004a) Disturbed surround inhibition in focal hand dystonia. Ann Neurol 56:595-599.

Sohn YH, Hallett M (2004b) Surround inhibition in human motor system. Exp Brain Res 158:397-404.

Starr PA, Kang GA, Heath S, Shimamoto S, Turner RS (2008) Pallidal neuronal discharge in Huntington's disease: support for selective loss of striatal cells originating the indirect pathway. Exp Neurol 211:227-233.

Stuphorn V, Emeric EE (2012) Proactive and reactive control by the medial frontal cortex. Front Neuroeng 5:9.

Swann NC, Cai W, Conner CR, Pieters TA, Claffey MP, George JS, Aron AR, Tandon N (2012a) Roles for the pre-supplementary motor area and the right inferior frontal gyrus in stopping action: electrophysiological responses and functional and structural connectivity. Neuroimage 59:2860-2870.

Swann NC, Tandon N, Pieters TA, Aron AR (2012b) Intracranial Electroencephalography Reveals Different Temporal Profiles for Dorsal- and Ventro-lateral Prefrontal Cortex in Preparing to Stop Action. Cereb Cortex.

Thorell LB, Lindqvist S, Bergman Nutley S, Bohlin G, Klingberg T (2009) Training and transfer effects of executive functions in preschool children. Developmental science 12:106-113.

Vonsattel JP, Myers RH, Stevens TJ, Ferrante RJ, Bird ED, Richardson EP, Jr. (1985) Neuropathological classification of Huntington's disease. J Neuropathol Exp Neurol 44:559-577.

Wakai M, Takahashi A, Hashizume Y (1993) A histometrical study on the globus pallidus in Huntington's disease. J Neurol Sci 119:18-27.

Wang M, Vijayraghavan S, Goldman-Rakic PS (2004) Selective D2 receptor actions on the functional circuitry of working memory. Science 303:853-856.

Wessel J, Reynoso HS, Aron AR (*under review*) Stopping eye movements has global motor effects. J Neurophysiol.

Wiesendanger E, Clarke S, Kraftsik R, Tardif E (2004) Topography of cortico-striatal connections in man: anatomical evidence for parallel organization. Eur J Neurosci 20:1915-1922.

Yassa MA, Stark CE (2009) A quantitative evaluation of cross-participant registration techniques for MRI studies of the medial temporal lobe. Neuroimage 44:319-327.

Young AB, Shoulson I, Penney JB, Starosta-Rubinstein S, Gomez F, Travers H, Ramos-Arroyo MA, Snodgrass SR, Bonilla E, Moreno H, et al. (1986) Huntington's disease in Venezuela: neurologic features and functional decline. Neurology 36:244-249.

Zandbelt BB, Bloemendaal M, Hoogendam JM, Kahn RS, Vink M (2012a) Transcranial Magnetic Stimulation and Functional MRI Reveal Cortical and Subcortical Interactions during Stop-signal Response Inhibition. J Cogn Neurosci.

Zandbelt BB, Bloemendaal M, Neggers SF, Kahn RS, Vink M (2012b) Expectations and violations: Delineating the neural network of proactive inhibitory control. Hum Brain Mapp.

Zandbelt BB, van Buuren M, Kahn RS, Vink M (2011) Reduced proactive inhibition in schizophrenia is related to corticostriatal dysfunction and poor working memory. Biol Psychiatry 70:1151-1158.

Zandbelt BB, Vink M (2010) On the role of the striatum in response inhibition. PLoS ONE 5:e13848.